A COMPARATIVE ASSESSMENT OF AVAILABLE METHODS FOR SEISMIC PERFORMANCE EVALUATION OF BURIED STRUCTURES

A THESIS SUBMITTED TO
THE GRADUATE SCHOOL OF NATURAL AND APPLIED SCIENCES
OF
MIDDLE EAST TECHNICAL UNIVERSITY

BY

ALİ GÜNEY ÖZCEBE

IN PARTIAL FULFILLMENT OF THE REQUIREMENTS
FOR
THE DEGREE OF MASTER OF SCIENCE
IN
CIVIL ENGINEERING

AUGUST 2009

Approval of the thesis:

A COMPARATIVE ASSESSMENT OF AVAILABLE METHODS FOR SEISMIC PERFORMANCE EVALUATION OF BURIED STRUCTURES

submitted by **ALİ GÜNEY ÖZCEBE** in partial fulfillment of the requirements for the degree of **Master of Science in Civil Engineering Department, Middle East Technical University** by,

Prof. Dr. Canan Özgen _____
Dean, Graduate School of **Natural and Applied Sciences**

Prof. Dr. Güney Özcebe _____
Head of Department, **Civil Engineering**

Assoc Prof Dr. Kemal Önder Çetin _____
Supervisor, **Civil Engineering Dept., METU**

Examining Committee Members:

Prof. Dr. Mehmet Yener Özkan _____
Civil Engineering Dept., METU

Assoc. Prof. Dr. Kemal Önder Çetin _____
Civil Engineering Dept., METU

Prof. Dr. Erdal Çokça _____
Civil Engineering Dept., METU

Intr. Dr. Kartal Toker _____
Civil Engineering Dept., METU

Instr. Dr. Berna Unutmaz _____
Civil Engineering Dept., Kocaeli University

Date: 28.08.2009

I hereby declare that all information in this document has been obtained and presented in accordance with academic rules and ethical conduct. I also declare that, as required by these rules and conduct, I have fully cited and referenced all material and results that are not original to this work.

Name, Last Name : ALİ GÜNEY ÖZCEBE

Signature :

ABSTRACT

A COMPARATIVE ASSESSMENT OF AVAILABLE METHODS FOR SEISMIC PERFORMANCE EVALUATION OF BURIED STRUCTURES

Özcebe, Ali Güney

M.Sc., Department of Civil Engineering

Supervisor: Assoc. Prof Dr. Kemal Önder Çetin

August 2009, 149 pages

In the last three decades, seismic performance assessment of buried structures has evolved through the following stages : i) buried structures are not prone to seismically-induced damages, thus no need for detailed investigations, ii) eliminating soil-structure-earthquake interaction and use of seismically-induced free field ground deformations directly as the basis for seismic demand, thus producing conservative results, and finally iii) soil-structure and earthquake interaction models incorporating both kinematic and inertial interactions. As part of soil-structure and earthquake interacting models, simplified frame analysis established the state of practice and is widely used. Within the confines of this thesis, the results of simplified frame analysis based response of buried structures are compared with those of 2-D finite element dynamic analyses. For the purpose, 1-D dynamic and 2-D pseudo-dynamic analyses of free field and buried structural systems are performed for a number of generic soil, structure and earthquake combinations. The analyses results revealed that, in general, available closed form solutions are in pretty good agreement with the results of finite element analyses. However, due to the fact

that dynamic analyses can model both kinematic and inertial effects; it should be preffered for the design of critical structures.

Keywords: Seismic Design of Rectangular Tunnels, Simplified Method, Nonlinear Soil Mass Participation Factor, Statistically-Based SFA Method, Alternative Structural SFA Method

ÖZ

GÖMÜLÜ YAPILARIN DEPREM DAVRANIŞININ BELİRLENMESİNDE KULLANILAN MEVCUT YÖNTEMLERİN KARŞILAŞTIRMALI DEĞERLENDİRİLMESİ

Özcebe, Ali Güney

Yüksek Lisans, İnşaat Mühendisliği Bölümü

Tez Yöneticisi: Doç. Dr. Kemal Önder Çetin

Ağustos 2009, 149 sayfa

Son otuz yılda, gömülü yapıların sismik davranışının belirlenmesine yönelik olarak gerçekleştirilen analiz aşamaları aşağıdaki gelişimi göstermiştir: i) deprem yükleri altında güvenli oldukları düşünüldüğünden bir analize gerek duyulmamıştır, ii) serbest zemin saha koşullarınca belirlenen deprem yer hareketine bağlı deplasmanlar doğrudan gömülü yapı üzerine uygulanmıştır, iii) zemin-yapı deprem ilişkisi kinematik ve atalet etkilerini de gözönüne alan sayısal modellemeler ile belirlenmiştir. Zemin yapı deprem etkileşimini gözönüne alan modeller arasında basitleştirilmiş çerçeve yöntemi pratikte yoğun olarak kullanılmıştır. Bu çalışma kapsamında, basitleştirilmiş çerçeve yöntemleriyle 2 boyutlu sonlu elemanlar temelli dinamik benzeri analiz sonuçlarının karşılaştırılması planlanmıştır. Netice olarak, mevcut analitik yöntemlerin, belirli kabuller altında, sonlu elemanlar yöntemiyle tutarlı sonuçlar verdiği gözlemlenmiştir. Fakat, önem katsayısı yüksek olan yapıların tasarımlarında, atalet etkilerini ve kinematik ilişkileri modelleyebilen dinamik analiz yöntemi önerilmektedir.

Anahtar Kelimeler: Dikdörtgen Tünellerin Sismik Tasarımı, Basitleştirilmiş Yöntem, Doğrusal Olmayan Zemin Kütle Katılım Katsayısı, İstatiksel BÇA Yöntemi, Alternatif Yapısal BÇA Yöntemi.

To All of My Family…

ACKNOWLEDGEMENTS

To start with, I would like to thank Assoc. Prof. Dr. Kemal Önder Çetin not only for his close guidance throughout my study but also for enlarging my horizons in the field of civil engineering.

I would like to express my special thanks to Dr. P.E. Ali Terzibaşoğlu for sharing his deep knowledge with me and his never ending support which has always kept me motivated.

I would like to express my gratefulness to Mr. Habib Tolga Bilge for his invaluable contributions while reviewing the draft of this thesis. I would also like to thank him due to his kind and patient personality.

I would like to offer my most sincere thankfulness to my family since they have always been by my side throughout my life.

I would like to express my deepest gratefulness, to my dear wife, Sevgi Özcebe for her continuous support, endless understanding during the thesis period. I would also present my thankfulness for her valuable contributions while finalizing this manuscript.

This study had financially been supported with a scholarship provided by TÜBİTAK-BİDEB, this support is gratefully acknowledged.

I would like to offer my special thanks to Dr. Ersan Yıldız for his scientific support in my thesis subject.

I would also like to thank Mr. Ömer Karamanlı for his guidance while I was writing my thesis.

TABLE OF CONTENTS

LIST OF FIGURES

FIGURES

LIST OF TABLES

TABLES

LIST OF SYMBOLS AND ABBREVIATIONS

a	: Greater dimension of the cross-section of box girder (measured from wall to wall).
a_{max}	: Maximum acceleration of the seismic excitation.
b	: Smaller dimension of the cross-section of box girder (measured from wall to wall).
g	: Gravitational acceleration
h_i	: Layer thickness of i^{th} layer (from top) of the soil profile
k_l	: Structural response to unit racking deformation (Penzien, 2000)
k_{si}	: Soil related parameter (Penzien, 2000)
k_{so}	: Soil related parameter (Penzien, 2000)
r_d	: Non-linear shear mass participation coefficient
z	: Embedment depth
E_c	: Modulus of elasticity of concrete
F	: Flexibility ratio. Relative rigidity of the soil with respect to structure (Wang (1993) and Penzien (2000))
G	: Degraded shear modulus of soil layer (Huo et al., 2006)
G_{eq}	: Equivalent shear modulus of soil layer (in this study)
G_m	: Degraded shear modulus of soil layer (Wang, 1993)
G_{max}	: Initial shear modulus of soil layer
G_{rep}	: Representative shear modulus for layered profiles
G_s	: Degraded shear modulus of soil layer (Penzien, 2000)
H	: Height of the structure, axis to axis distance (Wang, 1993 and this study)
M_w	: Moment magnitude of the seismic action

R : Coefficient of racking ratio, ratio of soil-structure deformation to free-field deformation (used in Wang (1993), Penzien (2000), Huo et al. (2005) and in this study)

$R_{proposed}$: Racking ratio of the proposed model (in this study)

S_1 : Structural response to unit racking deformation (Wang, 1993)

$V_{s,eq}$: Equivalent shear wave velocity of the layered profile

$V_{s,bot}$: Shear wave velocity of the soil layer in contact with the bottom slab of the box girder

$V_{s,top}$: Shear wave velocity of the soil layer in contact with the top slab of the box girder

V_{si} : Shear wave velocity of i^{th} layer (from top) of the soil profile

W : Width of the structure, axis to axis distance (in Wang (1993) and in this study)

α_s : Parameter related with soil and structural rigidity (Penzien, 2000)

γ_{eq} : Effective shear strain of the soil layer, used to determine equivalent shear modulus of the soil from modulus reduction curves

γ_{max} : Maximum shear strain of the soil layer

γ_{soil} : Unit weight of the soil layer

λ : Aspect ratio of the box girder, ratio of greater dimension to smaller dimension of the box girder, i.e. a/b

$\theta 1$: Variable of the median predictions of statistically based proposed racking relationship

$\theta 2$: Variable of the median predictions of statistically based proposed racking relationship

$\theta 3$: Variable of the median predictions of statistically based proposed racking relationship

$\theta 4$: Variable of the standard error term of statistically based proposed racking relationship

σ_d : Standard deviation

$\sigma_{\varepsilon rd}$: Standard deviation term of nonlinear shear mass factor method of Çetin and Seed (2000)

$\sigma_{proposed}$: Racking ratio of the proposed model (in this study)

σ'_v : Initial effective overburden pressure

$\tau_{hv,eq}$: Equivalent shear stress of soil which is assumed to be experienced by the soil layer during an earthquake

$\tau_{hv,max}$: Maximum shear stress of soil which is assumed to be experienced by the soil layer during an earthquake

τ_{max} : Shear stress occurring at a certain depth due to inertial effect of accelerating soil block

υ_s : Poisson's ratio of the soil media

Ω : Stiffness ratio, i.e. relative stiffness of structure to surrounding soil (Huo et al. (2005))

Δ_{FF} : Free-field deformation, i.e. deformation of soil without considering any interaction.

Δ^{FF}_{max} : The most critical free field deformation in the soil at the place of the structure among all time steps of the seismic action

Δ^{SSI}_{max} : Deformation of the structure corresponding to the most critical free-field deformation

Δ_{p2i} : Normalized deformation of assumed normal forces acting on the walls of the structure (Huo et al., 2006)

Δ_S : Deformation of the structure which is interacting with surrounding soil (Wang, 1993)

Δ_{STRU} : Deformation of the structure which is interacting with surrounding soil (Huo et al., 2006).

$\Delta_{\tau i}$: Normalized deformation of assumed uniform shear forces on the perimeter of the structure (Huo et al., 2006)

$(EI)_{str}$: Bending stiffness of the structure (Huo et al., 2006)

FR : Flexibility ratio. Relative rigidity of the soil with respect to structure (used in this study)

CSR : Cyclic stress ratio

CSR_{eq} : Equivalent cylic stress ratio

PGA : Peak ground acceleration

PGD : Peak ground displacement

PGV : Peak ground velocity

SSI : Soil structure interaction

CHAPTER 1

INTRODUCTION

Current seismic design practice of structures consists of two completely different approaches: (i) force-based and (ii) displacement (deformation)-based methods. Force-based method is the traditional approach and involves the prediction of equivalent seismic forces. Seismic design is then carried out by applying required response modification factors and force-based demand over capacity ratios. The latter approach includes calculation of the displacement demand and further seismic design checks are carried out based on this target displacement. However, in practice simpler approaches are more widely used, thus in most of the cases, force method replaces more “realistic” displacement method owing to its superior simplicity and acceptable performance predictions.

The seismic response of an underground structure is different from the response of a superstructure founded on the ground surface. The confining action of surrounding soil media is the main reason of this difference. In simpler words, while superstructures are free vibrating systems, underground structures deform compatibly with the surrounding soil stratum. This requirement encourages engineers to pursue deformation-based methods in the seismic design of underground structures, since none of the available force-based methods have been developed to take into account deformation compatibility.

There exists a common misbelief in the design practice claiming the redundancy of the seismic design of underground structures, since it is assumed that satisfactory seismic performance has been fulfilled when structural members are designed according to service loads.

In Turkish practice, current design codes for bridges listed as AASHTO LFD (2002) and AASHTO LRFD (2007) are used for the design of underground structures. In application sections of these codes, the following is stated (Imbsen, 2006):

"Seismic effects for box culverts and buried structures need not be considered, except when they are subject to unstable ground conditions (e.g., liquefaction, landslides, and fault displacements) or large ground deformations (e.g., in very soft ground)."

This statement uses significantly subjective and undefined terms such as "large ground deformations" or "very soft ground". The author believes that soil profiles composed of medium dense or medium stiff layers may also experience large deformations, if they are subjected to higher intensity strong ground motions. Author also believes that, it is engineer's responsibility to check that the designed structure can satisfactorily resist to probable seismic excitations, as well as service life loads. Hence, it is recommended to check seismic performances of underground structures in seismically active regions.

Many researchers, e.g. Duke and Leeds (1959), Stevens (1977), Dowding and Rozen (1978), Owen and Scholl (1981), Sharma and Judd (1991), Power et al. (1998), and Kaneshiro et al. (2000), have studied the seismic performance of underground structures after a wide range of seismic events. Sharma and Judd (1991) performed a comprehensive study on the damage patterns observed in buried structures and their findings are summarized in Figure 1.1.

Figure 1.1 reveals that underground structures are also vulnerable to seismically-induced failures and damage. Although they are considered to be seismically safe when designed for service loads, seismic performance of the underground structures should be checked especially for scenarios including high magnitude events and small overburden levels. Shallow tunnel, i.e. when overburden is less than 15 m, are usually designed as cut and cover structures and these structures are more vulnerable to seismically-induced damages compared to deeper tunnels (Hashash, 2001).

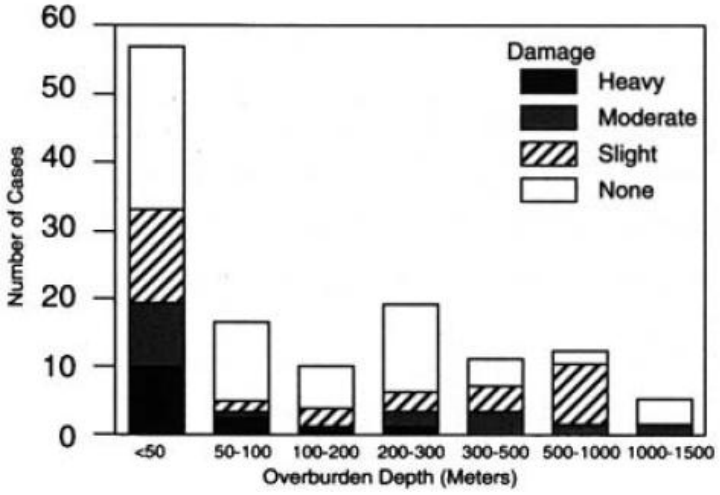

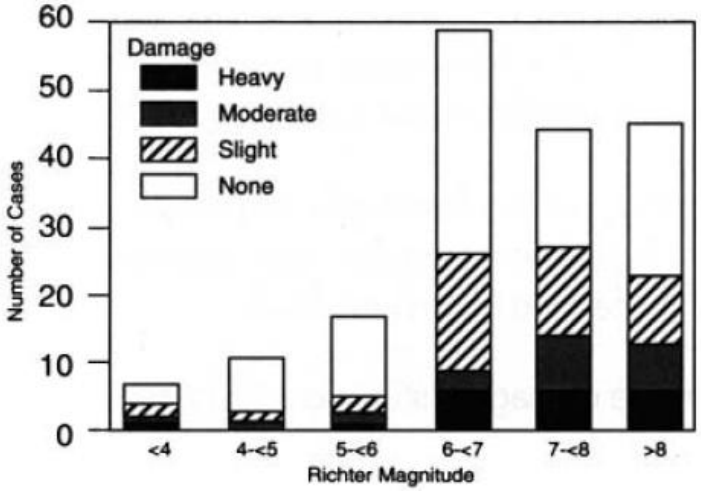

Figure 1.1. Damage statistics on underground structures (Sharma and Judd, 1991)

As stated by Wang (1993), as the depth of burial decreases:

i. lower confinement action results from lower overburden pressure, and

ii. higher amount of displacement is observed

Moreover, these shallow buried structures are subjected to higher levels of forces owing to their higher rigidities (Hashash et al., 2001).

1.1 Aim of the Thesis

The main focus of this study is to assess the seismic performance of rectangular, underground cut and cover structures constructed at relatively shallow depths. For this reason, special emphasis will be given on the following issues: a) the definition of a representative shear modulus concept in multi-layered systems, b) the development of a new racking deformation equation, i.e. equation which predicts earthquake-induced deformation of Soil-structure interacting system, by taking into account the uncertainties associated based on the results of finite element analyses, and c) the development of a simple preliminary assessment methodology for the estimation of flexibility ratios and free field ground deformations an alternative to advance numerical analyses for preliminary assessments.

1.2 Scope of the Thesis

Following this introduction, previous studies on the design of underground cut and cover structures will be summarized in Chapter 2. Different approaches used for the seismic assessment of these types of structures will be discussed; and moreover, existing simplified frame analysis methods will be introduced.

As will be discussed further in the following sections, all of the available analytical closed-form solutions are derived for uniform and homogeneous soil media. Thus, a representative equivalent modulus value is required for analysis of multi-layered systems. Chapter 3 is devoted to the determination of this

representative modulus concept and introduction of a new racking relationship, compatible with the assumption of representative modulus. The results of finite element analyses, and the proposed model, are compared with the results from existing studies within the confines of this chapter. Unlike other studies, uncertainty in predictions is also considered and mean plus and minus one standard deviation bands for multi-layered systems are presented.

In Chapter 4, a simplified procedure is proposed for the preliminary assessment of buried box type structure's seismic performance. The proposed procedure is developed based on the estimation of induced shear stresses by using nonlinear shear mass participation factor (r_d) of Çetin and Seed (2003). Then strain compatible modulus values are estimated through an iterative procedure.

Chapter 5 introduces an alternative racking method by using structural analysis software.

Chapter 6 summarizes major conclusions and findings.

CHAPTER 2

LITERATURE REVIEW

2.1 A Brief Review on Seismically-Induced Deformations at Tunnel Linings

This chapter presents a brief summary of deformation modes observed at tunnel linings under seismic excitations. Figure 2.1 is a summary of the work of Owen and Scholl (1981), which clearly illustrates all possible types of seismically-induced deformed shapes.

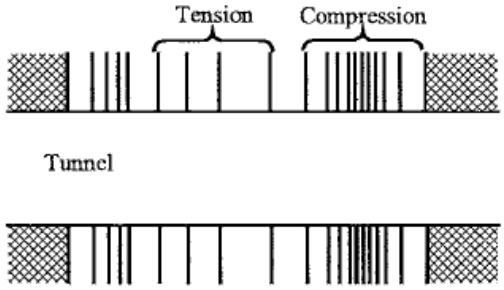

(i) Compression-extension

Figure 2.1. Types of deformations under seismic actions (after Owen and Scholl, 1981 and Hashash, 2001)

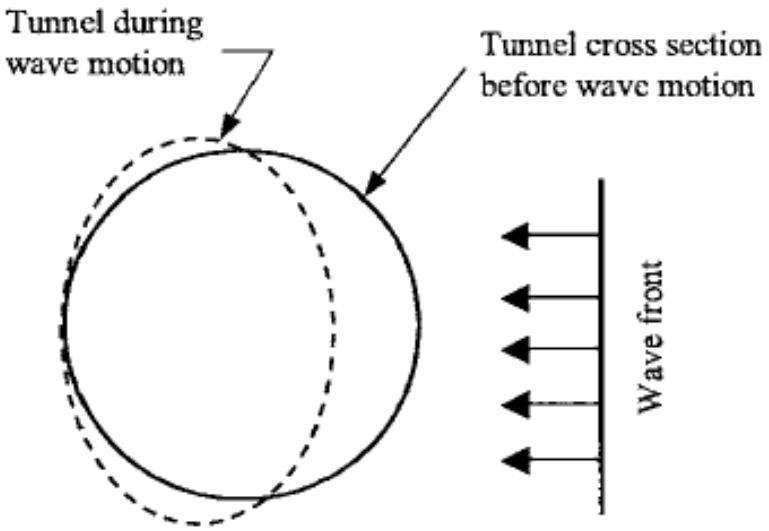

(ii) Compression of tunnel section

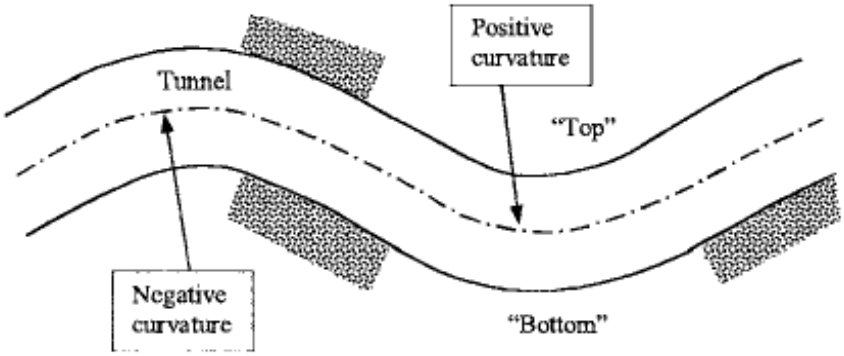

(iii) Longitudinal bending deformation

Figure 2.1 (cont'd). Types of deformations under seismic actions (after Owen and Scholl, 1981 and Hashash, 2001)

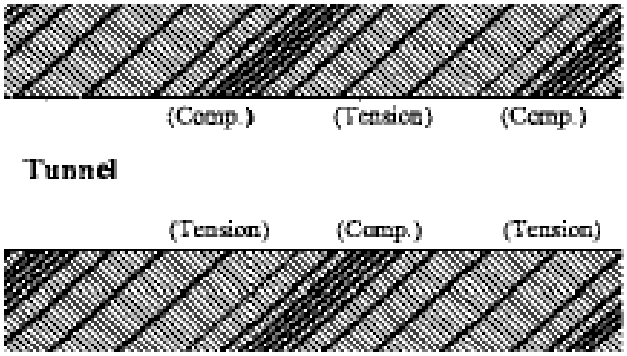

(iv) Diagonally propagating wave deformations

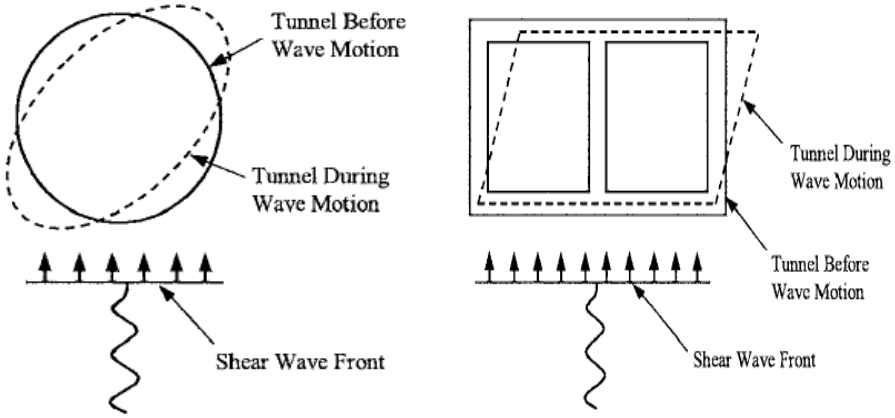

(v) Ovaling and racking deformations for
circular and rectangular tunnels, respectively

Figure 2.1 (cont'd). Types of deformations under seismic actions (after Owen and Scholl, 1981 and Hashash, 2001)

Along the deformation modes presented in Figure 2.1, racking deformations (v) are generally accepted as the most critical for tunnels subjected to seismic loading. This mode of deformation can be explained as in-plane deformation which creates shear and bending moment along the weak axis of rectangular tunnels.

2.2 Seismic Design Approaches for Rectangular Tunnel Sections

As part of the historical evolution, seismic designs of rectangular tunnels were carried out in two alternative ways:

i. dynamic pressure and

ii. free field deformation approach.

Dynamic pressure approach was originally developed for retaining structures by Mononobe-Okabe (Okabe, 1926). Due to its derivation, this method produces the most successful predictions for cantilever walls so that its use for underground box structures, especially in relatively higher embedment depths, leads to overestimated racking displacements (Wang, 1993). As mentioned by Wang (1993), this overestimation is mainly due to high amounts of surcharge.

In the free field deformation approach, seismic wave propagation-induced ground deformations are estimated by ignoring the presence of the structure and the excavation, then these deformations are applied on the de-coupled structure. Newmark (1968) and Kuesel (1969) developed analytical solutions for free field ground straining under harmonic waves. It had been widely believed that in case of stiff soil and flexible structure combination, free field deformation approach can be safely applied to the box frame. However, Hendron and Fernandez (1983) and Merritt et al. (1985) later found that these deformations could be amplified due to the presence of a cavity inside the free

field medium. Thus, free field approach may produce unconservative conclusions.

In 1987, St. John and Zahrah extended the studies of Newmark (1968) and Kuesel (1969) by modifying their equations considering shear and Rayleigh wave patterns of seismic excitation. Later, Penzien (2000) emphasized that if a cavity exists, the racking ratio, ratio of seismically-induced deformation of soil-structure system with respect to free-field soil deformation, approaches to 2 to 3, due to a discontinuity in the soil medium. St. John and Zahrah (1987) reported that free-field deformation method produces unrealistic results when the medium is softer relative to the embedded structure. They recommended performing finite element analyses for those cases. At present, there is a consensus for soft soil and rigid structure cases and it is known that this method results in very conservative racking displacements due to thicker member dimensions.

To sum up, free field method produces liberal or conservative results for very large and very low flexibility ratios, ratio of lateral rigidities of soil with respect to structure. As Hashash (2001) stated that, this method is a powerful tool which can be used for the preliminary design of underground structures.

It was in 1993 that, Wang proposed the first simplified frame analysis (SFA) method to assess the racking deformation of rectangular shaped box tunnel. The following factors have been identified to affect racking displacement of rectangular box tunnel structures:

i. relative stiffness between soil and structure

ii. structure geometry

iii. input earthquake motions

iv. tunnel embedment depth

Wang (1993) performed 36 dynamic finite element simulatons to assess the contributions of these factors on the overall performance. Assumptions behind the analyses are as defined:

i. no-slip condition along the interfaces,

ii. linear elastic and rigid frame which do not contain any plastic hinges,

iii. soil profiles consisting of soft layers overlying stiff layers, and

iv. rigid base (i.e. base rock) overlaid by soil profiles

This method basically linked the flexibility ratio (FR) to racking coefficient (R) for underground structures. By definition, the flexibility ratio is the effective linear shear thrust of soil relative to bending stiffness of the box frame structure. Figure 2.2 represents the method of Wang (1993) schematically.

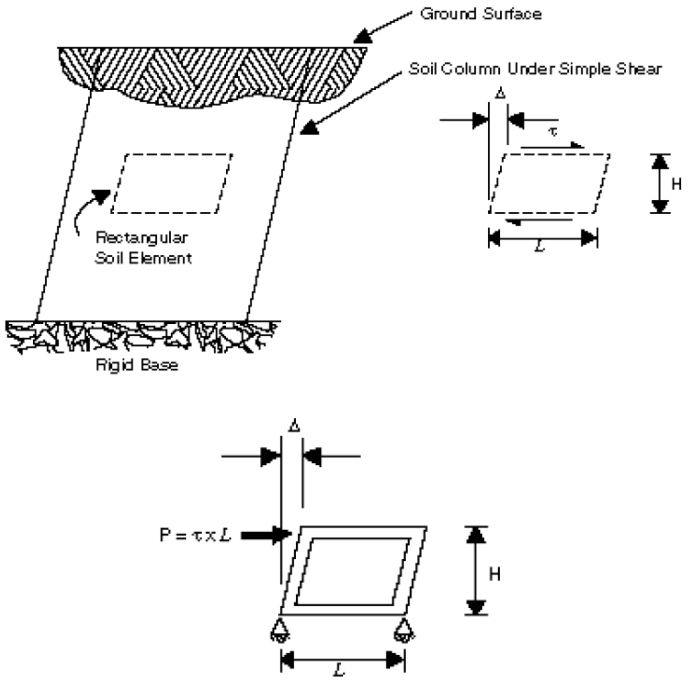

Figure 2.2. Definition of Simplified Frame Analysis (SFA) Method (Wang, 1993)

In 1998, Penzien and Wu developed a method, which estimates ovaling deformations of a circular tunnel by assuming plane strain conditions around the lining. In 2000, Penzien extended the previous work of Penzien and Wu (1998) for rectangular cut and cover structures. Different from Wang (1993), Penzien (2000) considered a uniform pressure along the structure consistent with plane strain conditions. Another difference is that Penzien (2000) directly estimates the deformation of the rectangular cavity with an approximation of circular cavity under constant shear stress conditions, whereas Wang (1993) suggests decreasing racking deformations of rectangular tunnels by 10% compared to circular tunnel deformations due to geometrical concerns.

The main assumptions of Penzien's method can be listed as:

i. height of the structure is smaller than the wavelength of the dominant ground motion frequency, and

ii. inertial effects are negligible.

These assumptions lead to constant shearing stress around the box frame, i.e. simple shear stress condition. The rest of the proposed procedure is similar to Wang's method. It simply relates the behavior of the combined system, i.e. soil and structure, to the components' relative rigidity with respect to each other.

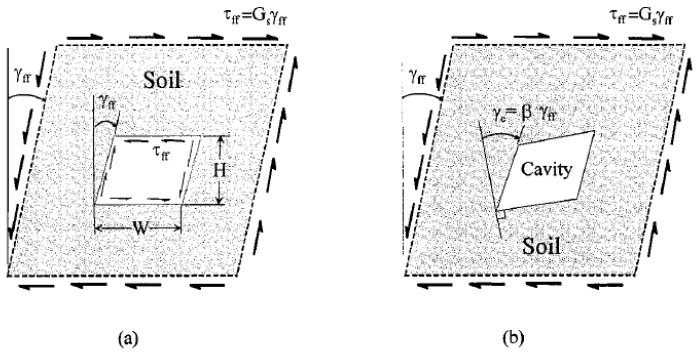

Figure 2.3. Deformation of free field with and without rectangular cavity under simple shear loading (Penzien, 2000)

Figure 2.3 schematically presented the deformation of the cavity under simple shear stress condition.

Figure 2.4 demonstrates the interaction effect on soil medium and box frame as proposed by Penzien (2000).

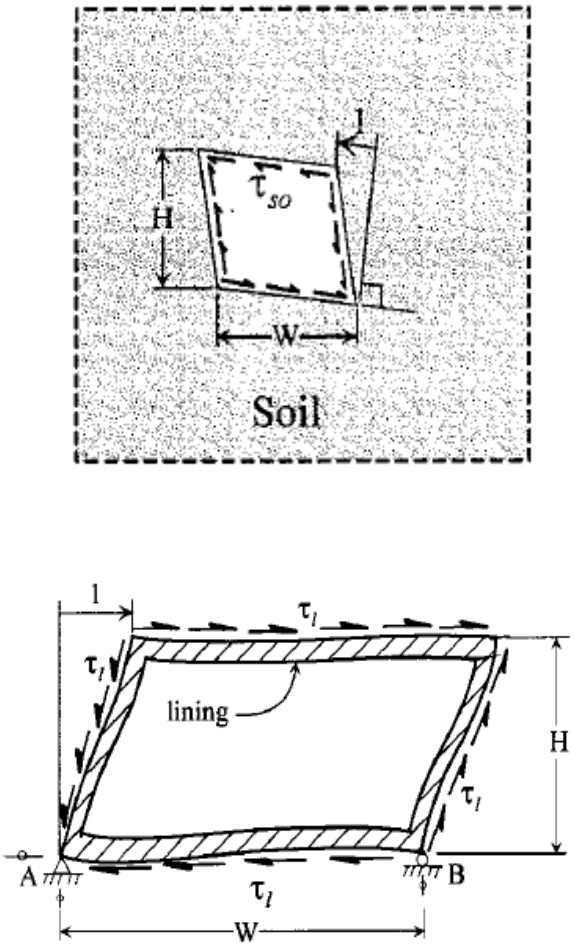

Figure 2.4. Stresses occuring along the perimeter of the cavity and structure under simple shear stress condition (Penzien, 2000)

In 2001, Hashash et al. performed a comprehensive study which includes a detailed literature survey on aspects of the design and analysis of underground structures. Besides many aspects of seismic design, this study especially covers the following issues:

- damage surveys on tunnels (Power et al., 1998),
- case studies all around the world,
- behaviour of underground structures to seismic waves (Owen and Scholl, 1981),
- seismic hazard analysis methods and corresponding design and analysis methods,
- ground motion and soil related parameters and generalizations (Power et al., 1996, St. John and Zahrah, 1987, etc.),
- types of ground responses to earthquakes,
- the response of underground structures to ground displacements (Newmark, 1968, Kuesel, 1969, St. John and Zahrah, 1987, Wang, 1993, Power et al., 1996, Penzien, 2000, etc.),
- seismic design issues (Hashash et al, 1998, Schmidt et al., 1998, Kiyomiya, 1995, etc.).

Besides this extensive literature survey, in their study, Hashash et al. (2001) provided illustrative examples regarding design and analysis of underground structures by using different methods.

Until 2006, all available soil structure interaction (SSI) methods assume only constant shear stress field around the box girder. By using conformal mapping techniques, complex variables theory, and theory of elasticity, Huo et al. (2005) incorporated normal stresses acting on walls to SSI analyses. In this method, in addition to normal stresses, aspect ratio (ratio of larger dimension to smaller dimension in the cross-section of the tunnel, $\lambda=a/b$), is also introduced.

It is important to note that, effect of the normal stresses become more important in cases where the soil rigidity is much higher than the rigidity of the structure. Therefore, for these conditions Huo et al. (2005) produces much higher racking ratios (i.e. $R= \Delta_{SSI}/\Delta_{FF}$) compared with Wang (1993) and Penzien (2000). For other cases, this solution converges to simple shear stress solutions since same constant shear stress is assumed around the structure (Huo et al., 2006).

Soil stresses and structure deformation are presented in Figure 2.5.

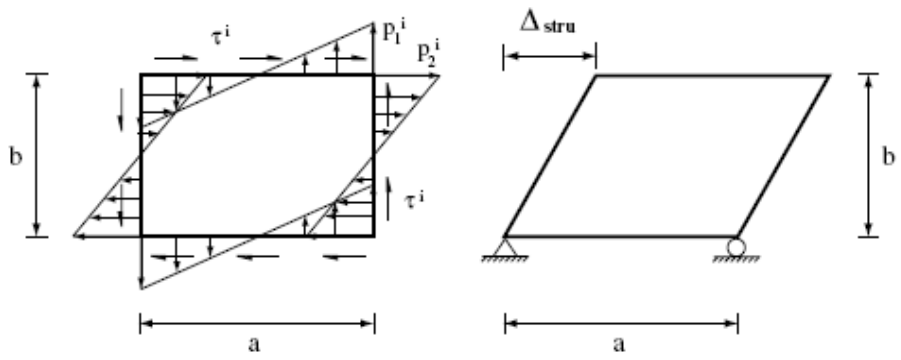

Figure 2.5. Structure loading and deformation (Huo et al., 2006)

Bobet et al. (2008) extended the study of Huo et al. (2005) by pointing out an important fact that soil stiffness may deviate significantly from that of the free field ones around the structure. Until 2008, the effect of soil medium had been modeled by using free field properties; but Bobet et al. (2008) proposed an iterative solution to find the modified shear modulus of the surrounding soil.

Next, the methodologies given by Wang (1993), Penzien (2000), and Huo et al (2006) are discussed.

2.3 Simplified Frame Analysis Methods

Simplified Frame Analysis (SFA) approach is a method which basically links racking deformation of soil-structure interacting system with relative stifnesses of soil medium with respect to structural stiffness.

2.3.1 Wang (1993)

The procedure proposed by Wang (1993) is applicable to cases where the structure geometry has been determined, soil profile is well known and earthquake record has been selected. The methodology involves the determination of the following variables:

- free field soil strains,
- free field soil deformation,
- Flexibility ratio, FR, as given in Equation 2.1.

$$FR = \frac{G_m \times W}{S_1 \times H} \tag{2.1}$$

In this equation,

G_m : Degraded shear modulus of the surrounding medium
W : Width of the structure
S_1 : Reciprocal of lateral racking deflection induced by unit force
H : Height of the structure
W and H are defined to be axis to axis distances.

- Racking coefficient, R, to be interpolated from Figure 2.6 and divided to a value of 1.1 so as to convert it to rectangular section coefficient (Wang, 1993).

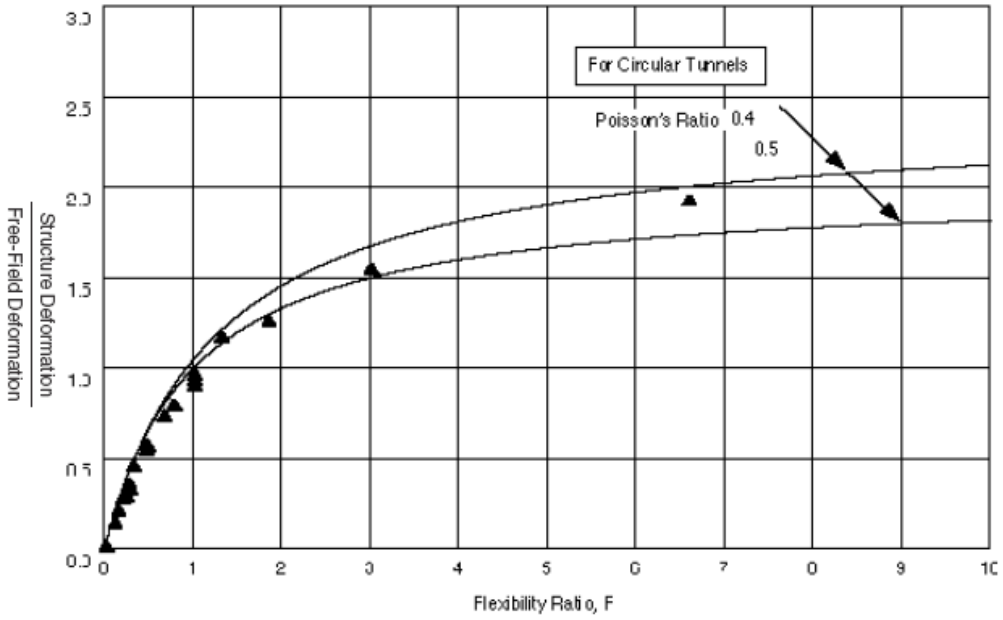

Figure 2.6. Racking curves (Wang, 1993)

- Racking deformation of structure, Δ_S, is calculated as given in Equation 2.2:

$$\Delta_S = R \times \Delta_{FF} \tag{2.2}$$

- So as to obtain racking deformation, equivalent triangular and concentrated forces are applied to the frame. Load case leading greater sectional forces is selected in order to obtain racking induced sectional forces.

2.3.2 Penzien (2000)

Penzien (2000) proposed a methodology for the purpose of determining the racking displacement and the sectional forces. The procedure is applicable to well defined structure geometry, soil profile, and seismic demand cases. The procedure can be summarized as follows:

- The lateral stiffness, k_l, of the structure under constant shear stress in plane strain condition, k_l, to be found by using any commercially available structural analysis program,
- Soil stiffness coefficient, k_{s0}, is calculated as given in Equation 2.3.

$$k_{s0} = \frac{G_s}{(3 - 4 \cdot \nu_s) * H} \tag{2.3}$$

Where;

H : height of the structure (axis to axis)

υ_s : Poisson's Ratio of surrounding soil medium

G_s : shear modulus of surrounding medium

- Second soil parameter, k_{si}, is calculated as follows.

$$k_{si} = \frac{G_s}{H} \tag{2.4}$$

- α_s, is calculated as given in Equation 2.5.

$$\alpha_s = (3 - 4 \cdot \nu_s) * \frac{k_l}{k_{si}} \tag{2.5}$$

Where;

k_l : lateral stiffness of structure

- Racking coefficient, R, is determined as follows.

$$R = \left[\frac{4 \cdot (1 - \nu_s)}{1 + \alpha_s} \right] \tag{2.6}$$

- Internal forces are calculated through applying the racking displacement to the structure.

2.3.3 Huo et al. (2005)

Recently, Huo (2006) has proposed a similar methodology. The procedure is applicable in case structure geometry is determined, soil profile is well known,

and earthquake record is selected. The procedure can be summarized as follows:

- Aspect ratio of the structure, λ, is calculated as follows:

$$\lambda = \frac{a}{b} \tag{2.7}$$

where,

a : larger dimension of the cross-section of the rectangular structure

b : smaller dimension of the cross-section of the rectangular structure

- Stiffness ratio, Ω, is estimated as given in Equation 2.8.

$$\Omega = \frac{(EI)_{STR}}{G \cdot b^3} \tag{2.8}$$

Where;

$(EI)_{STR}$: Bending rigidity of structural elements

G : Shear modulus of the surrounding layer

- Δ_{ti} and Δ_{p2i} to be calculated from Equation 2.9a and Equation 2.9b for one barrel simple structures.

$$\Delta_{ti} = \frac{(1+\lambda)}{24 \cdot (EI)_{STR}} \cdot \lambda \cdot b^4 \tag{2.9a}$$

$$\Delta_{p2i} = \frac{(1+\lambda)}{60 \cdot (EI)_{STR}} \cdot b^4 \qquad (2.9b)$$

- Correlation parameters, M, N, and L, are estimated by using Figure 2.7.

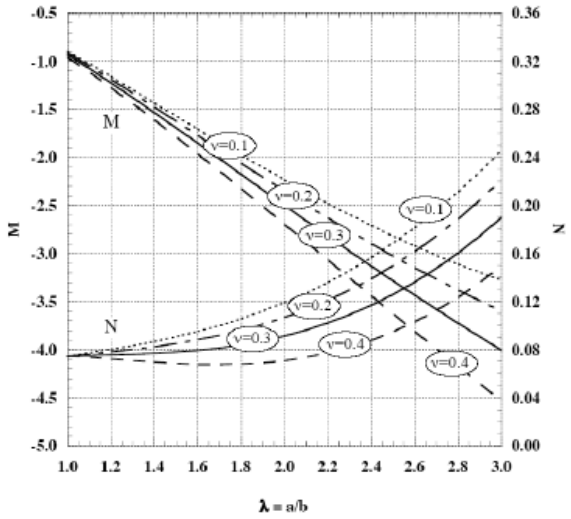

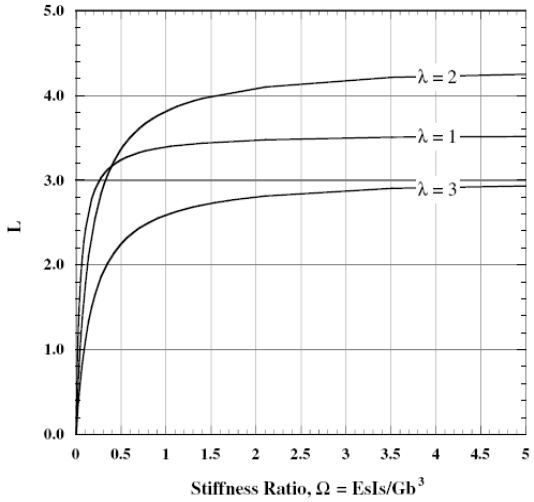

Figure 2.7. Model correlation parameters (Huo et al., 2005 and Huo, 2008)

- Normalized structural deformations can be calculated as follows:

$$R = \frac{\Delta_{STRU}}{\Delta_{FF}} = (1-\nu_s^{\,2}) \cdot \left[N \cdot \Delta_{p2i} + (M \cdot \Delta_{p2i} + \Delta_{\pi i}) \cdot L \right] \frac{G}{b} \qquad (2.10)$$

- Internal forces are calculated through applying the racking displacement to the structure.

In the following chapters, the procedures proposed by Wang (1993), Penzien (2000), and Huo et al. (2005) are going to be compared with finite element soil-structure interaction solutions obtained from PLAXIS 9.

CHAPTER 3

COMPARISON OF ANALYTICAL METHODS WITH THE PROPOSED RACKING RELATIONSHIP

This chapter is devoted to the discussion of finite element analyses details. Results of these analyses are compared with analytical closed-form solutions proposed by Wang (1993), Penzien (2000), and Huo et al. (2005). A new probabilistically-based racking relationship for multi-layered systems is developed based on finite element analyses (PLAXIS 9) results.

3.1 Parameters and Methodology of Site Response Analyses

The finite element analyses are performed by using PLAXIS 9.0-2D for all combinations, in which free field racking deformations exceed 1 mm. The analyses are performed for 6 different soil profiles, 14 different rock outcrop strong ground motions, 2 different structure types, and 2 different embedment depths (z=H and z=2H). Details of them are presented in the following sections.

3.1.1 Parameters

3.1.1.1 Soil Profiles

Six different generic soil profiles are used in both analytical solutions and finite element analyses. In order to examine the seismic response of underground structures in a heterogeneous soil profile, all soil profiles have been assumed to have soil interfaces (without considering any interface coefficient) along the walls of the embedded structures. Further information regarding the shear wave velocity and unit weight profiles are presented in Appendix A. For illustration purposes NEHRP C1 type soil profile is also shown in Table 3.1.

Table 3.1. Soil profile of NEHRP C1 type soil

C1				
Layer #	Material Type	Thickness (m)	U. Weight (kN/m^3)	S. Wave Velocity (m /s)
1	CLAY, PI = 15	1.00	16.97	396
2	CLAY, PI = 15	1.00	16.97	411
3	CLAY, PI = 15	1.00	16.97	427
4	CLAY, PI = 15	1.00	16.97	427
5	CLAY, PI = 15	1.00	16.97	442
6	CLAY, PI = 15	1.00	16.97	457
7	CLAY, PI = 15	1.00	16.97	488
8	CLAY, PI = 50	1.00	16.97	549
9	CLAY, PI = 50	1.00	16.97	579
10	CLAY, PI = 50	1.00	16.97	594
11	CLAY, PI = 50	1.00	16.97	625
12	CLAY, PI = 50	1.00	16.97	655
13	SAND	1.00	16.97	686

Table 3.1 (cont'd). Soil profile of C1 type soil

C1				
Layer #	Material Type	Thickness (m)	U. Weight (kN/m^3)	S. Wave Velocity (m /s)
14	SAND	1.00	16.97	686
15	SAND	1.00	16.97	762
16	SAND	1.00	16.97	762
17	SAND	1.00	16.97	762
18	SAND	1.00	16.97	762
19	SAND	1.00	16.97	762
20	SAND	1.00	16.97	762
21	DENSE SAND	1.00	16.97	838
22	DENSE SAND	1.00	16.97	838
23	DENSE SAND	1.00	16.97	838
24	DENSE SAND	1.00	16.97	914
25	DENSE SAND	1.00	16.97	914
26	DENSE SAND	1.00	16.97	914
27	W. ROCK	1.00	16.97	1067
28	W. ROCK	1.00	16.97	1067
29	W. ROCK	1.00	16.97	1067
30	W. ROCK	1.00	16.97	1067
31	BASE ROCK	-	16.97	1219

In order to be consistent with SHAKE 91, which is an equivalent linear site response analysis software, soil layers in finite element (Plaxis) assessments are modeled as linear elastic but with strain compatible modulus parameters consistent with SHAKE 91 analyses results.

Seismic loading, by nature, takes place very rapidly; therefore it is often associated with undrained conditions. To satisfy this condition, i.e. no volume change assumption leading to a Poisson ratio of 0.5 during seismic excitation is adopted for all soil layers.

3.1.1.2 Structural Information

In the analyses performed, one barrel and one bay box frame structures with different aspect ratios have been used. Figure 3.1 shows these frame structures illustratively (dimensions are in m).

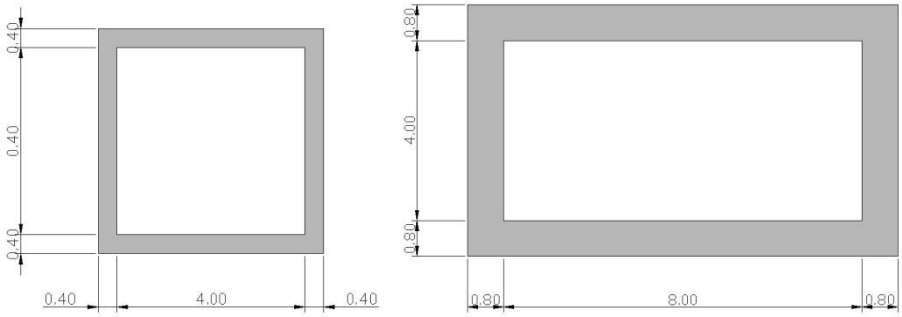

Figure 3.1. Frame structures

Structures are assumed to be R/C box frames, having uncracked modulus of elasticity of the concrete (E_c) equal to 30000 MPa (N/mm^2). In order to create realistic scenarios, dimension of wall thickness is very important. As a general design approximation, wall thicknesses have been assumed to be equal one tenth (1/10) of the clear span, i.e. clear distance measured from wall to wall.

Effect of aspect ratio to soil structure interaction analyses was first studied by Huo et al. (2005). Since the author believes that the aspect ratio plays a significant role in the behavior of an underground tunnel subjected to seismic action, it has been included as a parameter in the analyses. As a matter of fact, aspect ratio is not a structural variable like structural rigidity of the box frame reinforced concrete structure; since an increase in the aspect ratio means

increase in clear span which leads to a proportional increase in wall thickness and thus a proportional increase in rigidity of the structure. It is believed that as the majority of the structural resistance against earthquake loading is provided by vertical load carrying elements, i.e. walls, the condition corresponding to minimum wall thickness creates the most critical structural geometry.

Further information regarding structural parameters is presented in Appendix B.

3.1.1.3 Embedment Depth

It was in 1993 when the effect of the embedment depth was first referred to in the study of Wang. Later, Hashash (2001) clearly indicated that increase in the burial depth implied increasing shear wave velocities, leading to a greater shear moduli. Moreover, both Wang (1993) and Hashash (2001) stated that in uniform layers the maximum relative displacement between the roof and the slab of the structure decreased as the embedment depth increased due to the accumulation of displacements near the ground surface level. Wang (1993) and Penzien (2000) pointed out the fact that depth of burial should be at least equal to the height of the structure, H, (1.5 H in Wang's coordinate system) to sustain simple shear strain/stress conditions.

In general, an increase in embedment depth results in an increase in the racking ratio. Nevertheless, it is taken as a parameter so as to characterize this dependence.

In the FEM analyses and analytical solutions, two types of embedment depth (z) were used for each type of structure; i) z = H as the lower limit, and ii) z = 2H as the upper limit. Soil profiles, structural geometries, and embedment depths are presented in Figures 3.2 to 3.4 for NEHRP site classes B, C and D, respectively.

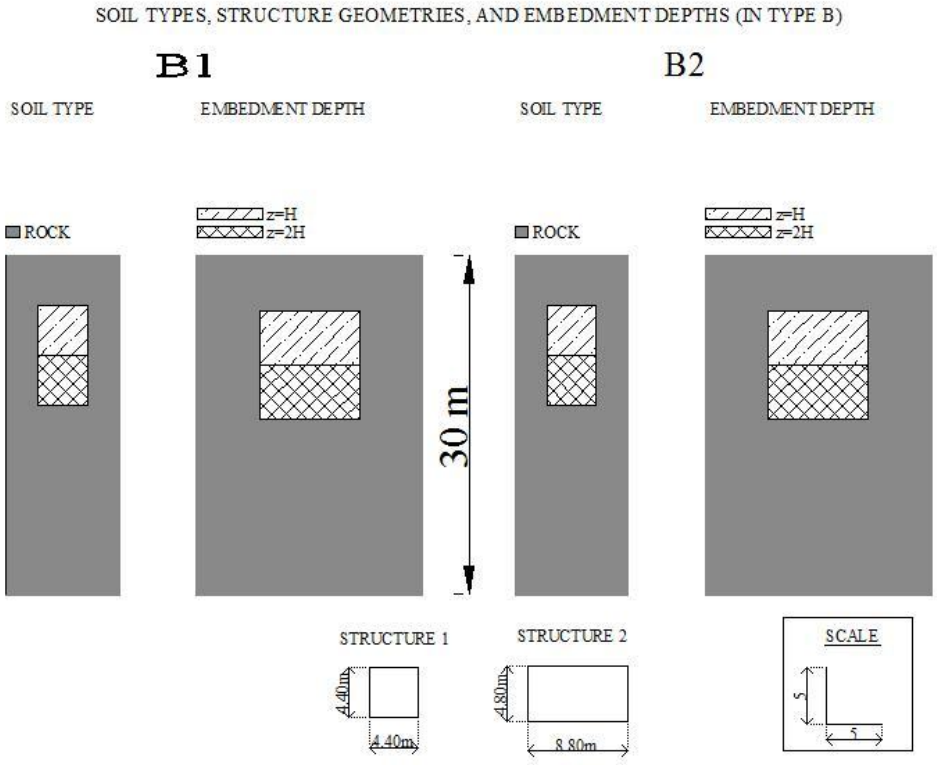

Figure 3.2. NEHRP B

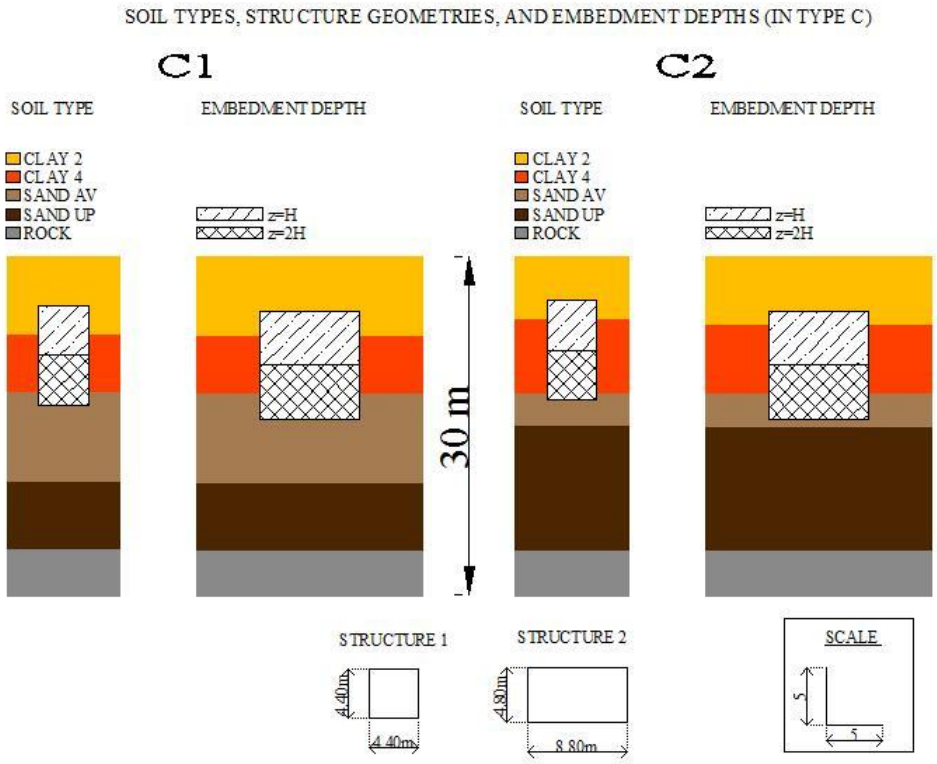

Figure 3.3. NEHRP C

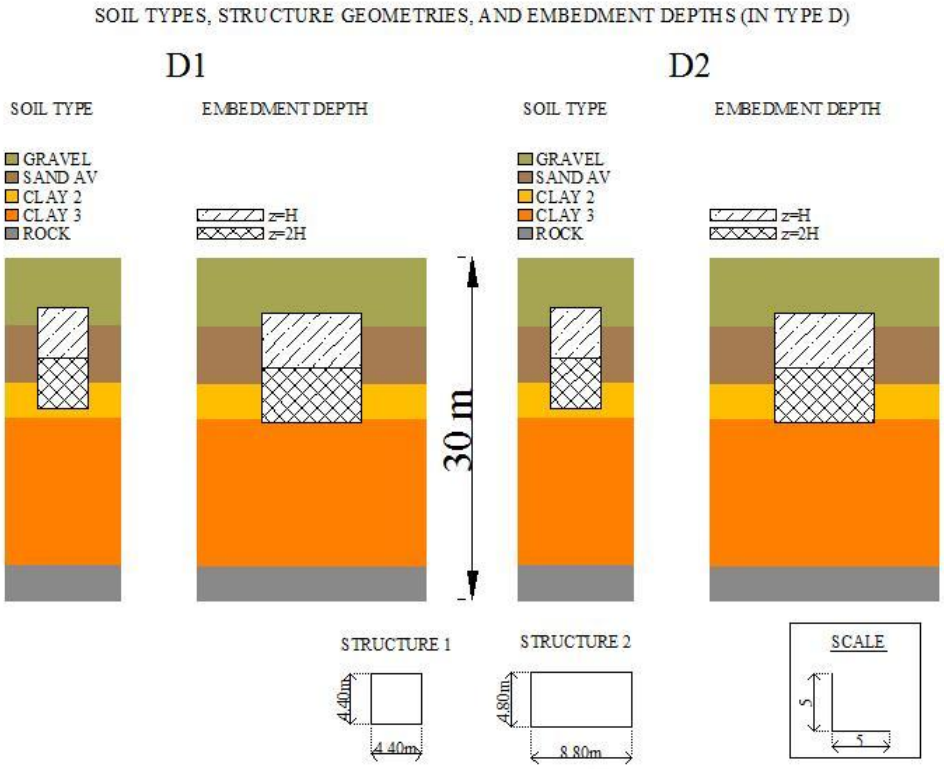

Figure 3.4. NEHRP D

The notation regarding the soil layers which are used in Figures 3.1 to 3.3 are summarized in Table 3.2. In this table, references of modulus degradation and damping ratio curves used in analyses are listed. Average sand is assumed to represent sand having average properties; on the other hand, sand up and sand low are assumed to be stiff and loose sand layers, respectively (Seed and Idriss, 1970).

Table 3.2. Summary of Notation

Name	Information
Sand Av.	Sand layer behaving as average sand, defined in Seed and Idriss (1970)
Sand Up.	Sand layer behaving as upper bound sand, defined in Seed and Idriss (1970)
Sand Low.	Sand layer behaving as lower bound sand, defined in Seed and Idriss (1970).
Clay, 2	Clay with PI=15
Clay, 3	Clay with PI=30
Clay, 4	Clay with PI=50

3.1.1.4 Strong Ground Motion Data

A representative set of strong ground motion (SGM) records including 13 rock outcrop and 1 stiff soil accelerograms were selected from NISEE (PEER) online database. Distance from the source, magnitude of the event, time domain parameters (peak ground acceleration, PGA, peak ground velocity, PGV, and peak ground displacement, PGD), and the frequency content were considered while selecting the SGM records. Duration was not taken as a parameter since SHAKE 91 analyses are in frequency domain, thus are insensitive to duration.

Time and frequency domain parameters are listed in Table 3.3. Further information may be obtained from Appendix C.

Table 3.3. Properties of SGM records used in this study

Name of EQ	Station of record	M_w (mom.)	PGA (g)	PGV cm/s	PGD cm	Dominant Frequency (Hz)	Maximum Frequency (Hz)
L.Prieta	Piedmont Jr.	6.93	0.084	8.17	2.94	-	-
Landers	S. Valley	7.30	0.050	3.73	1.96	-	-
Northridge	LA	6.70	0.112	8.66	1.78	0-15	50
N.P.Springs	S. Valley	6.00	0.139	3.94	0.55	5-15	100
Kocaeli	Izmit	7.40	0.219	29.78	17.13	0-5	100
Northridge	L. Hughes #9	6.70	0.216	9.83	2.77	3-9	25
Northridge	S. Gab. –E	6.70	0.256	9.72	2.79	0-9	-
L.Prieta	USCS	6.93	0.311	12.49	5.93	-	-
Whittier	S. Gab. –E	6.00	0.303	22.80	3.33	1-5	25
Hector Mine	Hec	7.13	0.265	28.56	22.54	0-8	50
L.Prieta	S. Cruz	6.93	0.450	18.67	3.83	0-10	100
L.Prieta	Gilroy Array	6.93	0.411	31.57	6.35	0-15	100
L.Prieta	Los Gatos	6.93	0.420	73.51	20.04	0-3	50
C.Mendocino	Petrolia	7.01	0.589	48.14	21.92	0-5	25

3.1.2 Methodology Adopted

Within the confines of this study, site response analyses were performed by using SHAKE91 software. Existing analytical solutions of Wang (1993), Penzien (2000) and Huo (2006) were used to study all combinations based on previously discussed parameters. Additionally, finite element based soil-structure interaction analyses were also performed for cases where free-field relative deformation, obtained from 1-D site-response analyses, exceeds 1 mm. 1 mm have been chosen to represent the lowest limit beyond which the structure begins to respond. Finally, finite element and analytical solutions are compared, whenever it is possible.

It is important to note that while determining relative stiffness of soil with respect to structure, shear rigidity of the surrounding soil medium is the most

important parameter. As all analytical solutions are developed for uniform soil conditions, it is a very difficult task to estimate a representative shear modulus (G_{eq}) for non-uniform soil conditions. This study recommends a procedure for the determination of G_{eq}.

Finally, at the end of this chapter an empirical relationship is going to be presented for non-uniform soil media cases.

The basic methodology is as follows:

1. Site response analysis were performed by using SHAKE 9 to obtain free field racking deformation, Δ^{FF}_{max}, between depths corresponding to the roof and the ceiling slab of the structure,
2. Analytical racking methods were followed and corresponding $(\Delta_{SSI})^{WANG}$, $(\Delta_{SSI})^{PENZIEN}$, and $(\Delta_{SSI})^{HUO}$ were estimated by using an representative shear modulus value by using Equations 3.2 and 3.3.
3. If Δ^{FF}_{max}>1 mm then 2D Finite element analysis was performed following the simplified frame methodology.
4. Findings are compared and tabulated. An illustrative finite element run is presented in Appendix D.

3.2 Comparison of Finite Element (PLAXIS 9) Analysis Results with Analytical Solutions

3.2.1 Introduction of Representative Modulus

A representative shear modulus needs to be estimated for multi-layered soil profiles. Figure 3.5 presents an example soil profile through which an equivalent shear wave is propagating.

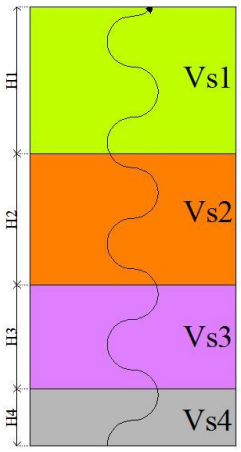

Figure 3.5. Equivalent shear wave velocity concept

In equivalent shear wave velocity concept, $V_{s,eq}$ is estimated by travel times as given in Equation 3.1.

$$\frac{\Sigma H}{Vs_{eq}} = \frac{H_1}{Vs_1} + \frac{H_2}{Vs_2} + \frac{H_3}{Vs_3} + \frac{H_4}{Vs_4} \tag{3.1}$$

As a particular case, for underground structures, rigidities of the layers surrounding the structure on the top and the bottom contributes most to the representative uniform shear rigidity. On the other hand, the thicknesses of the top and bottom layers have almost no effect on the representative modulus. Thus Equation 3.1 can be simplified to Equation 3.2.

$$\frac{2}{Vs_{eq}} = \frac{1}{Vs_{top}} + \frac{1}{Vs_{bot}} \tag{3.2}$$

Having determined the equivalent shear wave velocity, representative shear modulus (G_{rep}) can be calculated by using the following relation (Equation 3.3):

$$G_{rep} = Vs_{eq}^2 \times \rho_{eq} \quad (3.3)$$

Where;

G_{rep} : representative shear modulus

Vs_{eq} : equivalent shear wave velocity

ρ_{eq} : the equivalent density.

3.2.2 Comparison Between the Results of FEM and Analytical Methods

The use of Equation 3.2 and 3.3 together leads reasonable estimates of G_{eq} suitable to be used in PLAXIS 9 analyses.

In Figure 3.6, 3.7 and 3.8, racking coefficients determined by PLAXIS 9 analyses (R_{PLX}) are compared with available methods of Wang (1993), Penzien (2000) and Huo (2006), respectively.

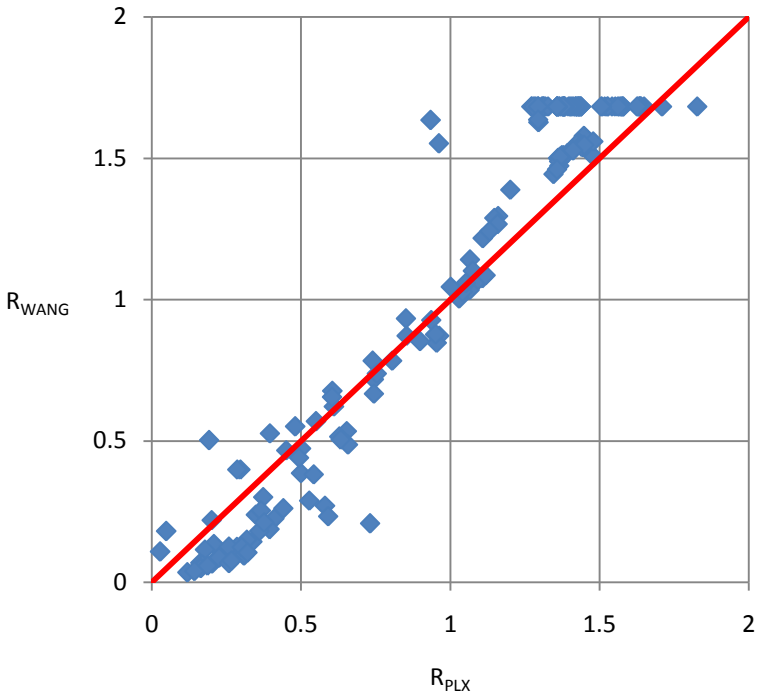

Figure 3.6. Comparison of FEM racking coefficients with Wang (1993)

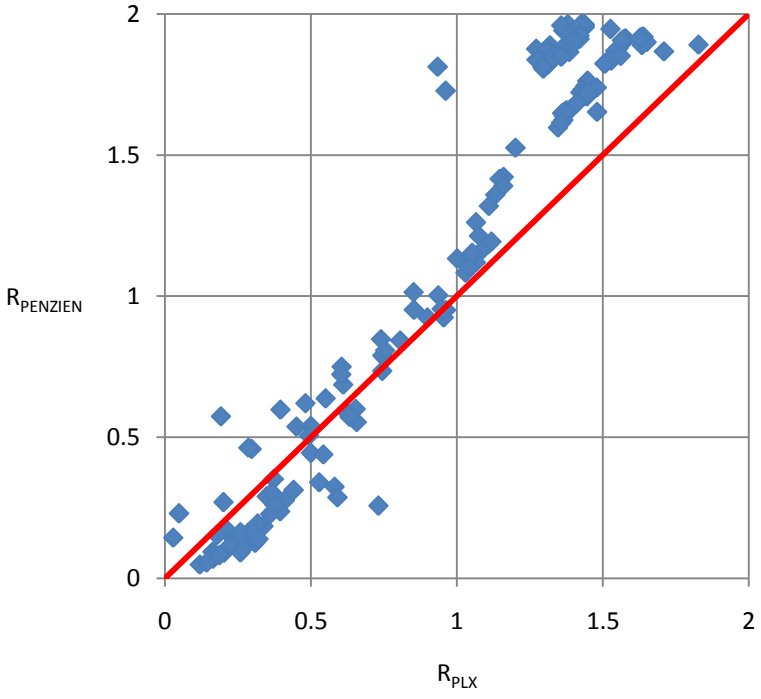

Figure 3.7. Comparison of FEM racking coefficients with Penzien (2000)

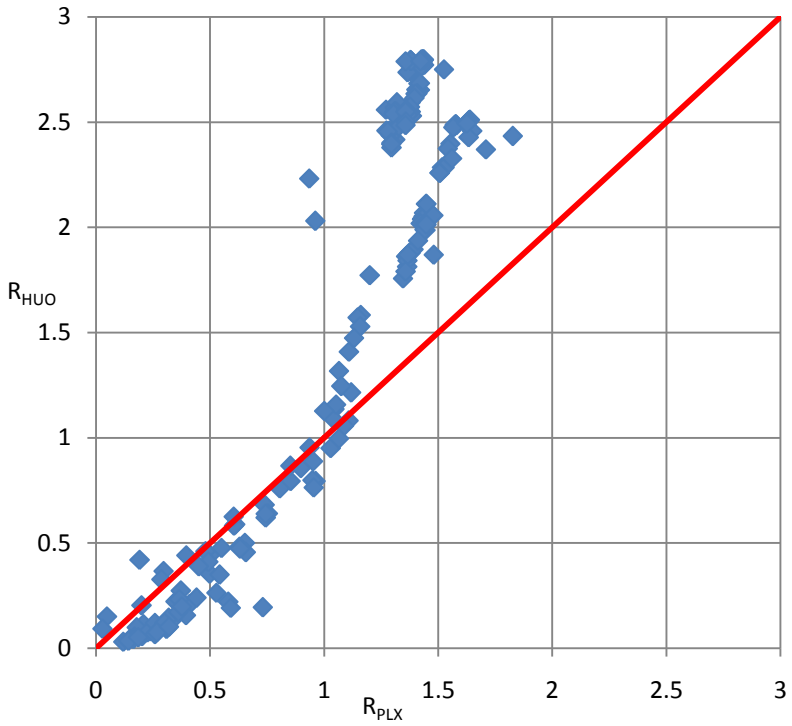

Figure 3.8. Comparison of FEM racking coefficients with Huo (2006)

For Flexibility Ratio (FR) < 1.0; all three methods seem to produce consistent results with FE assessments. However, for FR > 1.0, predictions by Huo et al. (2005), Penzien (2000), and Wang (1993) are 40%, 20%, and 10% higher than finite element analysis results.

Although analytical results obtained by methods of Wang (1993) and Penzien (2000) seem to be consistent with each other, they differ by about 10 to 15%. This is primarily because of the fact that, Wang (1993) recommends to reduce the racking ratios by a factor 1.10 in his study for rectangular structures; whereas, Penzien (2000) does not propose such a modification.

There is a notable difference between Huo et al. (2005) with Wang (1993) and Penzien (2000) for higher FR due to epistemic differences between these methods. As a racking force, different from two other methods, Huo et al. (2005) considers normal stresses in addition to shear stress along the structure,

as expected, normal stresses become more important as the rigidity of the soil increases. In fact, this difference is not very critical since with increasing rigidity of the surrounding soil, free field deformations become smaller. The displacement becomes so small that the amplified displacement can also be considered as negligible.

PLAXIS 9 solutions are observed to be in a good agreement with Wang (1993) and Penzien (2000). On the other hand, for flexibility ratios greater than unity, further magnification due to normal stresses offered by Huo et al. (2005) could not be observed in the FEM results.

All methods converge to similar results when the rigidity of soil decreases. In other words, as normal pressure of soil start to vanish, only uniform shear stress condition remains. A similar conclusion is also presented in Huo et al. (2005); as illustrated in Figure 3.9.

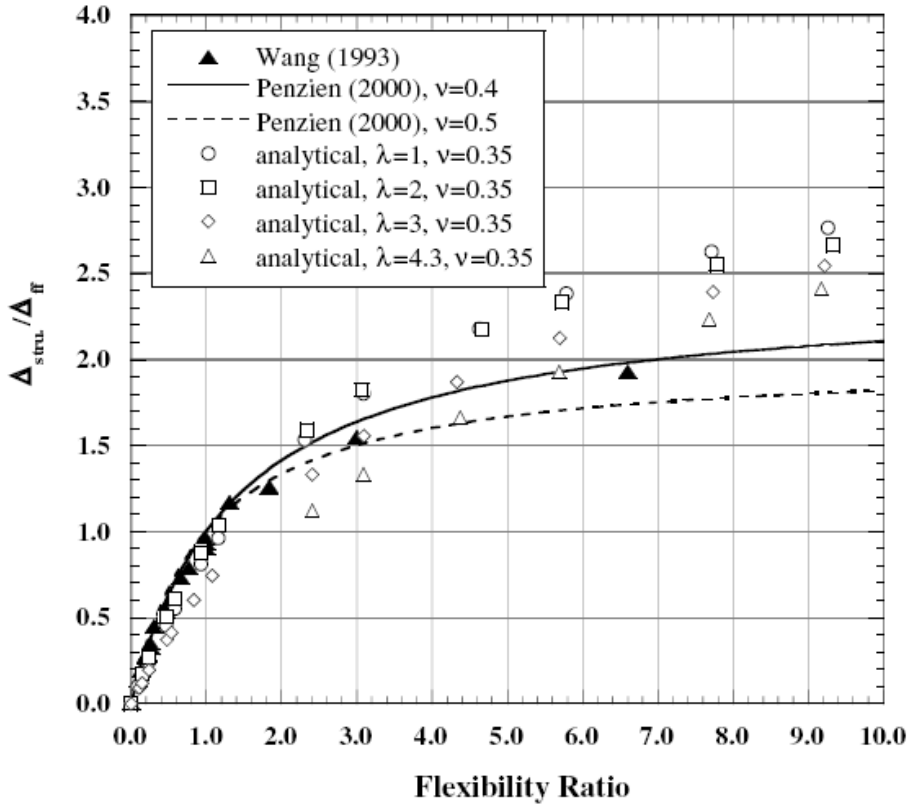

Figure 3.9. Comparison of Huo et al. (2005) with Wang (1993) and Penzien (2000) (Huo et al., 2006)

3.3 An Alternative SFA Method to Estimate Racking Deformation

Before discussing the proposed approach for the purpose of developing the racking relationship, the limit values and main assumptions that are used in this study will be discussed.

Flexibility ratio term is defined consistent with Penzien (2000), which makes use of the uniform shear stress assumption around the structure.

3.3.1 Main Assumptions

Followings are the major assumptions:

1. Plane strain conditions are valid around the underground structure.
2. Poisson ratio of the soil medium is very close to 0.5 to model incompressible soil media since earthquake loading is assumed to take place under undrained conditions.
3. Only shear forces are present around the structure. Uniform strain (thus stress) field assumption is valid.
4. Inertial effect of the lining is neglected.
5. No plastic deformation occurs in plastic hinge regions of the box girder.
6. Equivalent linear elastic shear modulus and damping are used as to represent the real cyclic degraded shear modulus and inelastic damping of soil.
7. Uncracked modulus of concrete has been used, i.e. lining remains elastic during an earthquake.

8. Flexibility ratio is calculated by using the method proposed by Penzien (2000). For this calculation, G_{eq} of the surrounding medium is calculated by using Equations 3.2 and 3.3.

In model development stage, the model uncertainty is also considered. For the purpose of developing an unbiased model, model error is assumed to be normally distributed with zero mean and standard deviation σ_ε .

3.3.2 Prediction of the Proposed Racking Curve

While developing a new formulation, FEM results obtained for NEHRP D and NEHRP C classes have been used by neglecting the extreme values from the analysis. Median values of the racking relationship (R) are assumed to have the mathematical form given in Equation 3.4.

$$R_{proposed} = \frac{\theta_1}{(\theta_2+\theta_3\times FR)} \times FR \tag{3.4}$$

The standard deviation of the model is observed to be a function of racking coefficient as follows:

$$\sigma_{proposed} = \theta_4 \times R_{proposed} \tag{3.5}$$

θ_1, θ_2, θ_3, and θ_4 were estimated by using maximum likelihood theory. Further information related to the framework of maximum likelihood method may be obtained from Çetin and Seed (2004).

Using maximum likelihood assessment for the determination of model coefficients, the flexibility ratio vs. racking coefficient relationship is estimated as defined in Equation 3.6.

$$R_{proposed} = \frac{2.214}{(1.01+1.41\times FR)} \times FR \tag{3.6}$$

Standard error term, $\sigma_{proposed}$, figures out to be as follows:

$$\sigma_{proposed} = 0.074 \times R_{proposed} \tag{3.7}$$

The proposed model presented in Equations 3.6 and 3.7 is drawn in Figure 3.10, along with $\pm 1\sigma_d$ uncertainty bands.

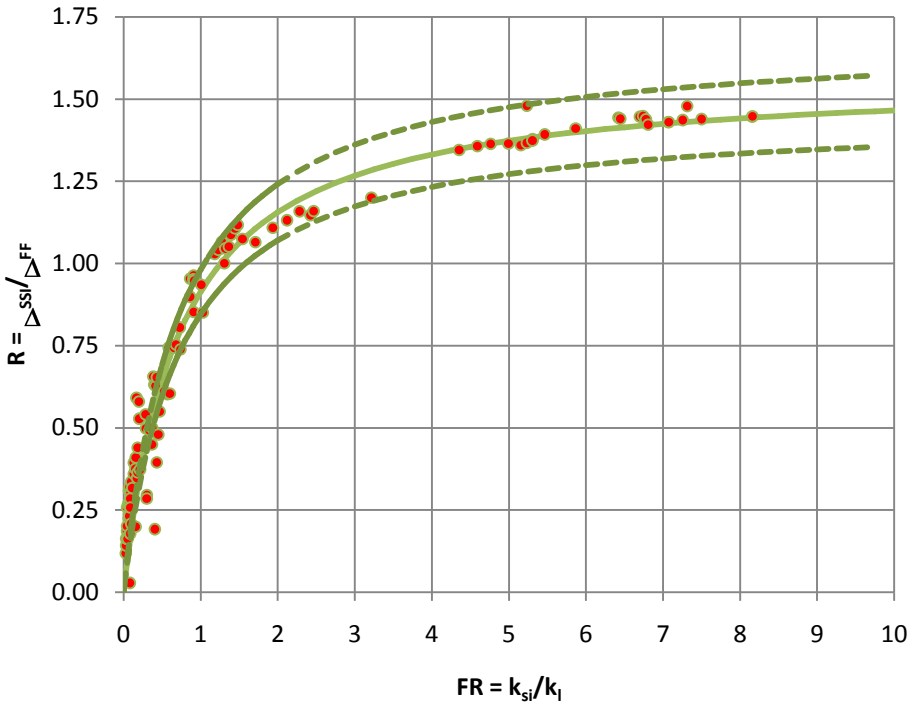

Figure 3.10. New racking curve plots showing mean ± one standard deviation bands

The results obtained from finite element analyses are compared with the model predictions in Figure 3.11. As revealed by this figure, the proposed model produces unbiased predictions with a quite high Pearson's Product (R^2) of 0.96 which is also an indication of the model success.

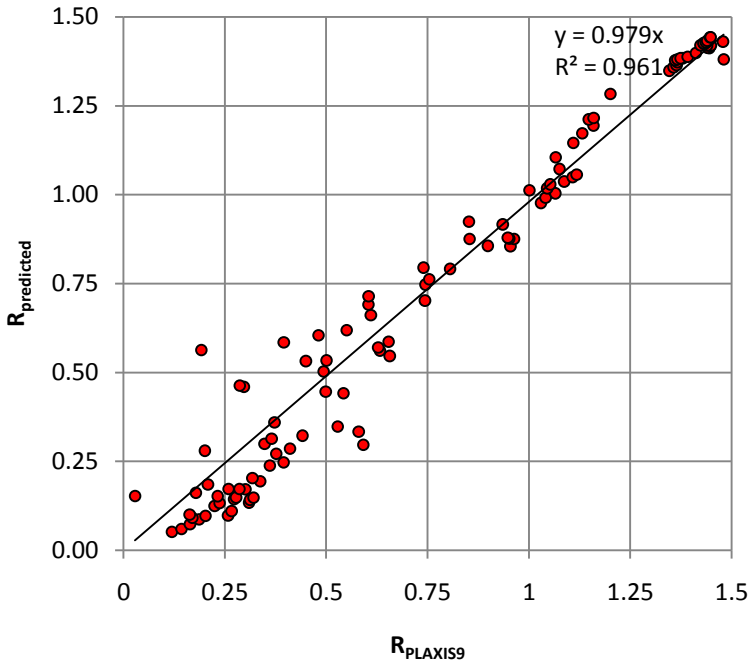

Figure 3.11. Comparison of racking coefficients of proposed model with finite element analyses

In the Figure 3.12, proposed median racking curve is compared with the curve obtained by Penzien's formulation (Penzien (2000)). As revealed by the figure Penzien's predictions are higher than FE based predictions in the range of FR greater than unity. Since Penzien approximates rectangular cavity deformation to be equal to circular cavity deformation, all values could be divided to nearly 1.10 to be compatible with Wang (1993)'s findings (Figure 3.13).

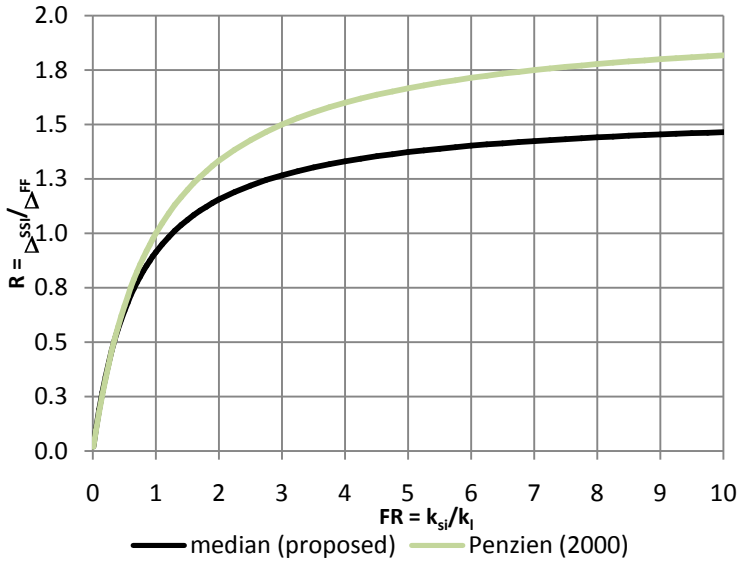

Figure 3.12. Comparison of proposed curve with Penzien (2000)

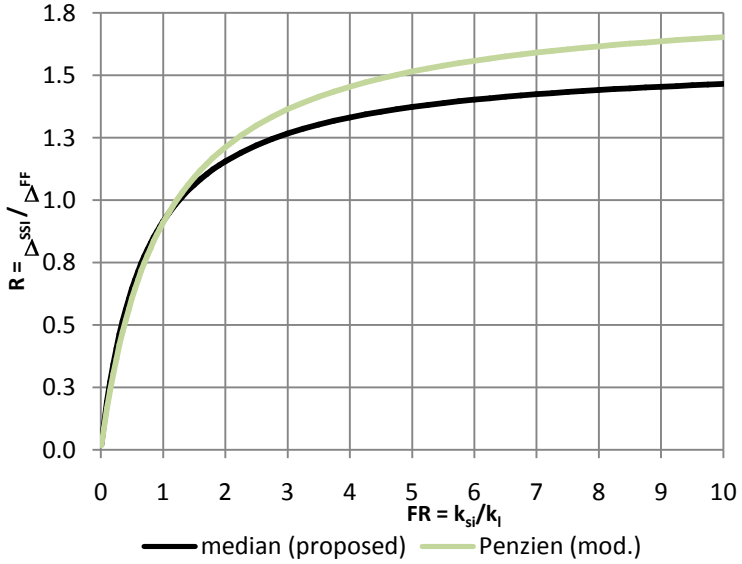

Figure 3.13. Comparison of proposed curve with Penzien (2000) modified racking relationship

CHAPTER 4

A SIMPLIFIED PROCEDURE FOR THE ESTIMATION OF FLEXIBILITY AND RACKING RATIOS

4.1 Background of the Method

Simplified frame analyses of buried structures have been carried out in a site and earthquake specific manner. However, for long pipelines or underground tunnels, performing site-specific analyses for all zones having different stratigraphy or seismic demand may be unpractical and cumbersome. Thus, a simplified procedure, based on nonlinear shear mass participation factor (r_d) concept, is introduced to cope with these difficulties and concerns. The proposed model is considered to produce unbiased preliminary assessment results for structures buried in heterogeneous soil formations in the longitudinal direction. However, it should be noted that proposed framework is suitable for preliminary assessment, and should never be used as a substitute to site and earthquake specific structural analyses.

4.1.1 The Theory of Nonlinear Shear Mass Participation Factor

Shear mass participation factor was first used by Seed and Idriss (1971) as a part of their simplified procedure and in time, Ishihara (1977), Iwasaki et al.

(1978), Imai et al. (1981), Golesorkhi (1989), and Çetin and Seed (2000) proposed alternative models.

4.1.1.1 Definition and the Methodology of the Method Proposed by Seed and Idriss (1971)

In their study, authors started the solution by calculating the maximum shear force of a rigid soil block having a unit weight of γ_{soil}, a height of h under a seismic event having maximum horizontal acceleration of a_{max} (Equation 4.1).

$$(\tau_{max})_{rigid\ body} = \gamma_{soil} \times h \times \frac{a_{max}}{g} \quad (4.1)$$

Where,

g : gravitational acceleration

h : height of the rigid block

γ_{soil} : unit weight of the soil layer

a_{max} : maximum ground acceleration (i.e. PGA)

Having determined the maximum shear force, $(\tau_{max})_{rgd}$, the rigid soil block experiences during seismic excitation, maximum shear stress in a deformable soil body is estimated by multiplying $(\tau_{max})_{rgd}$ by a factor called "Nonlinear Soil Mass Participation Factor" (r_d) so as to represent modal participation in the soil profile and non-linearity of the soil response, etc. (Equation 4.2).

$$\tau_{hv,max} = r_d \times (\tau_{max})_{rigid\ body} \quad (4.2)$$

By substituting Equation 4.1 into Equation 4.2, following expression is obtained (Equation 4.3).

$$\tau_{hv,max} = \frac{a_{max}}{g} \times \gamma_{soil} \times h \times r_d \quad (4.3)$$

As earthquake excitation is not harmonic and each loading cycle does not produce the same effect, a factor of 0.65 is used to represent the "equivalent uniform cyclic shear stress" (Equation 4.4).

$$(\tau_{hv})_{eq} = 0.65 \times \tau_{hv,max} \quad (4.4)$$

Having derived "equivalent uniform shear stress", "equivalent uniform cyclic stress ratio (CSR)" is obtained by normalizing "equivalent uniform cyclic stress" with initial effective overburden pressure, σ_v' (Equation 4.5).

$$CSR_{eq} = 0.65 \times \frac{a_{max}}{g} \times \frac{\gamma \times h}{\sigma_v'} \times r_d \quad (4.5)$$

Definition of the soil mass participation factor concept and values proposed by Seed and Idriss (1971) are schematically represented in Figure 4.1 and Figure 4.2, respectively.

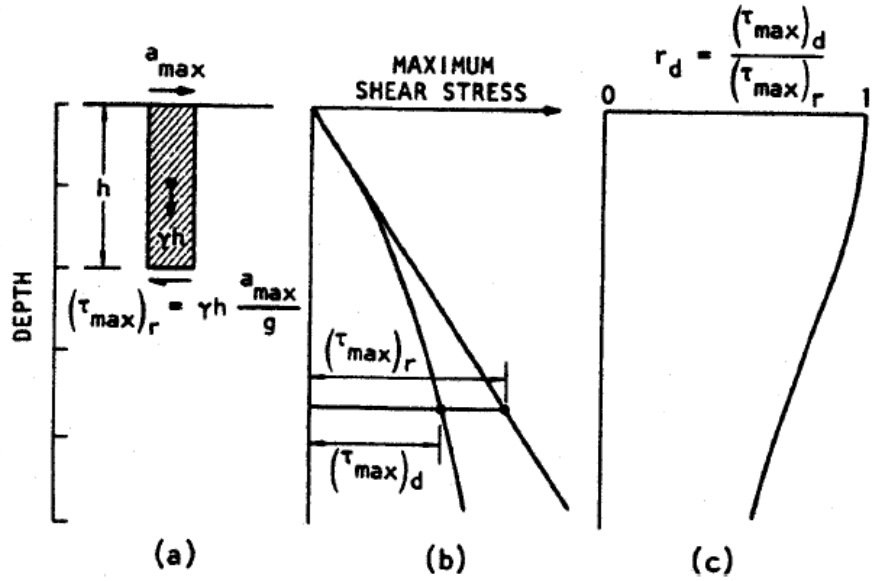

Figure 4.1. Definition of non-linear soil mass participation factor, r_d (Seed and Idriss, 1971)

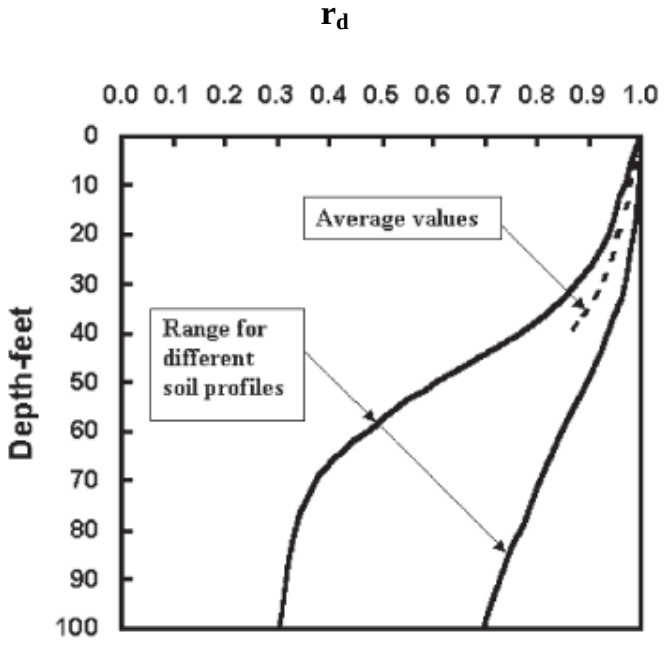

Figure 4.2. Illustration of shear mass participation (Seed and Idriss, 1971)

As mentioned previously, there exist alternative approaches (such as Ishihara (1977), Iwasaki et al. (1978), Imai et al. (1981), Golesorkhi (1989) to determine r_d; however the methodology defined by Çetin and Seed (2004) will be used and details of other approaches will not be reviewed. In their recent work, Çetin and Seed have compiled an extensive database and develop their correlations considering the uncertainties associated with the problem. These are the main reasons of selection of this method in further steps of this study. A brief review of this method will be given next.

4.1.1.2 Procedure Suggested by Çetin and Seed (2004)

In order to develop the correlation, Çetin and Seed (2000) performed 2153 site response analyses using 42 rock outcrop ground motions for 50 realistic soil profiles. The data has been processed probabilistically and the following models, which are sensitive to depth of the soil block, moment magnitude of the earthquake, peak ground acceleration, and equivalent shear wave velocity of top 12 m., have been proposed in Equations 4.6a and 4.6b for d<20 and d≥20 m, respectively.

If d < 20 m (~65 ft) Then

$$r_d\left(d, M_w, a_{max}, V^*_{s,12\ m}\right) = \frac{\left[1+\frac{-23.013-2.949\times a_{max}+0.999\times M_W+0.0525\times V^*_{s,12\ m}}{16.258+0.201\times exp^{0.341\times(-d+0.0785\times V^*_{s,12\ m}+7.586)}}\right]}{\left[\left[1+\frac{-23.013-2.949\times a_{max}+0.999\times M_W+0.0525\times V^*_{s,12\ m}}{16.258+0.201\times exp^{0.341\times(0.0785\times V^*_{s,12\ m}+7.586)}}\right]\right]} \mp \sigma_{\varepsilon_{r_d}} \quad (4.6a)$$

Else,

$$r_d\left(d, M_w, a_{max}, V^*_{s,12\ m}\right) = \frac{\left[1+\frac{-23.013-2.949\times a_{max}+0.999\times M_w+0.0525\times V^*_{s,12\ m}}{16.258+0.201\times exp^{0.341\times(-d+0.0785\times V^*_{s,12\ m}+7.586)}}\right]}{\left[\left[1+\frac{-23.013-2.949\times a_{max}+0.999\times M_w+0.0525\times V^*_{s,12\ m}}{16.258+0.201\times exp^{0.341\times(0.0785\times V^*_{s,12\ m}+7.586)}}\right]\right]} -$$

$$0.0046\times(d-20)\mp\sigma_{\varepsilon_{r_d}} \quad (4.6b)$$

Standard error terms of Equation 4.6a and Equation 4.6b are defined by Çetin and Seed (2004) as follows:

If d < 12 m (~40 ft) Then

$$\sigma_{\varepsilon_{r_d}}(d) = d^{0.850}\times 0.0198 \quad (4.7a)$$

If d>12 m or d=12 m Then

$$\sigma_{\varepsilon_{r_d}}(d) = 12^{0.850}\times 0.0198 \quad (4.7b)$$

In Figure 4.3, median values along with the uncertainty bands proposed by Çetin and Seed (2000) are illustrated.

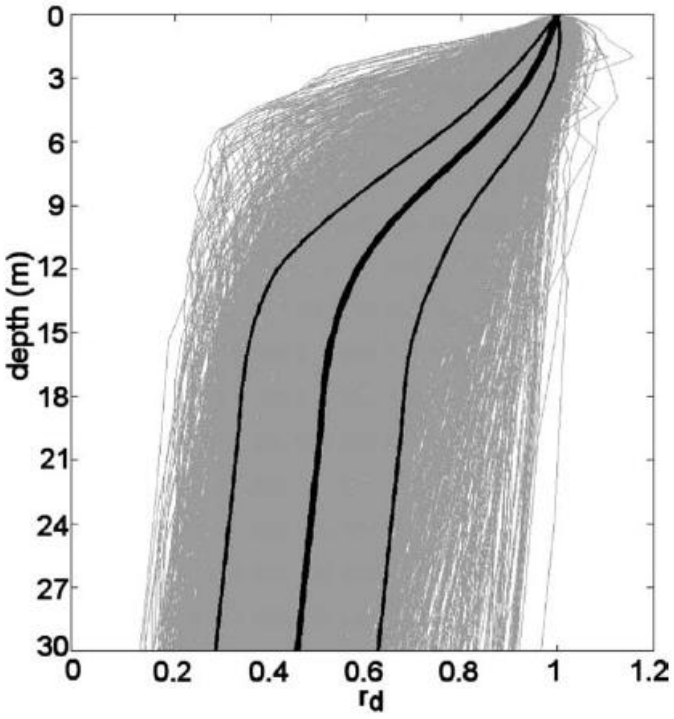

Figure 4.3. Illustration of median shear mass participation factor ± one standard deviation bands proposed by Çetin and Seed (2000) (Çetin and Seed, 2004)

4.1.2 Application of Participation Factor to Seismic Design of Buried Structures

4.1.2.1 Theory and the Methodology

By using Figure 4.3 or the proposed model given in Equations 4.6a and 4.6b, it is possible to estimate the mean value of seismically-induced maximum shear stress. Using the following simple relation, maximum shear strain can be estimated by the help of modulus degradation curves:

$$\gamma_{max} = \frac{\tau_{max}}{G_{eq}} \quad (4.8)$$

It is important to note that equivalent shear modulus is a function, of equivalent uniform shear stress (Equation 4.9a and Equation 4.9b).

$$\frac{G_{eq}}{G_{max}} = f(\gamma_{eq}) \quad (4.9a)$$

$$G_{max} = V_s^2 \times \rho_{soil} \quad (4.9b)$$

So as to relate equivalent shear strain to maximum shear strain, the author prefers to replace $(M_w\text{-}1)/10$ instead of constant value of 0.65 as defined in Equation 4.4 and recommended by Idriss (1992). The correlation between maximum cyclic strain and uniform equivalent cyclic strain is given in Equation 4.10.

$$\gamma_{eq} = \frac{(M_w - 1)}{10} \times \gamma_{max} \quad (4.10)$$

It can be inferred from Equations 4.8, 4.9, and 4.10 that if τ_{max} is known, γ_{max} and G_{eq} may be estimated by following an iterative procedure. For this purpose a computer code in Visual Basic Applications (VBA) is developed and presented in Appendix F.

The proposed simplified method for the determination of racking/ovaling deformations consists of the following steps;

- Estimation of τ_{max}, G_{eq}, and γ_{max} at a depth corresponding to the center of gravity of the structure.

- Flexibility ratio obtained by using Penzien's formulation under incompressible soil conditions as shown in Equation 4.11.

$$FR = \frac{k_{si}}{k_l} = \frac{{}^{G_{eq}}/_{H}}{k_l} \tag{4.11}$$

- Racking coefficient is then estimated by using the proposed racking relationship given in Equation 3.6 and 3.7.
- Free field deformation (Δ_{FF}) is calculated from Equation 4.12.

$$\Delta_{max}^{FF} = \gamma_{max} \times H \tag{4.12}$$

- Racking/ovaling deformation ($\Delta^{SSI}{}_{max}$) is calculated from Equation 4.13.

$$\Delta_{max}^{SSI} = R \times \Delta_{max}^{FF} \tag{4.13}$$

- By the application of $\Delta^{SSI}{}_{max}$ drift, structural response of the buried structure can be estimated.

4.1.2.2 Verification

Due to its strong dependence to the proposed model given on Çetin and Seed (2000), the author believes that the verification of the proposed method is

actually the verification of Çetin and Seed's model. Considering the success of Çetin and Seed's model, it is expected that the new simplified method is able to estimate flexibility ratios correctly in a mean sense. However, for the sake of completeness, the simplified method has been checked with SHAKE 91 results for 4 different soil profiles using 14 strong ground motions at 3 different depths.

4.1.2.2.1 Model Parameters

4.1.2.2.1.1 Soil profiles used in the verification

In the verification study, 4 different soil profiles have been used. 2 of them are selected to be composed of various layers; whereas, the rest are uniform profiles. In Tables 4.1, 4.2, 4.3, and 4.4; soil parameters are defined for Site A, B, C, and D respectively.

Table 4.1. Soil profile A and layering characteristics

Layer	Layer	H_i (m)	γ (kN/m^3)	V_s (m/s)
1	PI 15	1	17.3	244
2	PI 15	1	17.3	244
3	PI 15	1	17.3	244
4	Sand Av.	2	17.3	274
5	Sand Av.	2	17.3	274
6	Sand Av.	2	17.3	274
7	Sand Av.	2	17.3	290
8	Sand Av.	2	17.3	290
9	Sand Av.	2	18.1	290
10	Sand Av.	2	18.1	290
11	Sand Av.	2	18.1	320
12	Sand Av.	2	18.1	320
13	PI 30	2	18.1	320
14	PI 30	2	18.1	320
15	PI 30	2	18.1	320
16	PI 30	2	18.1	343
17	PI 30	2	18.1	343
18	PI 30	2	18.1	343
19	PI 30	2	18.1	343
20	PI 30	2	18.1	343
21	PI 50	2	18.1	381
22	PI 50	2	18.1	381
23	PI 50	2	18.1	381
24	PI 50	1	18.8	381
25	PI 50	1	18.8	381
26	PI 50	1	18.8	389
27	PI 50	1	18.8	389
28	PI 50	2	18.8	396
29	PI 50	2	18.8	396
30	PI 50	2	18.8	427
31	W. Rock	3	19.6	549
32	W. Rock	3	19.6	610
33	W. Rock	4	19.6	655
34	Rock		20.4	762

Table 4.2. Soil profile B and layering characteristics

Layer	Layer	H_i (m)	γ (kN/m^3)	V_s (m/s)
1	PI 30	2	17.4	150
2	PI 30	2	17.4	150
3	PI 30	2	17.4	150
4	PI 30	2	17.4	150
5	PI 30	2	17.4	150
6	PI 30	2	17.4	150
7	PI 30	2	17.4	150
8	PI 30	2	17.4	150
9	PI 30	2	17.4	150
10	PI 30	2	17.4	150
11	PI 30	2	17.4	200
12	PI 30	2	17.4	200
13	PI 30	2	17.4	200
14	PI 30	2	17.4	200
15	PI 30	2	17.4	200
16	PI 30	2	17.4	200
17	PI 30	2	17.4	200
18	PI 30	2	17.4	200
19	PI 30	2	17.4	200
20	PI 30	2	17.4	200
21	PI 30	2	17.4	225
22	PI 30	2	17.4	225
23	PI 30	2	17.4	225
24	PI 30	2	17.4	225
25	PI 30	2	17.4	225
26	PI 30	2	17.4	225
27	PI 30	2	17.4	225
28	PI 30	2	17.4	225
29	PI 30	2	17.4	225
30	PI 30	2	17.4	225
31	W. Rock	1	17.4	450
32	W. Rock	1	17.4	518
33	W. Rock	1	17.4	610
34	W. Rock	1	17.4	762
35	W. Rock	1	17.4	914
36	W. Rock	1	17.4	1067
37	W. Rock	1	17.4	1219
38	Rock		17.4	1219

Table 4.3. Soil profile C and layering characteristics

Layer	Layer	H_i (m)	γ (kN/m^3)	V_s (m/s)
1	Sand Av.	2	16.5	125
2	Sand Av.	2	16.5	125
3	Sand Av.	2	16.5	125
4	Sand Av.	2	16.5	125
5	Sand Av.	2	16.5	125
6	Sand Av.	2	16.5	175
7	Sand Av.	2	16.5	175
8	Sand Av.	2	16.5	175
9	Sand Av.	2	16.5	175
10	Sand Av.	2	16.5	175
11	Sand Av.	2	16.5	175
12	Sand Av.	2	16.5	175
13	Sand Av.	2	16.5	250
14	Sand Av.	2	16.5	250
15	Sand Av.	2	16.5	250
16	Sand Av.	2	16.5	351
17	Sand Av.	2	16.5	351
18	Sand Av.	2	16.5	351
19	Sand Av.	2	16.5	351
20	Sand Av.	2	16.5	351
21	Sand Av.	2	16.5	351
22	Sand Av.	2	16.5	351
23	Sand Av.	2	16.5	450
24	Sand Av.	2	16.5	450
25	Sand Av.	2	16.5	450
26	Sand Av.	2	16.5	450
27	Sand Av.	2	16.5	450
28	Sand Av.	2	16.5	450
29	Sand Av.	2	16.5	450
30	Sand Av.	2	16.5	450
31	W. Rock	1	16.5	450
32	W. Rock	1	16.5	518
33	W. Rock	1	16.5	610
34	W. Rock	1	16.5	762
35	W. Rock	1	16.5	914
36	W. Rock	1	16.5	1067
37	W. Rock	1	16.5	1219
38	Rock		16.5	1219

Table 4.4. Soil profile D and layering characteristics

Layer #	Layer	H_i (m)	γ (kN/m^3)	V_s (m/s)
1	PI 50	0.45	17.3	107
2	PI 50	0.45	17.3	110
3	Sand Av.	1.5	17.3	190
4	Sand Av.	1	17.3	200
5	Sand Av.	1	17.3	210
6	Sand Av.	3	17.3	230
7	Sand Av.	3	17.3	250
8	Sand Av	3	17.3	270
9	Gravel	2.6	18.8	350
10	Gravel	3	18.8	360
11	Gravel	3	18.8	375
12	Gravel	3	18.8	390
13	Gravel	3	18.8	400
14	Gravel	3	18.8	410
15	Gravel	3	18.8	425
16	Gravel	3	18.8	435
17	Gravel	3	18.8	450
18	W.Rock	5	19.6	500
19	W.Rock	5	19.6	550
20	W.Rock	5	19.6	650
21	W.Rock	5	20.4	700
22	Rock		20.4	750

4.1.2.2.1.2 Earthquake Records

Same records, discussed in previous sections, were used in the verification study. Details of these records are presented in Chapter 3.

4.1.2.2.1.3 Sample Depths

τ_{max} and γ_{max} were calculated at 3 depths of 4.4 m, 8.8 m, and 13.2 m for 4 soil profiles under 14 strong ground motions.

4.1.2.2.2 Results of the Verification of the Parameters

In order to assess the applicability of the proposed simplified approach, τ_{max} and γ_{max} values obtained from simplified iterative analyses were compared with SHAKE91 findings.

Maximum shear stresses obtained by the proposed methodology are compared with results of SHAKE91 analysis as shown in Figure 4.4. It can be concluded from this figure that the simplified method is in a fair agreement with SHAKE 91 results and produces unbiased estimates of induced shear stresses.

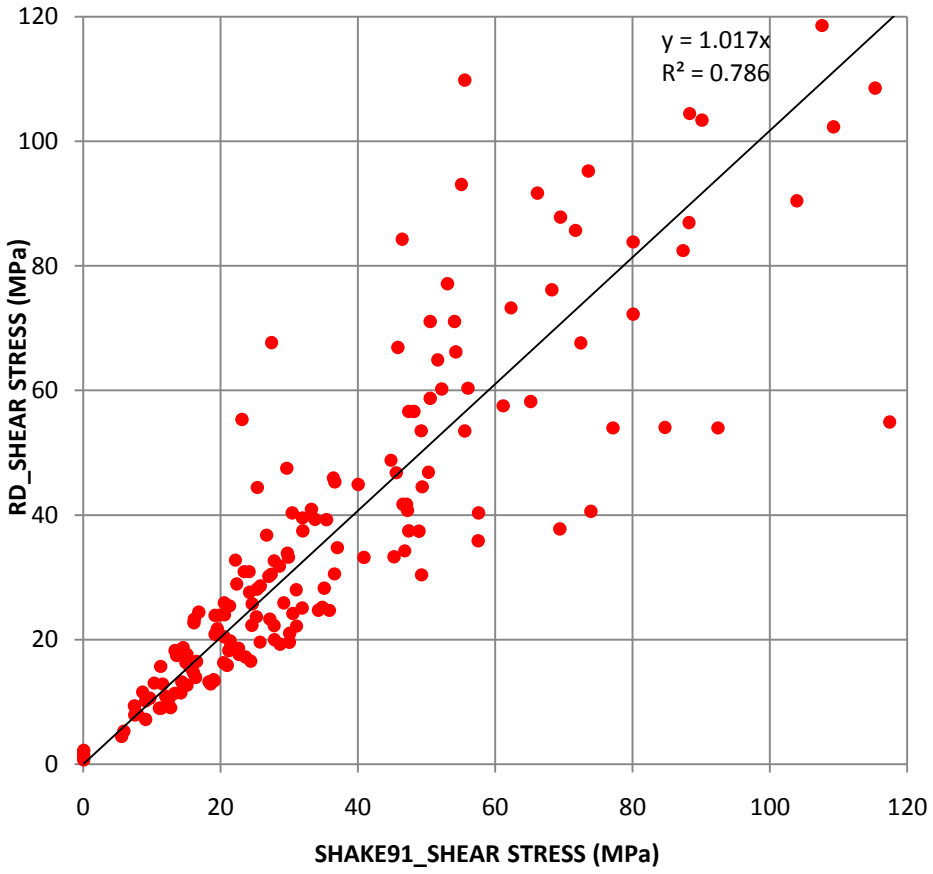

Figure 4.4. Comparison maximum shear stress obtained from SHAKE 91 analyses with the median predictions of simplified method

In Figure 4.5, the cyclic uniform shear strains obtained from SHAKE 91 are compared with cyclic uniform shear strains estimated by the simplified method. As expected, correlation of strains is not as well as correlation of stresses (has much higher scatter) due to the fact that an iterative solution has been carried out to find the best of the probable multiple roots of shear strain. However, as it can be observed from Figure 4.5 that application of the proposed method to determine shear strains still produces unbiased estimates and for cyclic uniform strains smaller than 0.2 – 0.5 %, the values obtained by the simplified method is in an acceptable agreement with SHAKE 91 results.

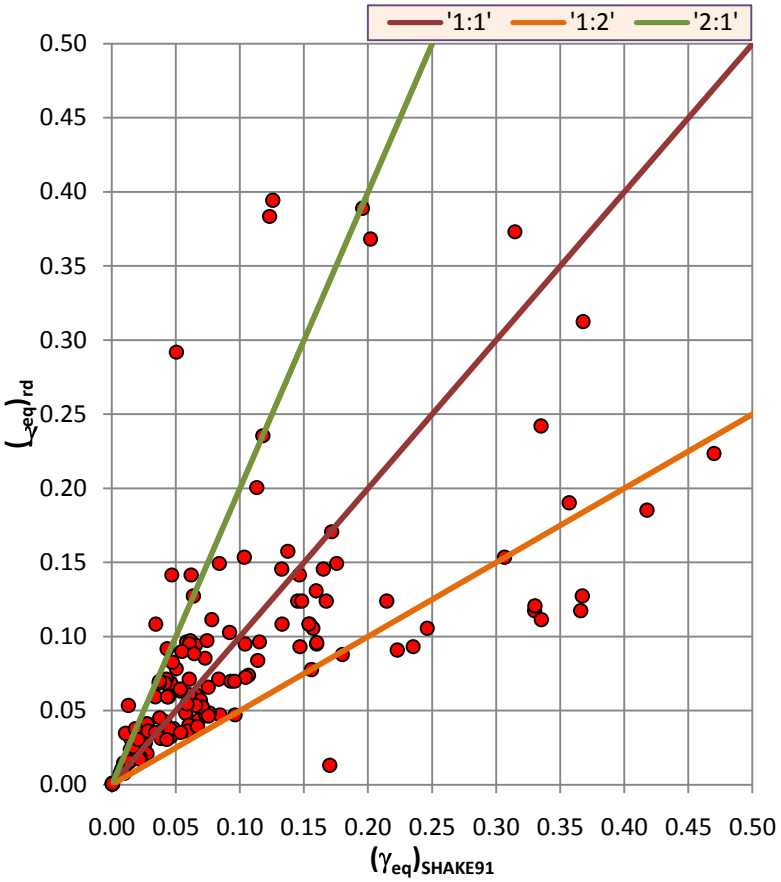

Figure 4.5. Comparison of cyclic uniform shear strain obtained by SHAKE 91 analyses with values estimated by simplified method

4.1.2.2.3 Limitations and Applicability of the Simplified Method

1. Proposed method predicts shear strains and shear stresses, thus equivalent moduli, in an unbiased manner. However, author still strongly recommends that this method should be used for pre-evaluation only since it may not fully model the participation of higher modes.

2. The scatter of the predictions by the simplified method increases as the strains increase. Thus, at medium to large strain ranges, the method becomes ineffective which is also valid for the other methods. Therefore, this method should be used with caution at medium to large strain levels.

CHAPTER 5

AN ALTERNATIVE STRUCTURAL ANALYSIS APPROACH

This chapter is dedicated to the development of an alternative methodology which also confirms the existing analytical solutions. The proposed methodology is applicable with any available commercial structural analysis software. The details of the proposed approach are explained via an illustrative example in the following sections of this chapter.

5.1 Introduction of the Alternative Method

The proposed methodology provides an alternative to existing analytical approaches and lets the user develop solutions for the problematic seismic analyses of buried structures by using any commercially available structural analysis software (Terzibaşoğlu, 2008-2009). The author believes that due to widespread use of structural analysis programs in design offices, the proposed methodology may draw attention of design engineers.

The proposed methodology will be explained via an illustrative example for the sake of clarification.

5.1.1 Steps for the Construction of Mathematical Model:

SAP2000 (CSI, 1995) structural analysis software was used for this illustrative example.

Steps to be followed are:

1. Definition of the Construction Material: Serviceability conditions seem to be the most important criterion in selection of construction material and the properties of the materials used in this example are presented in Table 5.1.

Table 5.1. Construction material properties

Material Name :	Concrete (Representative)	-
Material Type :	Concrete	-
Mass Per Unit Volume :	2.55	ton/m^3
Modulus of Elasticity :	30	GPa
Poisson's Ratio :	0.25	-

2. Definition of Geometry: Structural system is defined in regular manner. In Figure 5.1, an example of single bay and single span rectangular R/C box girder is presented.

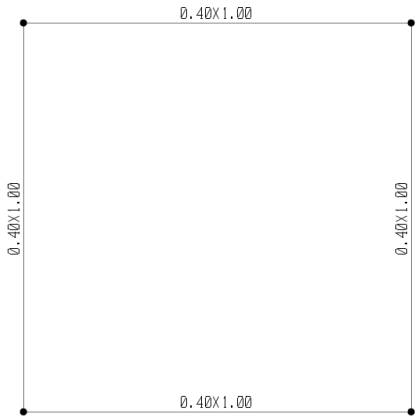

Figure 5.1. Structural system

3. Assignment of Structural Members: Structural members are assigned to the geometry defined in the previous step. Member properties are defined as presented in Table 5.2 and Figure 5.2.

Table 5.2. Cross-sectional properties of the section used in the example analysis

Cross-Sectional Area :	0.40	m^2
Moment of Inertia (I_x) :	0.0333	m^4
Moment of Inertia (I_y) :	5.33 E-3	m^4
Torsional Constant (J) :	0.016	m^4

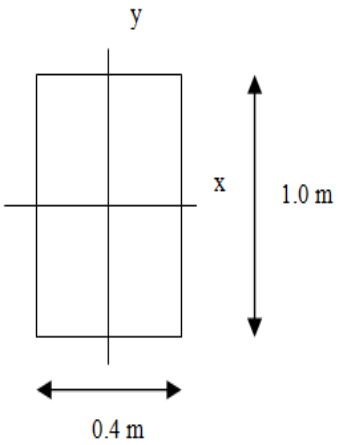

Figure 5.2. Cross-section of the structural members

3. Assignment of Loads: An initial constant distributed load, 1 kN/m, was applied to the top and bottom slabs of the structure as presented in Figure 5.3.

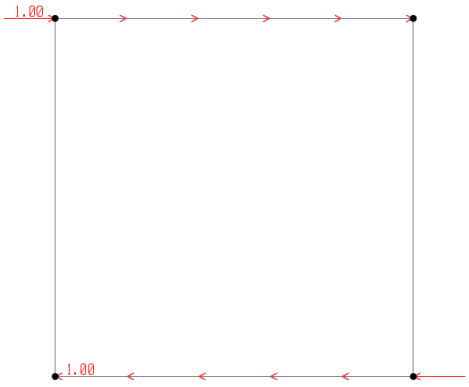

Figure 5.3. Assignment of initial loads to top and bottom slabs of the structure

4. Assignment of Soil Rigidities: Soil around the buried structure also contributes to the seismic response of the structure as discussed in Chapter 3. It was concluded that the shear rigidities of top and bottom layers have significant influence; whereas, soils located around side walls have negligible effect on the in phase seismic response of the structure. Thus, in the numerical model, equivalent linear springs were used to simulate the effects of soil rigidities at the top and bottom slabs. Equivalent spring constants are defined to be the functions of structure width (Figure 5.4, dimensions are in m), and shear rigidity of the surrounding soil as given in Equation 5.1.

$$k_{spring} = G_{eq} \times \mathrm{W/H} \tag{5.1}$$

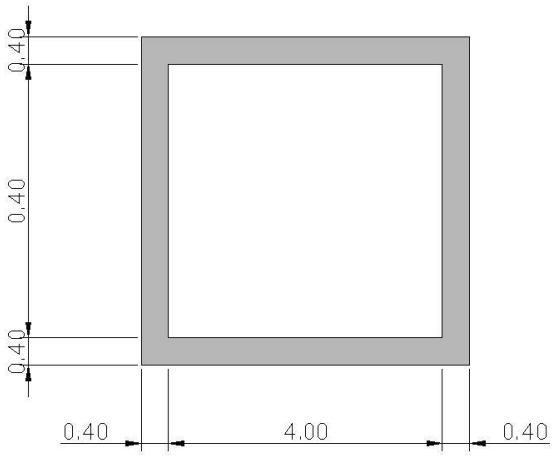

Figure 5.4. Structural system used in the illustrative example

For the selected example,

G_{eq} = 342049 kPa

W = 4.40 m

H = 4.40 m

Hence, k_{spring} = 342049 x 4.40 / 4.40 = 342049 kN/m

5. Spring coefficient, k_{spring}, is assigned to four corners of the structure as shown in Figure 5.5.

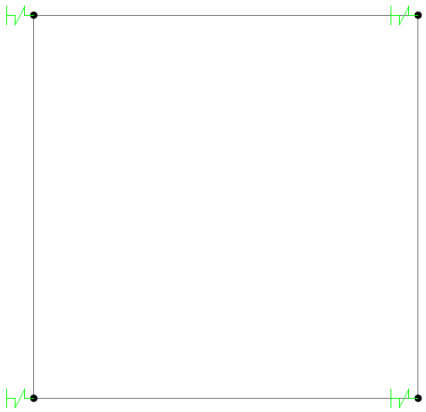

Figure 5.5. Definition of soil rigidities

6. Assignment of Restraints: Two vertical restraints, located at the bottom slab, are assigned to the nodes as they are required to maintain the stability (Figure 5.6).

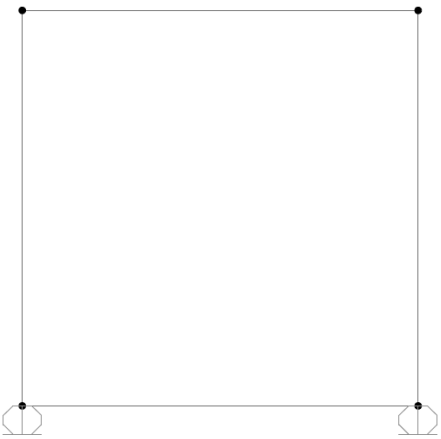

Figure 5.6. Assignment of vertical restraints

7. Having completed all the steps, an iterative procedure is followed to obtain deformation of the soil environment around the cavity, exact for circular section and slightly overconservative for rectangular type of sections, as shown in Equation 5.2 as recommended by Penzien and Wu (1998).

$$\Delta_{\max}^{\text{cavity}} = 4 \times (1 - \upsilon_{soil}) \times \Delta_{\max}^{\text{FF}} \qquad (5.2)$$

In this example,

Δ^{FF}_{max} = 1.79 mm.

υ_{soil} = 0.5

Δ^{cavity}_{max} = 4 x (1-0.5) x 1.79 mm = 3.57 mm.

a. In order to represent the cavity condition, bending rigidity of the structure has to be reduced to a very small value. Bending rigidities of the structure can be reduced by stiffness multipliers, or any other theoretically correct method. Moment of inertia of the structure is suggested to be decreased at least 1000 times of the real value.

b. After the bending stiffness of the structure is modified in proper manner, uniform distributed loading, as defined in Step 4, is applied in an iterative manner until the difference in deformation between the top and the bottom slabs converges to the value obtained from Equation 5.2.

c. By changing stiffness multipliers defined in Step 7a to unity, i.e. real structure is placed instead of the cavity, the same uniform distributed load is applied and racking deformation is obtained.

In this example,

$\Delta_{soil\text{-}structure}$ = 3.34 mm (very close to Penzien's value of 3.4 mm)

8. Soil structure interaction displacement should be exerted ***only*** on the structure, ***i.e. springs and loading should be removed from the model***, to determine the sectional forces.

5.1.2 Main Assumptions of the Proposed FEM Method

As part of this procedure,

1. Inertial effects are neglected,
2. Free-field deformation and equivalent linear shear modulus should be already determined by either performing equivalent linear site response analysis or using Simplified Procedure proposed in Chapter 4, and
3. Deformation of the cavity must be estimated so as to represent cavity conditions precisely.

CHAPTER 6

SUMMARY AND CONCLUSIONS

Within the confines of this thesis, seismic performance of buried single span and bay box type structures is assessed through site-earthquake and structure specific simplified frame analyses, as well as currently available methods of Wang (1993) and Penzien (2000) and Huo et al. (2005). Based on the results of simplified frame analyses, a new statistically-based relationship between flexibility ratio and racking coefficient is developed. As an input to the proposed procedure, seismically induced maximum shear stresses and strains and corresponding equivalent shear modulus are developed by a simplified iterative procedure as opposed to time consuming seismic site response analyses. It is shown that the proposed procedure and relationship produce unbiased estimates of racking coeffients, eliminating the need for lengthy numerical analyses for **preliminary design** of buried structures located in heteregenous soil and seismic environments. For structural engineers who are willing to tackle the problem by softwares lacking soil elements, an alternative assessment methodology attempting to model soil interaction through equivalent springs is also developed.

More specific conclusions of the thesis study are summarized as given below:

Compared with the finite element-based seismic soil-structure and earthquake interaction model predictions in the racking ratio (R) vs. flexibility ratio (FR) domain:

- Wang (1993), Penzien (2000) and Huo et al (2006) predictions are concluded to be consistent for FR values less than 1 (i.e: a laterally stiffer structure replaces the excavated soil).

- For FR values greater than 1 (i.e: a more flexible structure replaces the excavated soil) Wang (1993), Penzien et al. (2000) and Huo et al (2006) predictions are higher by 10 %, 20 % and 40 %, respectively. Thus, these methods are concluded to produce higher seismically-induced roof drifts.

Due to fact that Penzien (2000) solution is developed for circular sections, direct use of it for rectangular box type sections produce 10 to 15 % higher R values as compared to the predictions of Wang (1993).

Inspired from inconsistent predictions in the high FR range, an alternative simplified procedure is proposed. Analysis steps of this procedure are summarized in a flowchart in Appendix G (Figure G.1).

As presented in **Figure G.1**, the proposed simplified method in the preliminary analyses scheme eliminates 1-D seismic site response analyses (e.g.: SHAKE-91) and 2-D static numerical analyses (e.g. Plaxis) and still presented unbiased estimates of the response as discussed in Chapter 4. Major assumptions of the proposed procedure are: i) participation of higher modes do not contribute significantly at small to medium strain ranges, (ii) equivalent linear elastic shear modulus and damping are used to represent the real cyclic degraded shear modulus and inelastic damping of soil, (iii) inertial effects of both lining and the surrounding soil are not taken into consideration, (iv) no plastic deformation is modeled in structural members

For engineers, who are willing to tackle the problem by softwares lacking soil elements, an alternative assessment methodology, as summarized in **Figure G.1**, is developed. Major assumptions of the proposed procedure are: i) inertial effects are neglected and ii) deformation of the cavity must be estimated correctly to obtain realistic results.

Both of the proposed assessment methodologies are recommended to be used for only preliminary assessments and **should never** be perceived as a substitute to static and dynamic soil-structure-earthquake interaction models which may be required in the final design stage.

REFERENCES

AASHTO, American Association of State Highway and Transportation Officials, Standard Specifications of Highway Bridges, 17th Edition., Washington D.C., 2002.

AASHTO LRFD, American Association of State Highway and Transportation Officials, Standard Specification for Highway Bridges, 4th Edition., Washington D.C., 2007.

Bobet, A., Fernández, G., Huo, H., and Ramírez, J., A Practical Iterative Procedure to Estimate Seismic-Induced Deformations of Shallow Rectangular Structures, Canadian Geotechnical Journal, 2008.

Brinkgreve, R.B.J., Broere, W., and Waterman, D., General Information Manual for PLAXIS 2D v9.0, University of Delft and Plaxis BV, The Netherlands, 2008.

Charney, Dr. F. A., NONLIN: "An Educational Program for Learning the Concepts of Structural Dynamics and Earthquake Engineering, Advanced Structural concepts, Golden, Colorado and Schnabenl Engineering, Denver, Colorado.

Çetin K. Ö. and Seed R. B., Earthquake-induced nonlinear shear mass participation factor (r_d), Geotechnical Engineering Research Report No. UCB/GT-00/02, 2000.

Çetin K. Ö. and Seed R. B., Nonlinear shear mass participation factor (r_d) for cyclic shear stress ratio evaluation, Soil Dynamics and Earthquake Engineering Volume 24, Issue 2, February 2004, Pages 103-113, Elsevier, 2004.

Dowding, C.H., Rozen, A., Damage to rock tunnels from earthquake shaking, J. Geotech. Eng. Div., ASCE 104 (GT2)., 175-191, 1978.
Duke, C.M., Leeds, D.J., Effects of Earthquakes on Tunnels, Paper Presented at the RAND Second Protective Construction Symposium, March 24-26, 1959.

Ersoy, U., Özcebe, G., Betonarme, Evrim Dağıtım, İstanbul, 2001.

Golesorkhi R., Factors influencing the computational determination of earthquake-induced shear stresses in sandy soils, Dissertation submitted in partial satisfaction of the requirements for the degree of Doctor of Philosophy, University of California at Berkeley, 1989.

Hashash, Y.M.A., Hook, J.J., Schmidt, B., Yao, J.I., Seismic design and analysis of underground structures, Tunneling and Underground Space Technology 16, 247–293, 2001.

Hashash, Y.M.A., Tseng, W.S., Krimotat, A., Seismic soil-structure interaction analysis for immersed tube tunnels retrofit, Geotech. Earthquake Eng. Soil Mech. III 2, 1380 1391. ASCE Geotechnical Special Publication no. 75., 1998.

Hendron, A.J., Fernandez, G., Dynamic and static design considerations for underground chambers, In: Howard, T.R. (Ed.), Seismic Design of Embankments and Caverns. ASCE, New York, pp. 157–197, 1983.

Huo, H., Bobet, A., Fernández, G. and Ramírez, J., Load Transfer Mechanisms between Underground Structure and Surrounding Ground: Evaluation of the Failure of the Daikai Station, Journal of Geotechnical and Geoenvironmental Engineering, ASCE, Vol. 131, No. 12, pp. 1522-1533, 2005.

Idriss, I.M. and Sun, J.I., User's Manual for Shake-91. Richmond: University of California, 1992.

Imai, T., Tonouchi, K., Kanemori, T., The Simple Evaluation Method of Shear Stress Generated by Earthquakes in Soil Ground, Bureau of Practical Geological Investigation, Report No. 3, pp. 39-58, 1981.

Imbsen, R., Recommended LRFD Guidelines for the Seismic Design of Highway Bridges, Report Prepared to American Association of State Highway and Transportation Officials (AASHTO), Highway Subcommittee on Bridge and Structures. TRC/Imbsen & Associates, Inc., 2006.

Ishihara, K., Simple Method of Analysis for Liquefaction of Sand Deposits During Earthquakes, Soils and Foundations, Vol. 17, No. 3, September 1977, pp. 1-17, 1977.

Iwasaki, T., Tatsuoka, F., Tokida, K. I., Yasuda, S., A Practical Method for Assessing Soil Liquefaction Potential Based on Case Studies at Various Sites in Japan, Proceedings of 2nd International Conference on Microzonation for Safer Construction-Research and Application, Vol. II, San Francisco, California, November 1978, pp. 885-896., 1978.

Kaneshiro, J.Y., Power, M., Rosidi, D., Empirical correlations of tunnel performance during earthquakes and aseismic aspects of tunnel design, Proceedings of the Conference on Lessons Learned From Recent Earthquakes On Earthquakes in Turkey 1999, November 8 11, 2000.

Kiyomiya, O., Earthquake-resistant design features of immersed tunnels in Japan, Tunneling Underground Space Technol. 10 (4)., 463-475, 1995.

Kuesel, T.R., Earthquake Design Criteria for Subways, J. Struct. Div., ASCE ST6, 1213-1231, 1969.

Merritt, J.L., Monsees, J.E., Hendron, A.J., Jr., Seismic design of underground structures, Proceedings of the 1985 Rapid Excavation Tunneling Conference, vol. 1, pp. 104-131, 1985.

Mononobe, N., Matsuo, H., On The Determination of Earth Pressures During Earthquakes, Proceedings, World Engineering Congress, 1929.

Newmark, N.M., Problems in wave propagation in soil and rock, Proceedings of the International Symposium on Wave Propagation and Dynamic Properties of Earth Materials, 1968.

http://nisee.berkeley.edu., Website of National Information Service for Earthquake Engineering. PEER, NGA Strong Motion Database. Last Update: May 16, 2007. PEER, 1999. Last visited on: August, 7th, 2009.

Okabe, S., General theory on earth pressure and seismic stability of retaining wall and dam, Journal of Japan Society of Civil Engineers, Vol. 12, No. 1, pages 123 to 134, 1926.

Owen, G.N., Scholl, R.E., Earthquake engineering of large underground structures, Report no. FHWA RD-80 195. Federal Highway Administration and National Science Foundation, 1981.

Penzien, J., Seismically induced raking of tunnel linings, Earthquake Engineering and Structure Dynamics 29, 683–691, 2000.

Penzien, J., Wu, C.L., Stresses in linings of bored tunnels, Earthquake Engineering and Structure Dynamics 27, 283–300, 1998.

Power, M., Rosidi, D., Kaneshiro, J., Seismic vulnerability of tunnels-revisited, In: Ozedimir, L.,(Ed.). Proceedings of the North American Tunneling Conference. Elsevier, Long Beach, CA, USA, 1998.

Schmidt, B., Hashash, Y., Stimac, T., US immersed tube retrofit, Tunnels Tunneling Int. 30 (11)., 22-24, 1998.

Schnabel, P.B., Lysmer, J., Seed, B.H., SHAKE: a computer program for earthquake response analysis of horizontally layered sites, Report no. EERC 72 12. University of California, Berkeley, CA, USA, 1972.

Schnabel, P. B., Effects of Local Geology and Distance from Source on Earthquake Ground Motions, PhD Thesis, University of California, Berkeley, California, 1973.

Seed, H.B., Idriss, I.M.,, Soil moduli and damping factors for dynamic response analyses, Earthquake Engineering Research Center, Report No. EERC 70-10, University of California, Berkeley, California, 1970.

Seed, H. B., Idriss, I. M., Simplified Procedure for Evaluating Soil Liquefaction Potential, Journal of the Soil Mechanics and Foundations Division, ASCE, Vol. 97, No. SM9, September 1971.

Seed, H. B., Wong, R. T., Idriss, I. M., Tokimatsu, K., Moduli and Damping Factor for Dynamic Analyses of Cohesionless Soils, Geotechnical Engineering Report No. UCB/EERC-84/14, University of California at Berkeley, September 1984.

Sharma, S., Judd, W.R.,, Underground opening damage from earthquakes, Eng. Geol. 30, 263-276, 1991.

St. John, C.M., Zahrah, T.F.,, Aseismic design of underground structures, Tunneling Underground Space Technol. 2 (2)., 165 197, 1987.

Stevens, P.R., A review of the effects of earthquakes on underground mines, United States Geological Survey Open File Report 77 313, US Energy Research and Development Administration, Reston, VA, 1977.

Terzibaşoğlu, A., Personal communications, 2008-2009.

TS 500, Betonarme Yapıların Tasarım ve Yapım Kuralları, Türk Standartları Enstitüsü, Ankara, 2000.

Vucetic, M., Dobry, R., Effect of Soil Plasticity on Cyclic Response, Journal of Geotechnical Engineering, ASCE, Vol. 117, No. 1., 1991.
Wang, J.N., Seismic Design of Tunnels, Monograph 7, Parsons Brinckerhoff Quade & Douglas, Inc., 1993.

Wilson, E.L. And Habibullah, A., SAP 2000, Structural Analysis Program, Computer and Structures Inc., Berkeley, California, USA, 1995.

APPENDIX A

MODELLING PARAMETERS

In this appendix, modeling parameters of soil layers, used in Chapter 3, are going to be presented with relevant modulus degradadation and damping curves. These parameters include shear wave velocity plots and unit weight plots vs. depth. Phreatic level has not been taken into consideration in the analyses.

Soil Profiles :

Not degraded seismic properties of the soil profile B1 is indicated in Table A.1.

Table A.1. Initial properties of Site B1

B1				
Number	**Material**	**h_i (m)**	**γ (kN/m^3)**	**V_s (m /s)**
1	ROCK	1.00	17.44	594
2	ROCK	1.00	17.44	594
3	ROCK	1.00	17.44	594
4	ROCK	1.00	17.44	671
5	ROCK	1.00	17.44	671
6	ROCK	1.00	17.44	671
7	ROCK	1.00	17.44	671
8	ROCK	1.00	17.44	732
9	ROCK	1.00	17.44	732
10	ROCK	1.00	17.44	732
11	ROCK	1.00	17.44	792
12	ROCK	1.00	17.44	792
13	ROCK	1.00	17.44	792
14	ROCK	1.00	17.44	838
15	ROCK	1.00	17.44	838
16	ROCK	1.00	17.44	838
17	ROCK	1.00	17.44	914
18	ROCK	1.00	17.44	914
19	ROCK	1.00	17.44	991
20	ROCK	1.00	17.44	991
21	ROCK	1.00	17.44	1021
22	ROCK	1.00	17.44	1021
23	ROCK	1.00	17.44	1067
24	ROCK	1.00	17.44	1067
25	ROCK	1.00	17.44	1067
26	ROCK	1.00	17.44	1143
27	ROCK	1.00	17.44	1219
28	ROCK	1.00	17.44	1280
29	ROCK	1.00	17.44	1341
30	ROCK	1.00	17.44	1402
31	W. ROCK	30.00	17.44	1463

Not degraded seismic properties of the soil profile B2 is indicated in Table A.2.

Table A.2. Initial properties of Site B2

B2				
Number	**Material**	**h_i (m)**	**γ (kN/m^3)**	**V_s (m /s)**
1	ROCK	1.00	17.44	750
2	ROCK	1.00	17.44	750
3	ROCK	1.00	17.44	750
4	ROCK	1.00	17.44	750
5	ROCK	1.00	17.44	800
6	ROCK	1.00	17.44	800
7	ROCK	1.00	17.44	800
8	ROCK	1.00	17.44	800
9	ROCK	1.00	17.44	850
10	ROCK	1.00	17.44	850
11	ROCK	1.00	17.44	850
12	ROCK	1.00	17.44	850
13	ROCK	1.00	17.44	850
14	ROCK	1.00	17.44	850
15	ROCK	1.00	17.44	900
16	ROCK	1.00	17.44	900
17	ROCK	1.00	17.44	900
18	ROCK	1.00	17.44	900
19	ROCK	1.00	17.44	950
20	ROCK	1.00	17.44	950
21	ROCK	1.00	17.44	950
22	ROCK	1.00	17.44	950
23	ROCK	1.00	17.44	950
24	ROCK	1.00	17.44	950
25	ROCK	1.00	17.44	1000
26	ROCK	1.00	17.44	1000
27	ROCK	1.00	17.44	1000
28	ROCK	1.00	17.44	1000
29	ROCK	1.00	17.44	1100
30	ROCK	1.00	17.44	1100
31	ROCK	30.00	17.44	1100

Not degraded seismic properties of the soil profile C1 is indicated in Table A.3.

Table A.3. Initial properties of Site C1

C1				
Number	**Material**	**h_i (m)**	**γ (kN/m^3)**	**V_s (m /s)**
1	CLAY, PI = 15	1.00	16.97	396
2	CLAY, PI = 15	1.00	16.97	411
3	CLAY, PI = 15	1.00	16.97	427
4	CLAY, PI = 15	1.00	16.97	427
5	CLAY, PI = 15	1.00	16.97	442
6	CLAY, PI = 15	1.00	16.97	457
7	CLAY, PI = 15	1.00	16.97	488
8	CLAY, PI = 50	1.00	16.97	549
9	CLAY, PI = 50	1.00	16.97	579
10	CLAY, PI = 50	1.00	16.97	594
11	CLAY, PI = 50	1.00	16.97	625
12	CLAY, PI = 50	1.00	16.97	655
13	SAND, AV.	1.00	16.97	686
14	SAND, AV.	1.00	16.97	686
15	SAND, AV.	1.00	16.97	762
16	SAND, AV.	1.00	16.97	762
17	SAND, AV.	1.00	16.97	762
18	SAND, AV.	1.00	16.97	762
19	SAND, AV.	1.00	16.97	762
20	SAND, AV.	1.00	16.97	762
21	SAND, UP.	1.00	16.97	838
22	SAND, UP.	1.00	16.97	838
23	SAND, UP.	1.00	16.97	838
24	SAND, UP.	1.00	16.97	914
25	SAND, UP.	1.00	16.97	914
26	SAND, UP.	1.00	16.97	914
27	ROCK	1.00	16.97	1067
28	ROCK	1.00	16.97	1067
29	ROCK	1.00	16.97	1067
30	ROCK	1.00	16.97	1067
31	ROCK	30.00	16.97	1219

Not degraded seismic properties of the soil profile C2 is indicated in Table A.4.

Table A.4. Initial properties of Site C2

C2				
Number	**Material**	**h_i (m)**	**γ (kN/m^3)**	**V_s (m /s)**
1	CLAY, PI = 15	1.00	16.97	366
2	CLAY, PI = 15	1.00	16.97	366
3	CLAY, PI = 15	1.00	16.97	366
4	CLAY, PI = 15	1.00	16.97	396
5	CLAY, PI = 15	1.00	16.97	396
6	CLAY, PI = 15	1.00	16.97	396
7	CLAY, PI = 50	1.00	16.97	427
8	CLAY, PI = 50	1.00	16.97	427
9	CLAY, PI = 50	1.00	16.97	457
10	CLAY, PI = 50	1.00	16.97	457
11	CLAY, PI = 50	1.00	16.97	518
12	CLAY, PI = 50	1.00	16.97	549
13	SAND, AV.	1.00	16.97	610
14	SAND, AV.	1.00	16.97	610
15	SAND, AV.	1.00	16.97	610
16	SAND, UP.	1.00	16.97	686
17	SAND, UP.	1.00	16.97	686
18	SAND, UP.	1.00	16.97	732
19	SAND, UP.	1.00	16.97	732
20	SAND, UP.	1.00	16.97	762
21	SAND, UP.	1.00	16.97	762
22	SAND, UP.	1.00	16.97	762
23	SAND, UP.	1.00	16.97	808
24	SAND, UP.	1.00	16.97	808
25	SAND, UP.	1.00	16.97	838
26	SAND, UP.	1.00	16.97	838
27	ROCK	1.00	16.97	914
28	ROCK	1.00	16.97	914
29	ROCK	1.00	16.97	1067
30	ROCK	1.00	16.97	1067
31	ROCK	30.00	16.97	1219

Not degraded seismic properties of the soil profile D1 is indicated in Table A.5

Table A.5. Initial properties of Site D1

D1				
Number	**Material**	**h_i (m)**	**γ (kN/m^3)**	**V_s (m /s)**
1	GRAVEL	1.00	16.50	100
2	GRAVEL	1.00	16.50	100
3	GRAVEL	1.00	16.50	125
4	GRAVEL	1.00	16.50	125
5	GRAVEL	1.00	16.50	125
6	GRAVEL	1.00	16.50	150
7	SAND, AV.	1.00	16.50	175
8	SAND, AV.	1.00	16.50	200
9	SAND, AV.	1.00	16.50	225
10	SAND, AV.	1.00	16.50	250
11	SAND, AV.	1.00	16.50	275
12	CLAY, PI = 15	1.00	16.50	275
13	CLAY, PI = 15	1.00	16.50	300
14	CLAY, PI = 15	1.00	16.50	300
15	CLAY, PI = 30	1.00	16.50	325
16	CLAY, PI = 30	1.00	16.50	325
17	CLAY, PI = 30	1.00	16.50	350
18	CLAY, PI = 30	1.00	16.50	375
19	CLAY, PI = 30	1.00	16.50	400
20	CLAY, PI = 30	1.00	16.50	425
21	CLAY, PI = 30	1.00	16.50	450
22	CLAY, PI = 30	1.00	16.50	475
23	CLAY, PI = 30	1.00	16.50	500
24	CLAY, PI = 30	1.00	16.50	525
25	CLAY, PI = 30	1.00	16.50	550
26	CLAY, PI = 30	1.00	16.50	575
27	CLAY, PI = 30	1.00	16.50	600
28	ROCK	1.00	16.50	650
29	ROCK	1.00	16.50	650
30	ROCK	1.00	16.50	700
31	ROCK	30.00	16.50	750

Not degraded seismic properties of the soil profile D2 is indicated in Table A.6

Table A.6. Initial properties of Site D2

D2				
Number	**Material**	**h_i (m)**	**γ (kN/m^3)**	**V_s (m /s)**
1	GRAVEL	1.00	16.50	100
2	GRAVEL	1.00	16.50	100
3	GRAVEL	1.00	16.50	100
4	GRAVEL	1.00	16.50	100
5	GRAVEL	1.00	16.50	100
6	GRAVEL	1.00	16.50	100
7	SAND, AV.	1.00	16.50	125
8	SAND, AV.	1.00	16.50	150
9	SAND, AV.	1.00	16.50	150
10	SAND, AV.	1.00	16.50	175
11	SAND, AV.	1.00	16.50	175
12	CLAY, PI = 15	1.00	16.50	200
13	CLAY, PI = 15	1.00	16.50	225
14	CLAY, PI = 15	1.00	16.50	250
15	CLAY, PI = 30	1.00	16.50	300
16	CLAY, PI = 30	1.00	16.50	350
17	CLAY, PI = 30	1.00	16.50	400
18	CLAY, PI = 30	1.00	16.50	450
19	CLAY, PI = 30	1.00	16.50	500
20	CLAY, PI = 30	1.00	16.50	550
21	CLAY, PI = 30	1.00	16.50	575
22	CLAY, PI = 30	1.00	16.50	575
23	CLAY, PI = 30	1.00	16.50	575
24	CLAY, PI = 30	1.00	16.50	575
25	CLAY, PI = 30	1.00	16.50	575
26	CLAY, PI = 30	1.00	16.50	575
27	CLAY, PI = 30	1.00	16.50	600
28	ROCK	1.00	16.50	650
29	ROCK	1.00	16.50	700
30	ROCK	1.00	16.50	750
31	ROCK	30.00	16.50	800

Depth Plots :

Unit Weight Plots :

Unit weight distribution along the depth of the soil profile B1 is illustrated in Figure A.1.

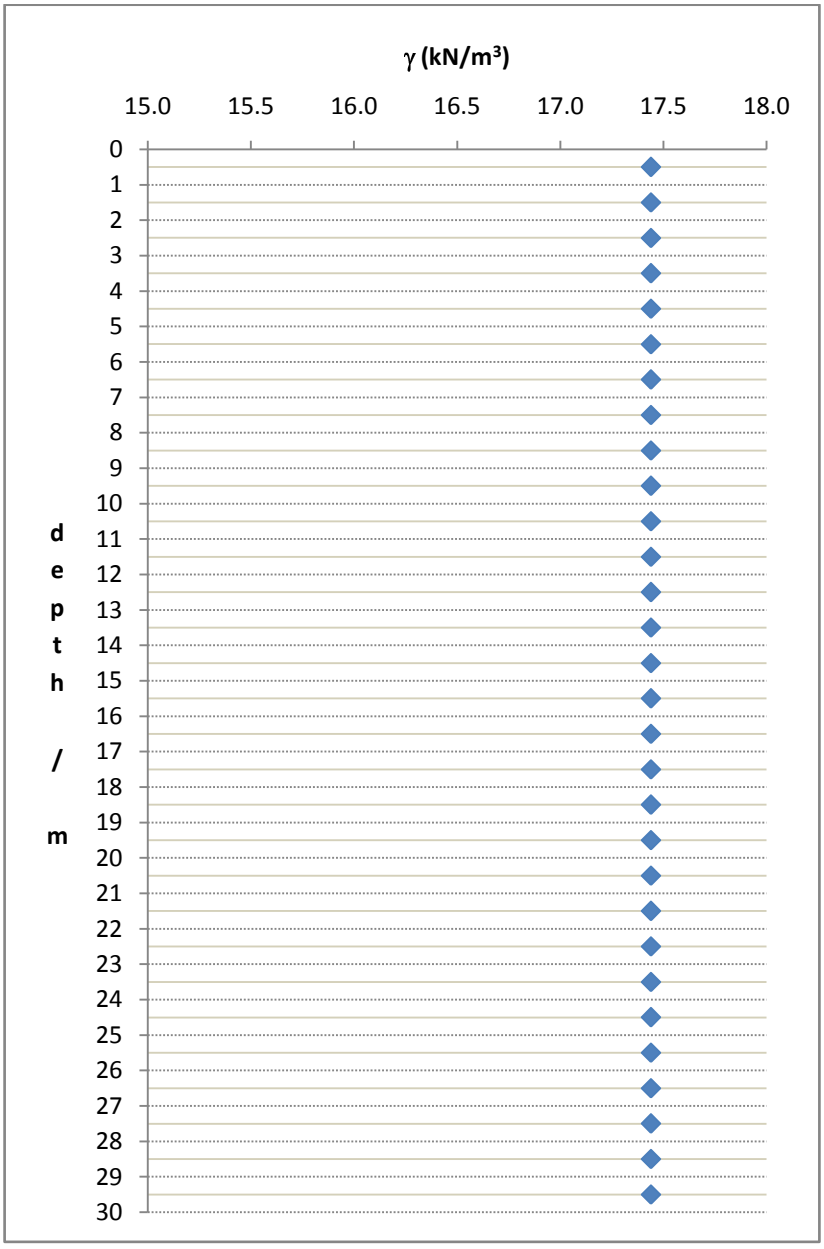

Figure A.1. Unit weight vs depth plot for the site B1

Unit weight distribution along the depth of the soil profile B2 is illustrated in Figure A.2.

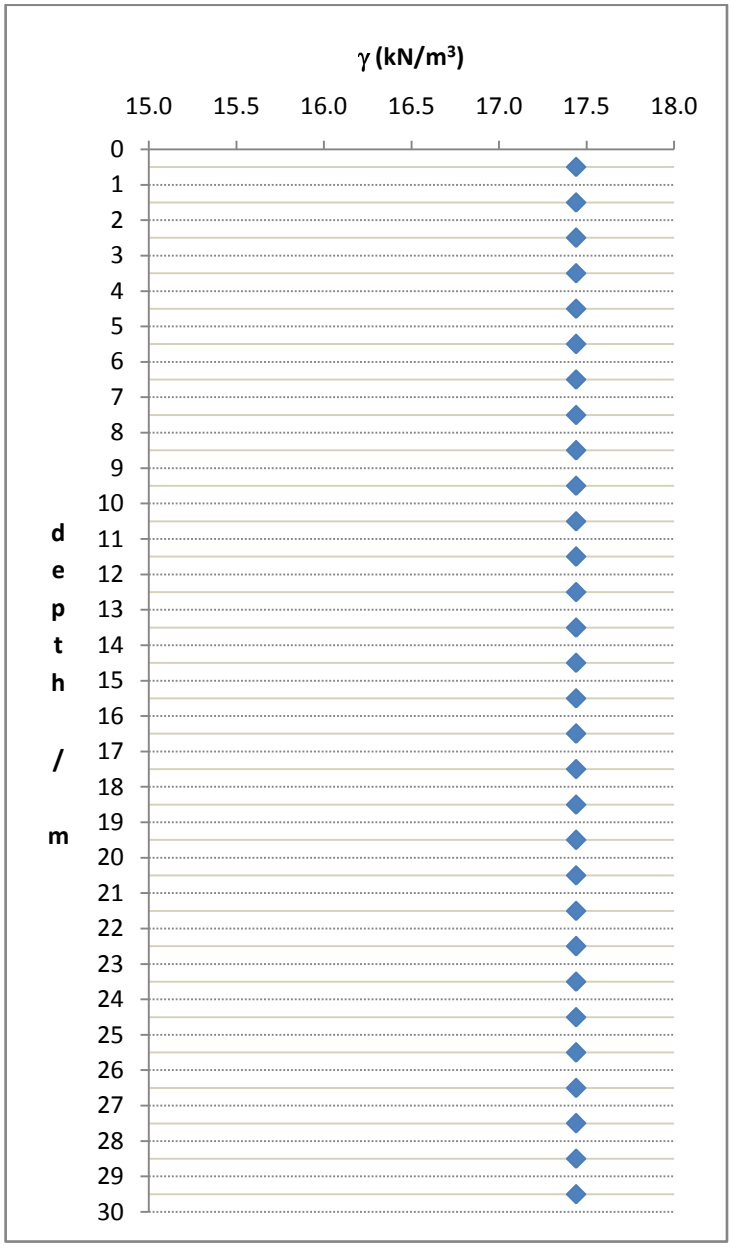

Figure A.2. Unit weight vs depth plot for the site B2

Unit weight distribution along the depth of the soil profile C1 is illustrated in Figure A.3.

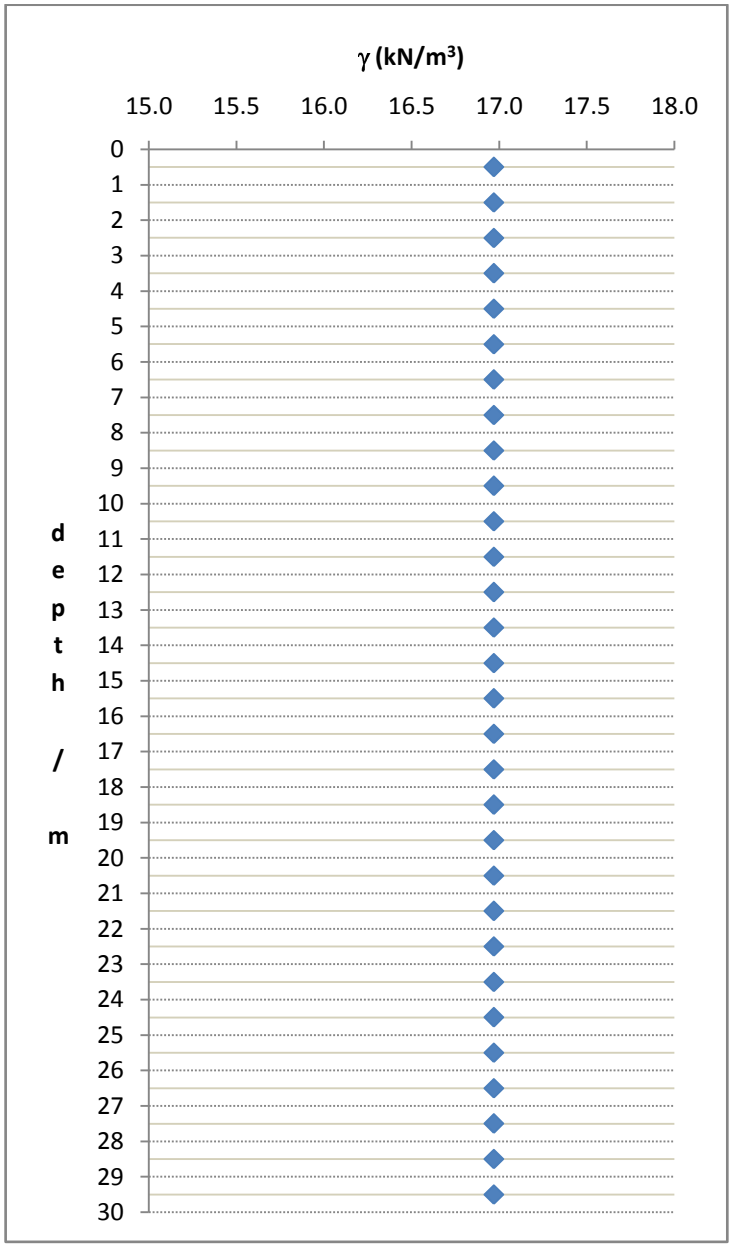

Figure A.3. Unit weight vs depth plot for the site C1

Unit weight distribution along the depth of the soil profile C2 is illustrated in Figure A.4.

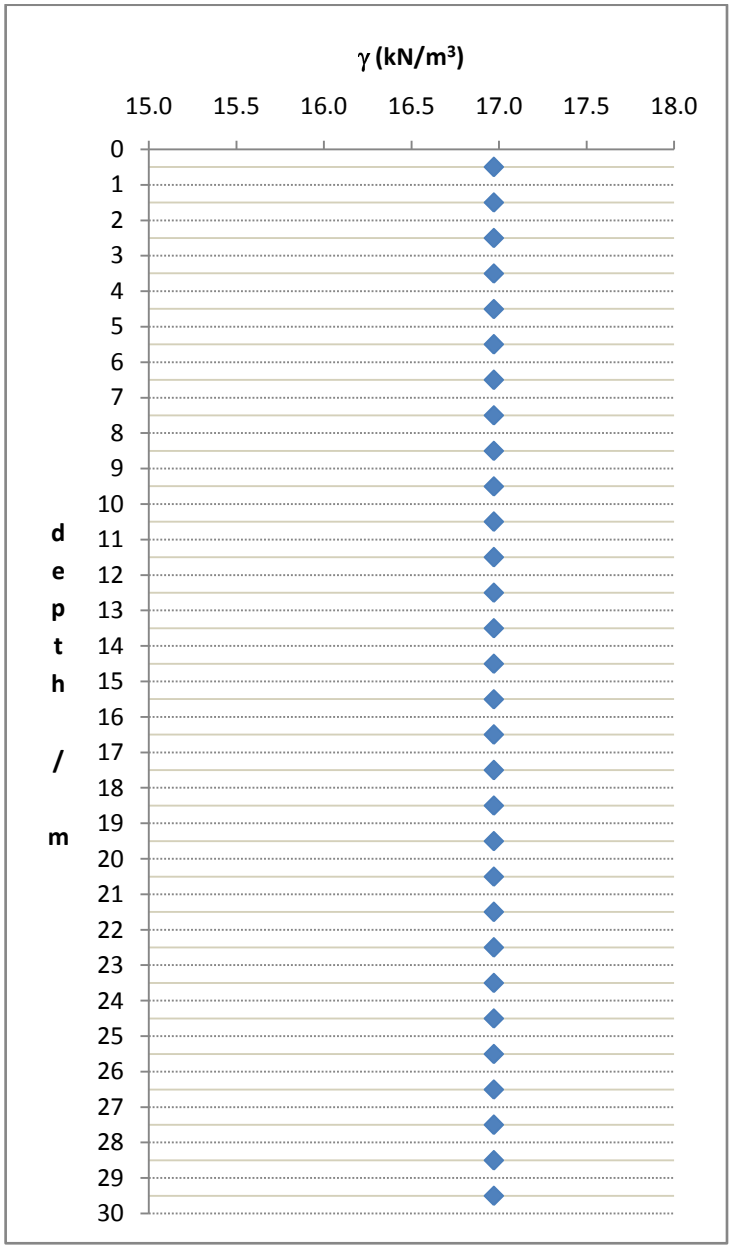

Figure A.4. Unit weight vs depth plot for the site C2

Unit weight distribution along the depth of the soil profile D1 is illustrated in Figure A.5.

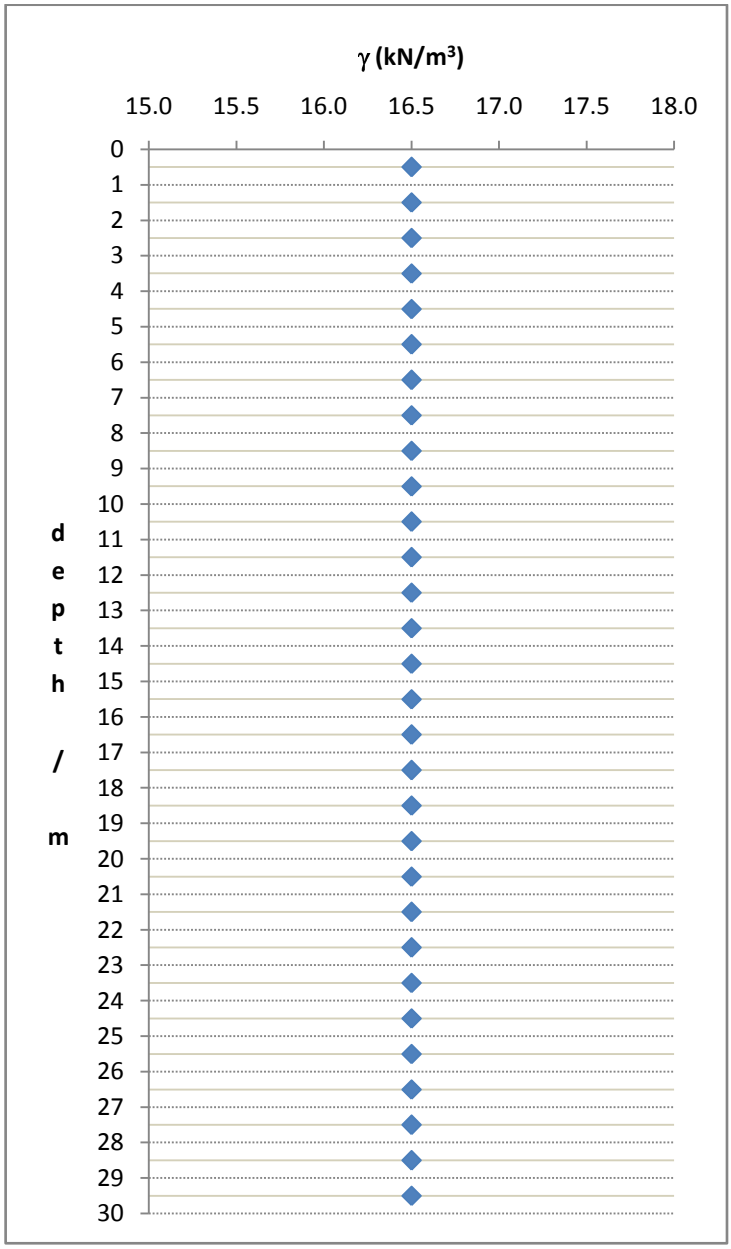

Figure A.5. Unit weight vs depth plot for the site D1

Unit weight distribution along the depth of the soil profile D2 is illustrated in Figure A.6.

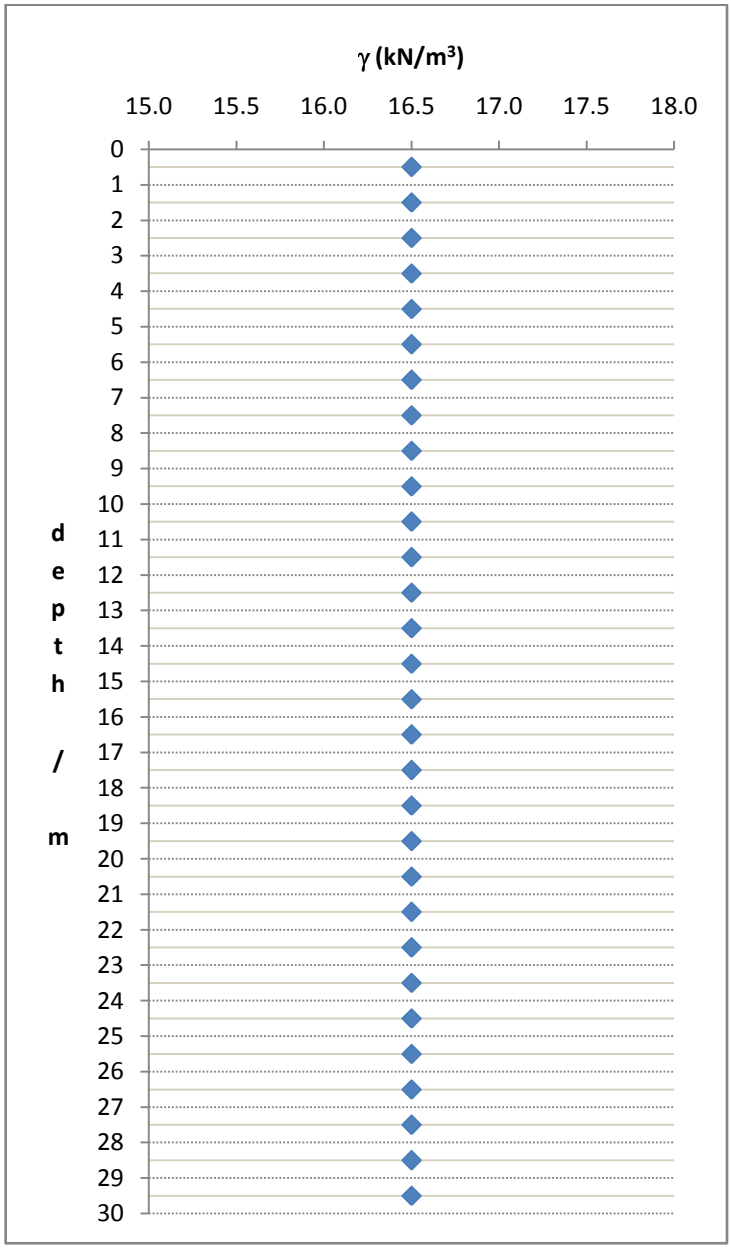

Figure A.6. Unit weight vs depth plot for the site D2

Shear Wave Velocity Plots :

Initial shear wave velocity distribution along the depth of the soil profile B1 is illustrated in Figure A.7.

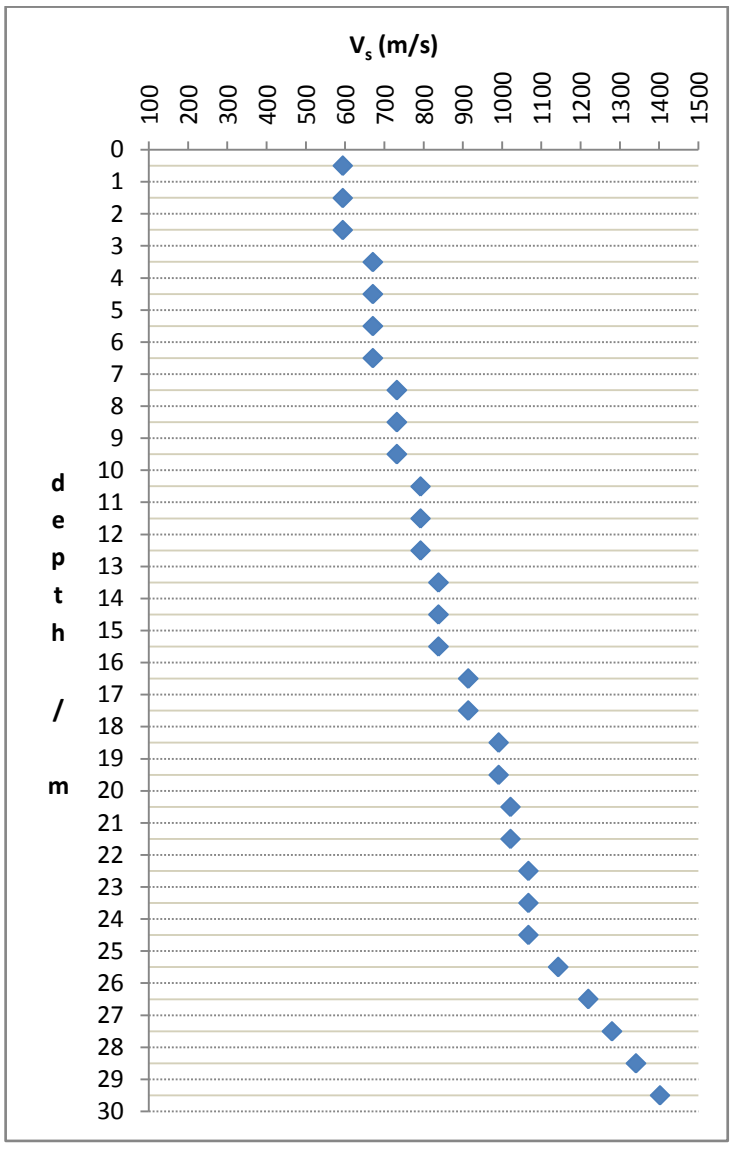

Figure A.7. Initial shear wave velocity vs depth plot for the site B1

Initial shear wave velocity distribution along the depth of the soil profile B2 is illustrated in Figure A.8.

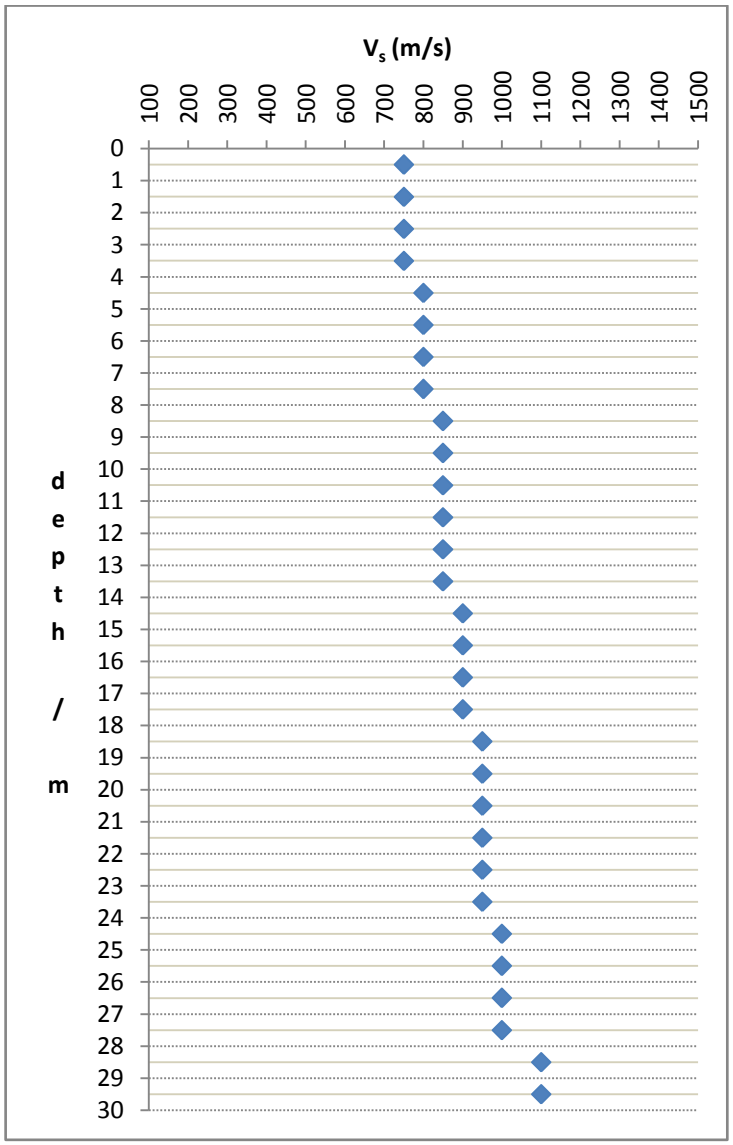

Figure A.8. Initial shear wave velocity vs depth plot for the site B2

Initial shear wave velocity distribution along the depth of the soil profile C1 is illustrated in Figure A.9.

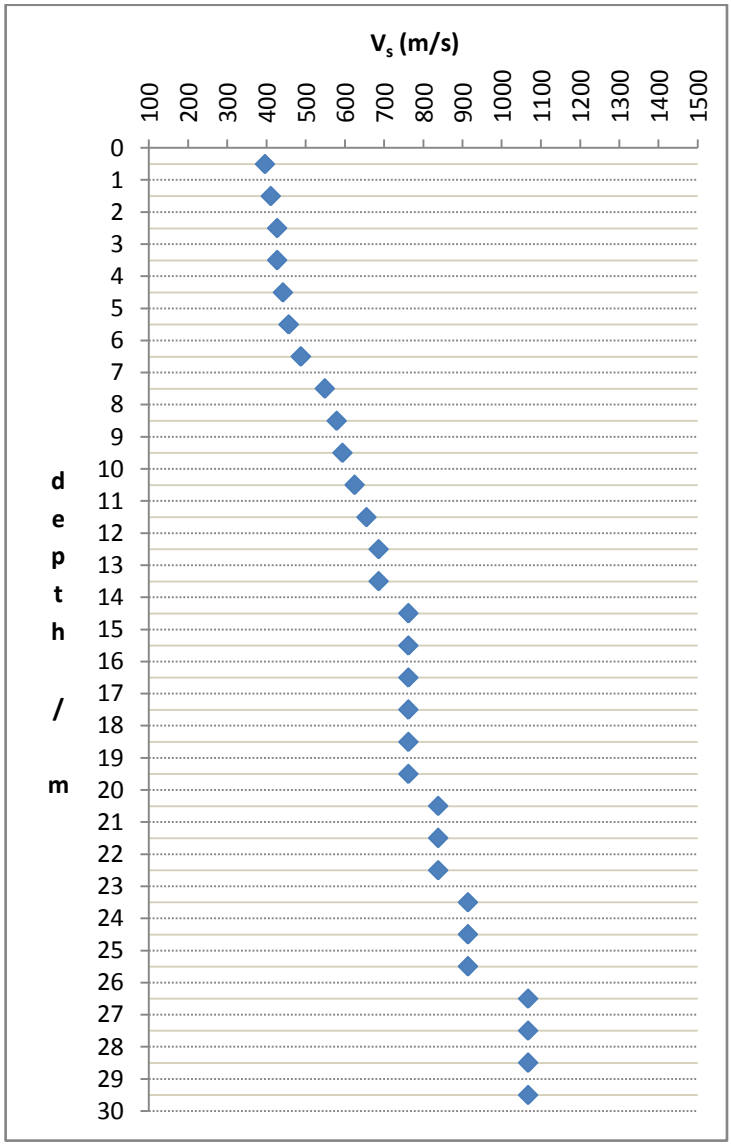

Figure A.9. Initial shear wave velocity vs. depth plot for the site C1

Initial shear wave velocity distribution along the depth of the soil profile C2 is illustrated in Figure A.10.

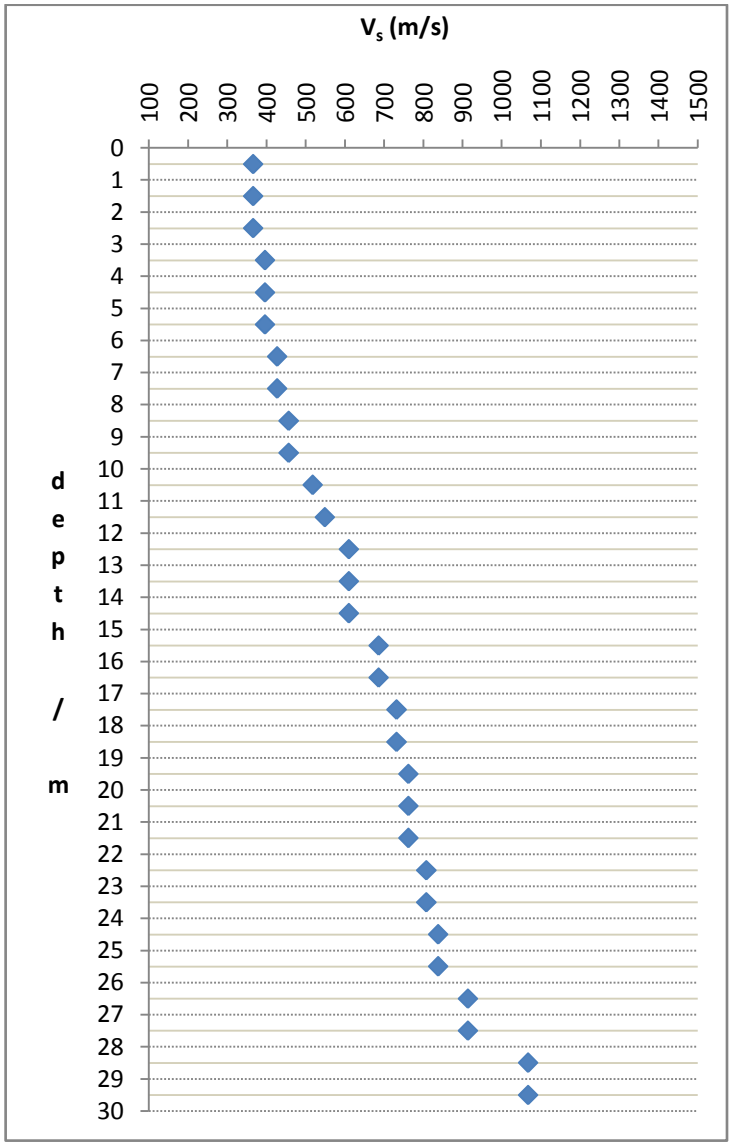

Figure A.10. Initial shear wave velocity vs. depth plot for the site C2

Initial shear wave velocity distribution along the depth of the soil profile D1 is illustrated in Figure A.11.

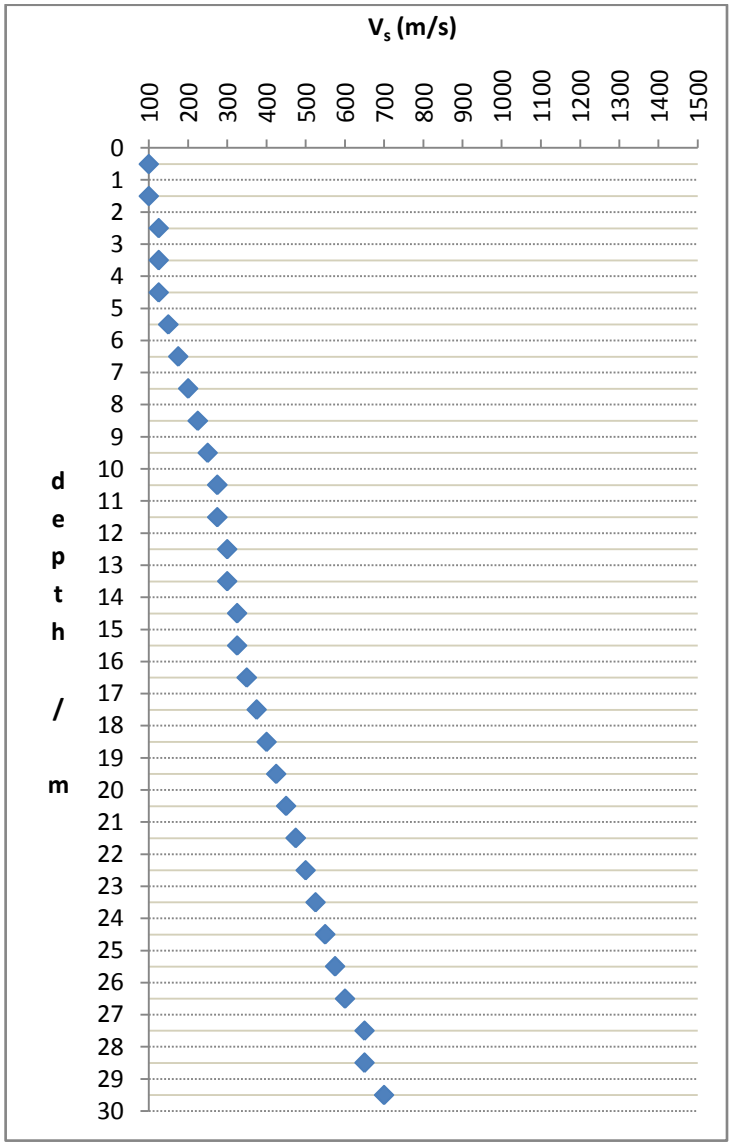

Figure A.11. Initial shear wave velocity vs. depth plot for the site D1

Initial shear wave velocity distribution along the depth of the soil profile D2 is illustrated in Figure A.12.

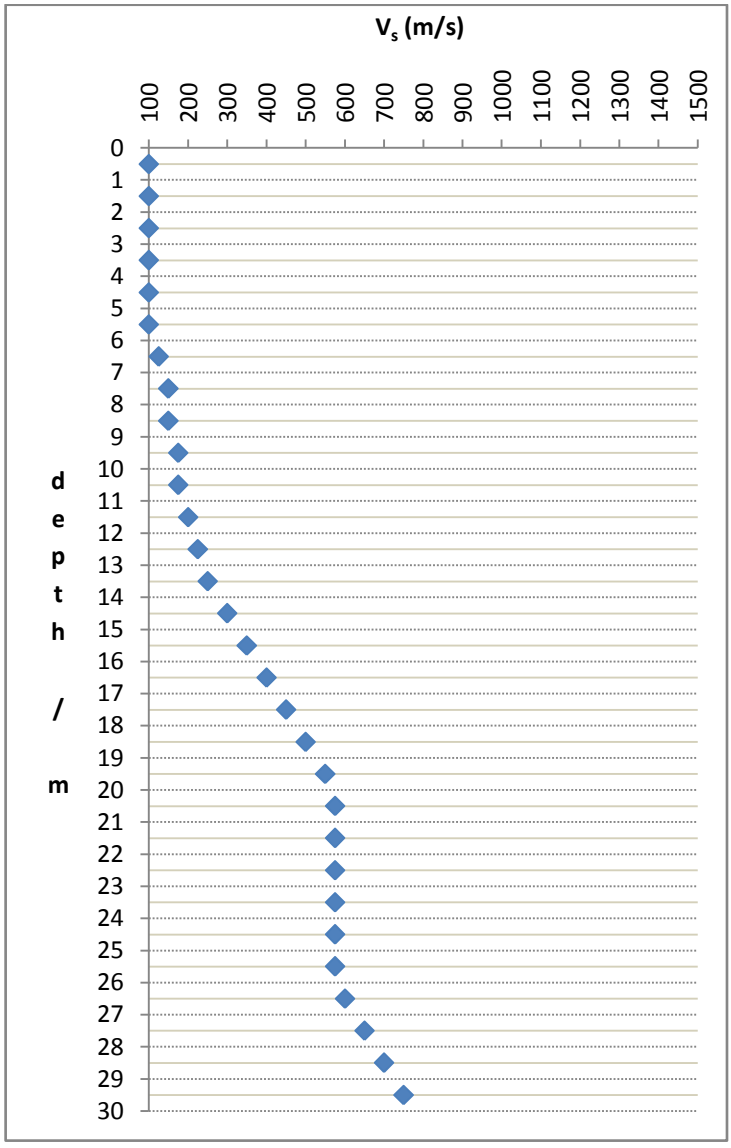

Figure A.12. Initial shear wave velocity vs. depth plot for the site D2

Modulus Degradation and Damping Curves Used In the Analyses :

Modulus degradation and damping relations with respect to cyclic uniform shear strain are listed in Table A.7.

Table A.7. Modulus Degradation and Damping Ratio Relationships

MATERIAL TYPE	MODULUS DEGRADATION RELATIONSHIP	DAMPING RATIO RELATIONSHIP
Rock	Schnabel (1973)	Schnabel (1973)
Clay, PI = 15	Vucetic and Dobry (1991)	Vucetic and Dobry (1991)
Clay, PI = 30	Vucetic and Dobry (1991)	Vucetic and Dobry (1991)
Clay, PI = 50	Vucetic and Dobry (1991)	Vucetic and Dobry (1991)
Clay, PI = 100	Vucetic and Dobry (1991)	Vucetic and Dobry (1991)
Gravel	Seed et al. (1988)	Seed et al. (1988)
Sand Low	Seed and Idriss (1970)	Seed and Idriss (1970)
Sand Av.	Seed and Idriss (1970)	Seed and Idriss (1970)
Sand Up.	Seed and Idriss (1970)	Seed and Idriss (1970)

Plots of the Modulus Degradation and the Damping Ratio Curves:

Rock (Schnabel (1973))

Modulus degradation curve and damping ratio curve proposed by Schnabel (1973) for rock layers are demonstrated in Figure A.13 and A.14, respectively.

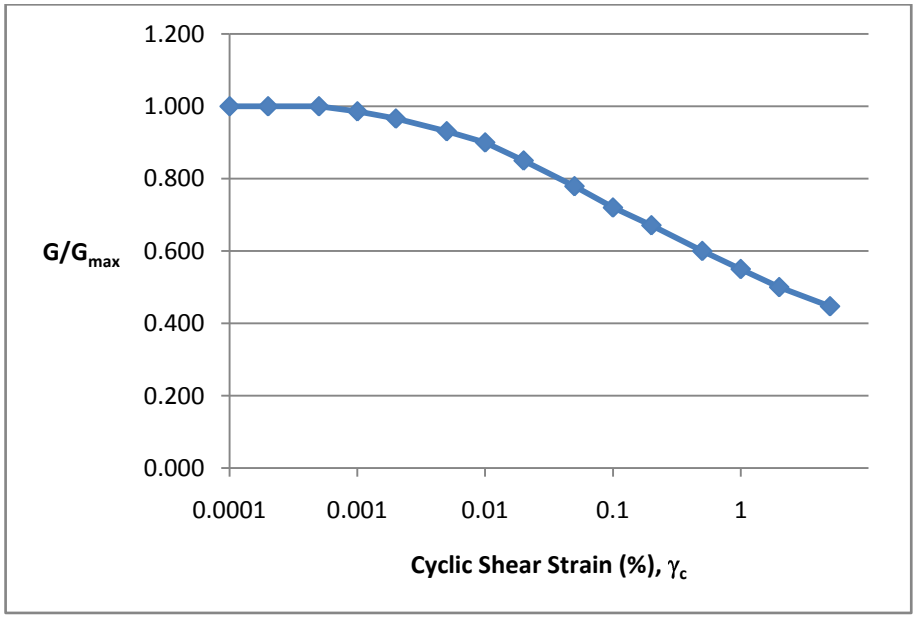

Figure A.13. Modulus degradation curve for rock layers (after Schnabel, 1973)

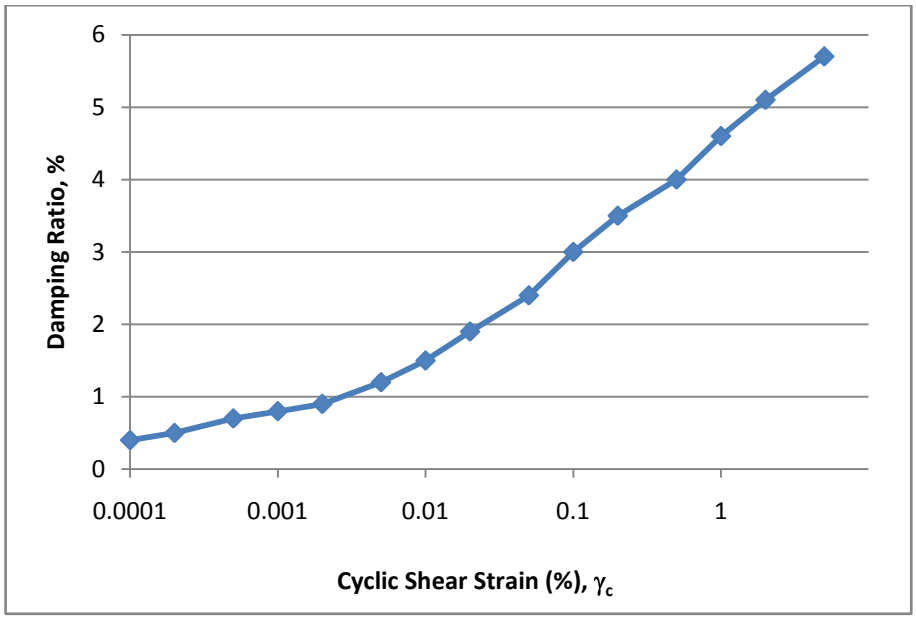

Figure A.14. Damping ratio curve for rock layers (after Schnabel, 1973)

Clay, PI = 15 (Vucetic and Dobry, 1991)

Modulus degradation curve and damping ratio curve proposed by Vucetic and Dobry (1991) for clay layers with PI = 15 are demonstrated in Figure A.15 and A.16, respectively.

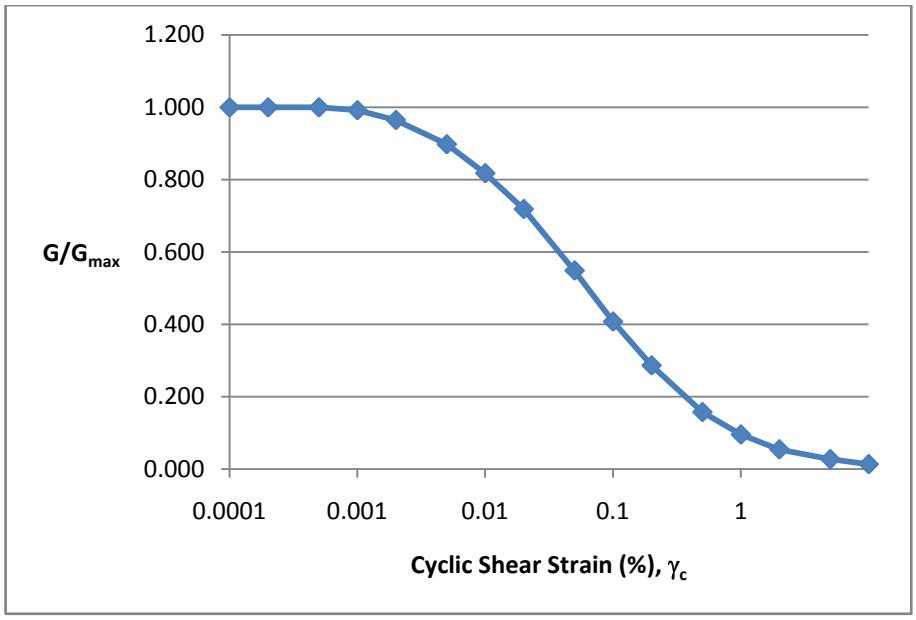

Figure A.15. Modulus degradation curve for clay layers (PI = 15) layers (after Vucetic and Dobry, 1991)

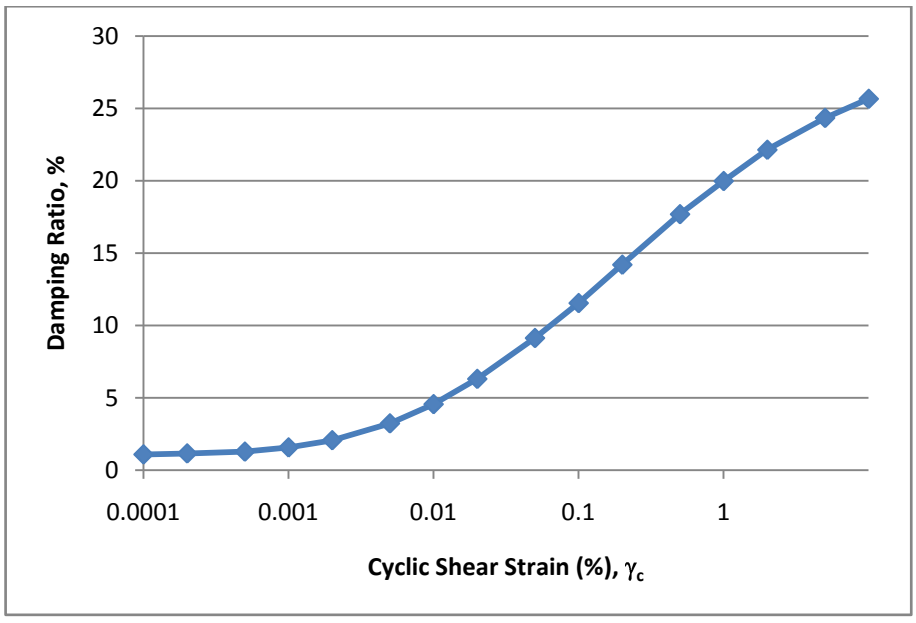

Figure A.16. Damping ratio curve for clay layers (PI = 15) layers (after Vucetic and Dobry, 1991)

Clay, PI = 30 (Vucetic and Dobry, 1991)

Modulus degradation curve and damping ratio curve proposed by Vucetic and Dobry (1991) for clay layers with PI = 30 are demonstrated in Figure A.17 and A.18, respectively.

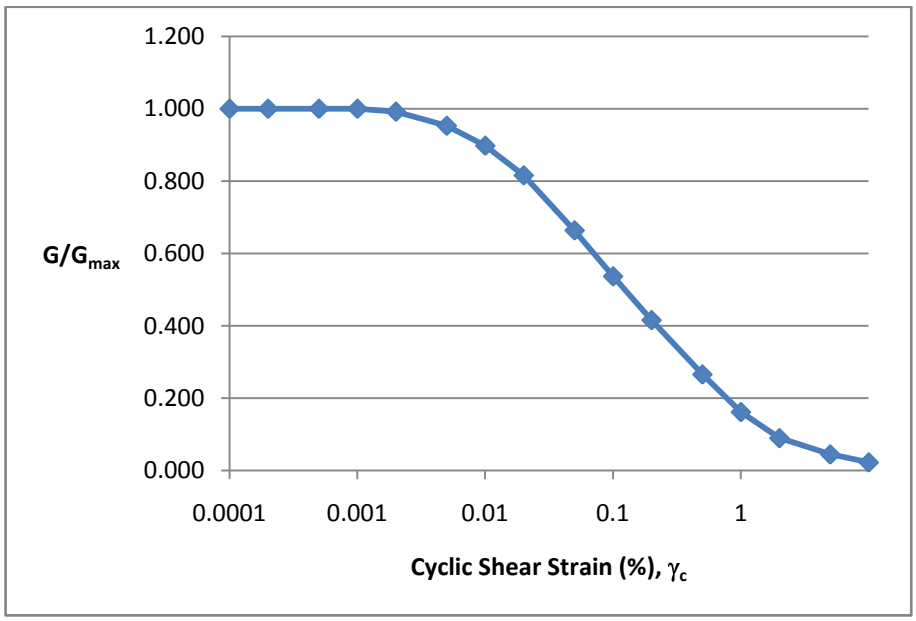

Figure A.17. Modulus degradation curve for clay layers (PI = 30) layers (after Vucetic and Dobry, 1991)

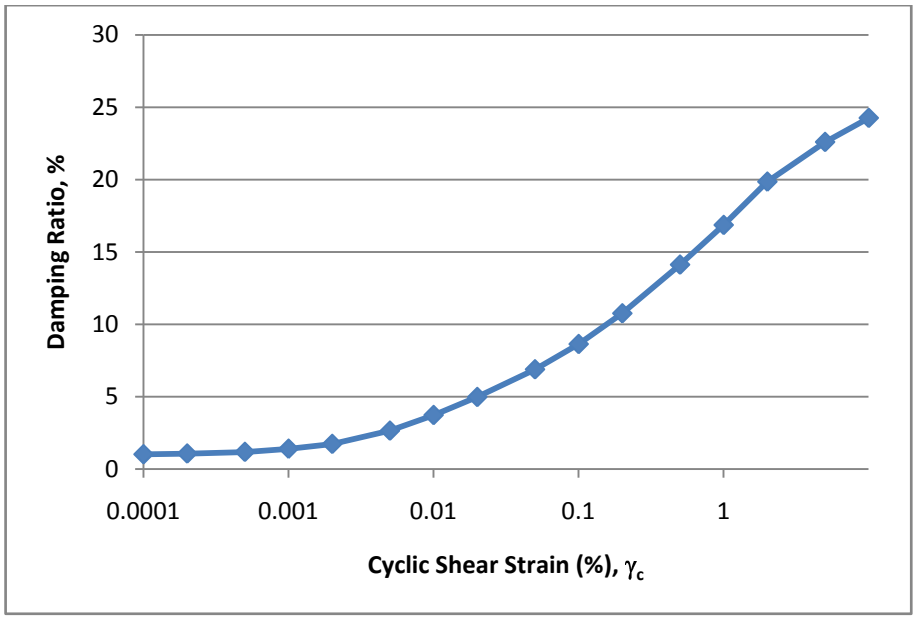

Figure A.18. Damping ratio curve for clay layers (PI = 30) layers (after Vucetic and Dobry, 1991)

Clay, PI = 50 (Vucetic and Dobry, 1991)

Modulus degradation curve and damping ratio curve proposed by Vucetic and Dobry (1991) for clay layers with PI = 50 are demonstrated in Figure A.19 and A.20, respectively.

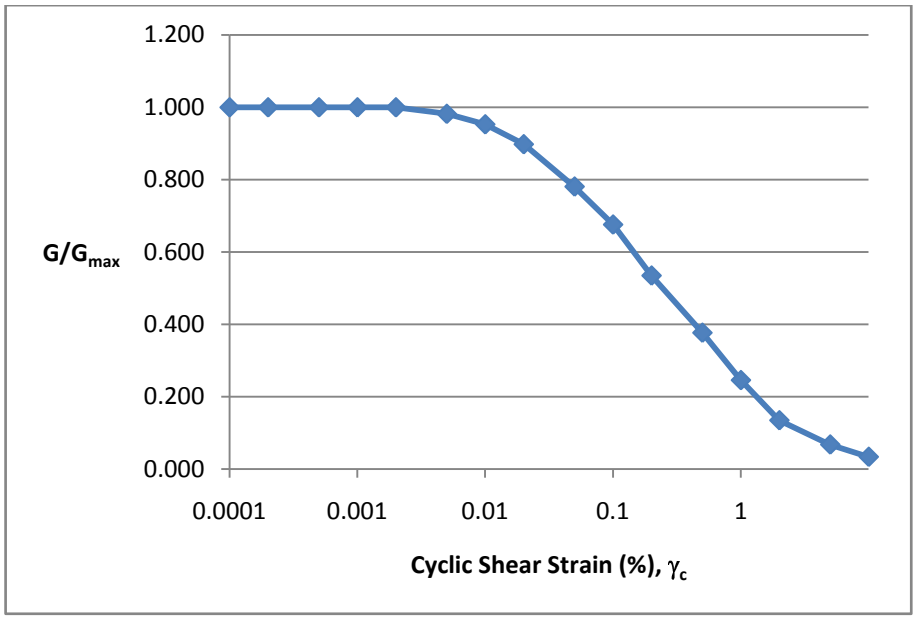

Figure A.19. Modulus degradation curve for clay layers (PI = 50) layers (after Vucetic and Dobry, 1991)

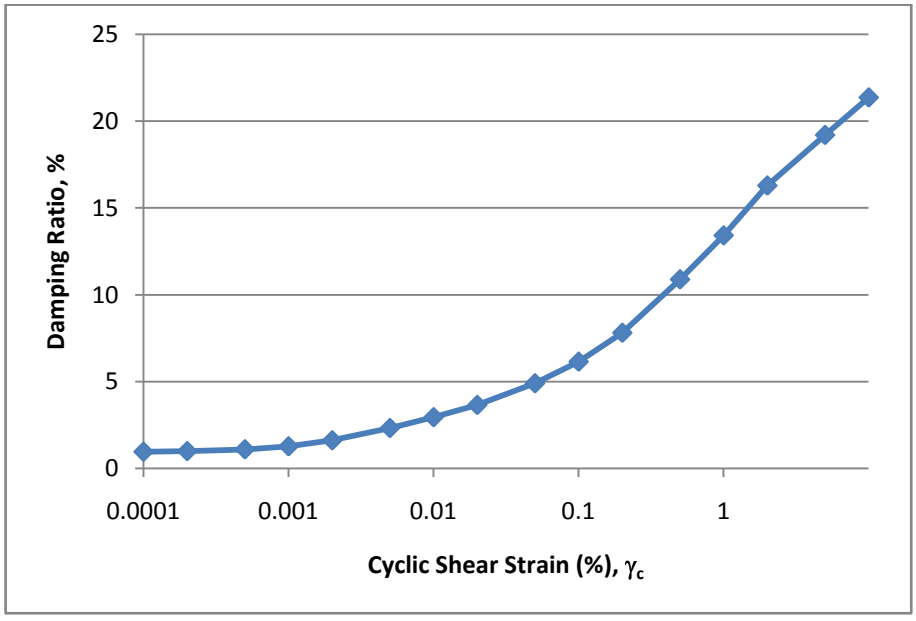

Figure A.20. Damping ratio curve for clay layers (PI = 50) layers (after Vucetic and Dobry, 1991)

Clay, PI = 100 (Vucetic and Dobry, 1991)

Modulus degradation curve and damping ratio curve proposed by Vucetic and Dobry (1991) for clay layers with PI = 100 are demonstrated in Figure A.21 and A.22, respectively.

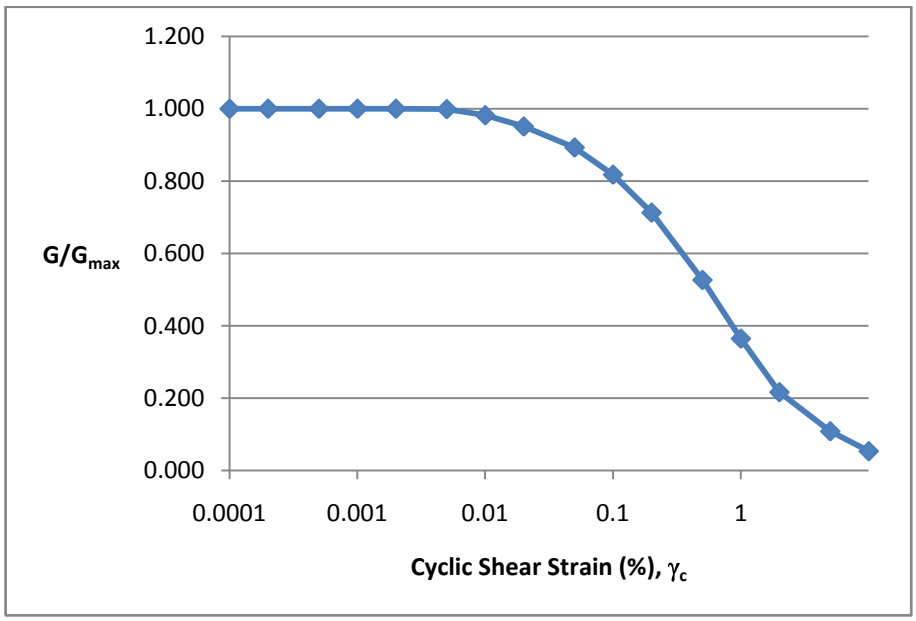

Figure A.21. Modulus degradation curve for clay layers (PI = 100) layers (after Vucetic and Dobry, 1991)

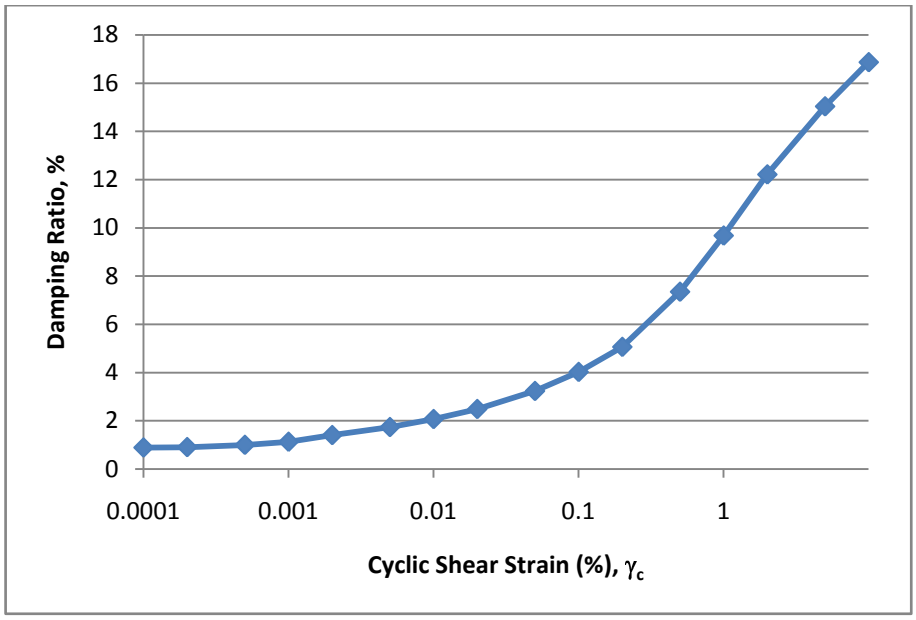

Figure A.22. Damping ratio curve for clay layers (PI = 100) layers (after Vucetic and Dobry, 1991)

Gravel (Seed et al. , 1988)

Modulus degradation curve and damping ratio curve proposed by Seed et al. (1988) for gravel layers are demonstrated in Figure A.23 and A.24, respectively.

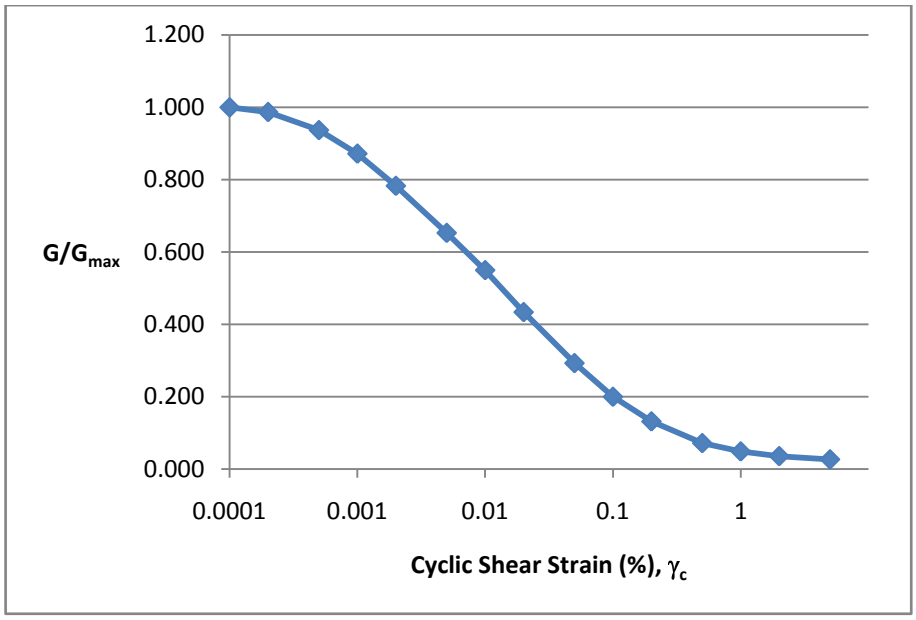

Figure A.23. Modulus degradation curve for gravel layers (after Seed et al. , 1988)

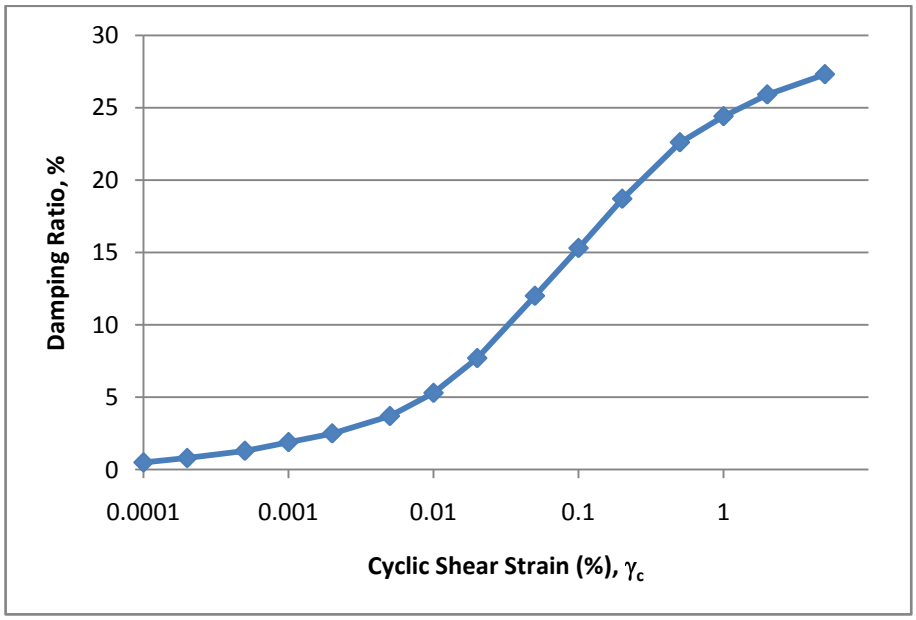

Figure A.24. Damping ratio curve for gravel layers (after Seed et al., 1988)

Loose Sand (Seed and Idriss, 1970)

Modulus degradation curve and damping ratio curve proposed by Seed and Idriss (1970) for loose sand layers are demonstrated in Figure A.25 and A.26, respectively. Modulus degradation curve has been used from **"Lower Bound"** predictions of Seed and Idriss (1970) and so as to be compatible with loose sand layer conditions **"Higher Bound"** predictions proposed by Seed and Idriss (1970) have been applied.

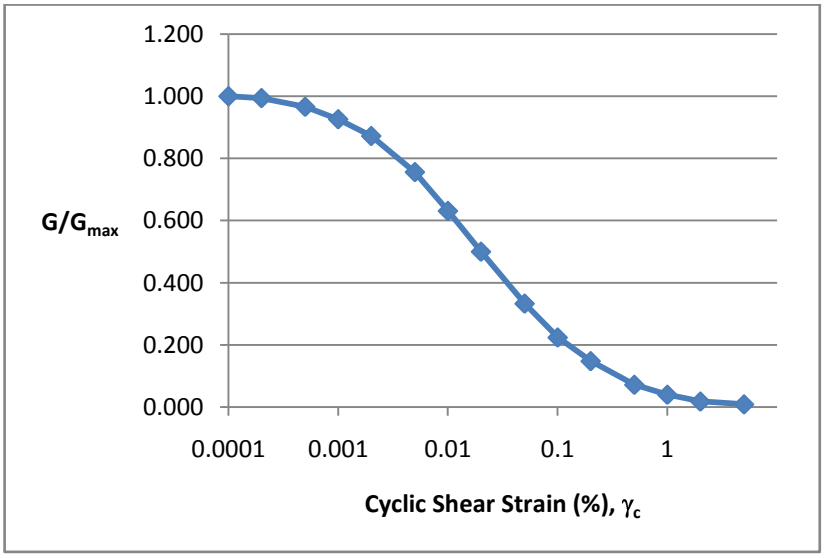

Figure A 25. Modulus degradation curve for sand layers, lower bound predictions (after Seed and Idriss, 1970)

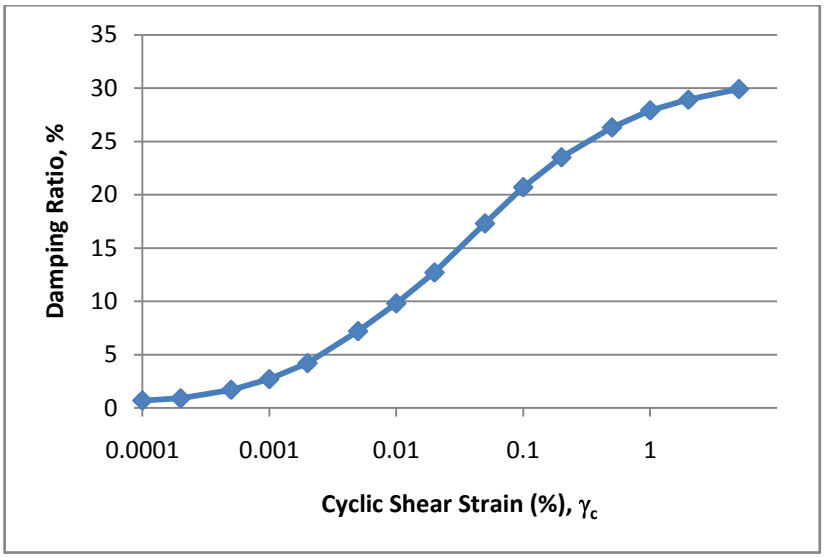

Figure A.26. Damping ratio curve for sand layers, higher bound predictions (after Seed and Idriss, 1970)

Sand (Seed and Idriss, 1970)

Modulus degradation curve and damping ratio curve proposed by Seed and Idriss (1970) for sand layers are demonstrated in Figure A.27 and A.28, respectively.

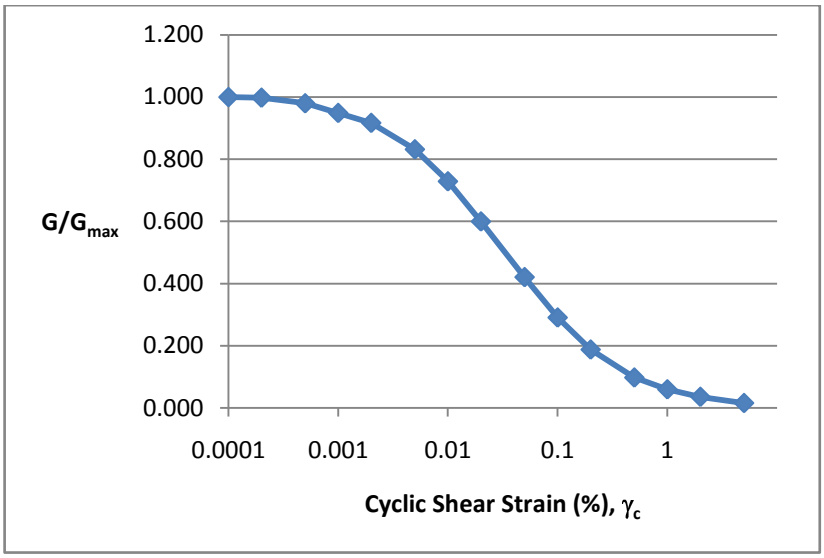

Figure A.27. Modulus degradation curve for sand layers, average predictions (after Seed and Idriss, 1970)

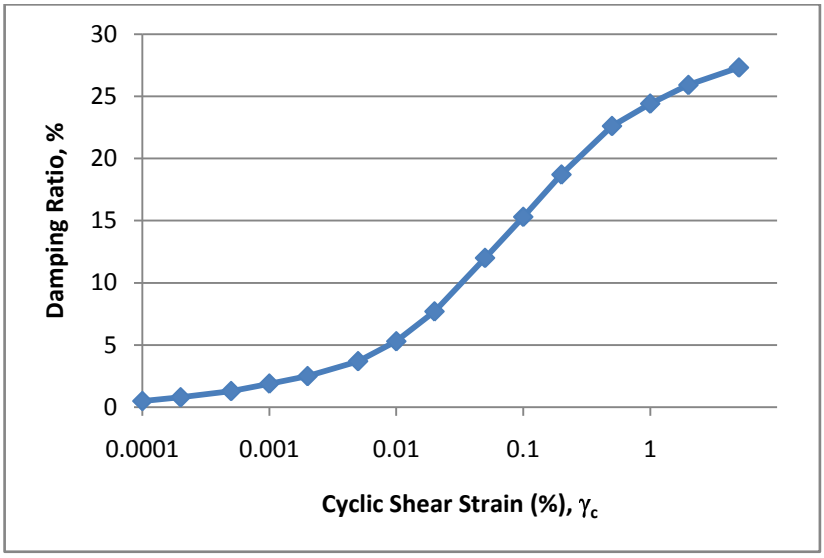

Figure A.28. Damping ratio curve for sand layers, average predictions (after Seed and Idriss, 1970)

Dense Sand (Seed and Idriss, 1970)

Modulus degradation curve and damping ratio curve proposed by Seed and Idriss (1970) for dense sand layers are demonstrated in Figure A.29 and A.30, respectively. Modulus degradation curve has been used from **"Higher Bound"** predictions of Seed and Idriss (1970) and so as to be compatible with dense sand layer conditions **"Lower Bound"** predictions proposed by Seed and Idriss (1970) have been applied.

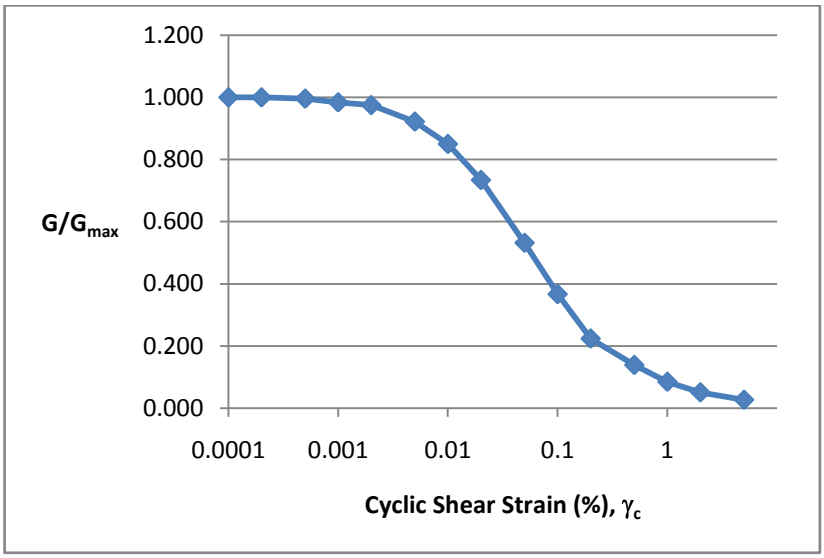

Figure A.29. Damping ratio curve for sand layers, higher bound (after Seed and Idriss, 1970)

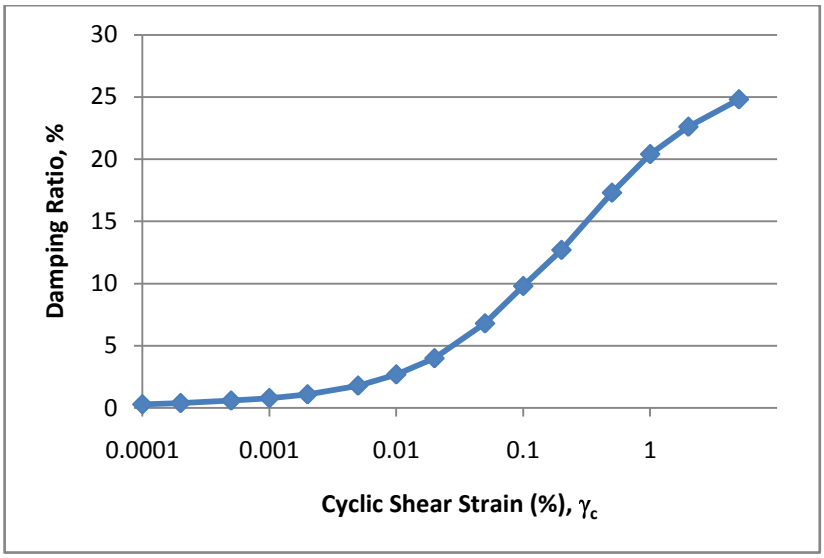

Figure A.30. Damping ratio curve for sand layers, lower bound predictions (after Seed and Idriss, 1970)

APPENDIX B

STRUCTURAL PARAMETERS

Geometry:

Two types of one bay and one span box girder tunnel have been used. Interior dimensions are (from wall to wall) listed below (Notation: Clear Height x Clear Width).

1. Structure 1 : 4.00 m x 4.00 m
2. Structure 2 : 8.00 m x 4.00 m

Member thicknesses have been assumed to be constant for all structural members for the sake of simplicity. Wall thicknesses have been defined to be one tenth of the clear span of the structure, which can be a good approximation for the preliminary design under service life loadings. Structure geometries are illustrated in Figure B.1 and Figure B.2 for *Structure 1* and *Structure 2*, respectively.

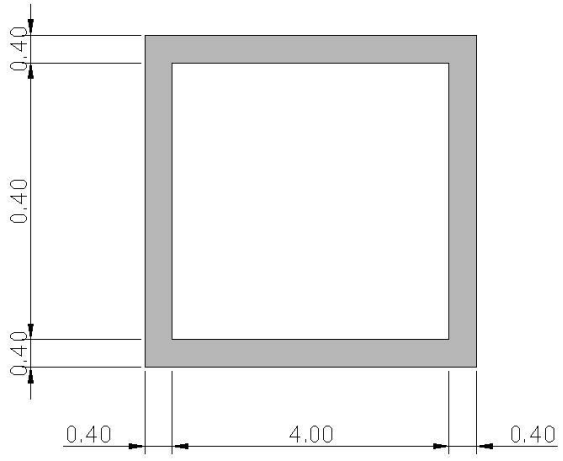

Figure B.1. Cross-sectional structure geometry and member dimensions of Structure 1

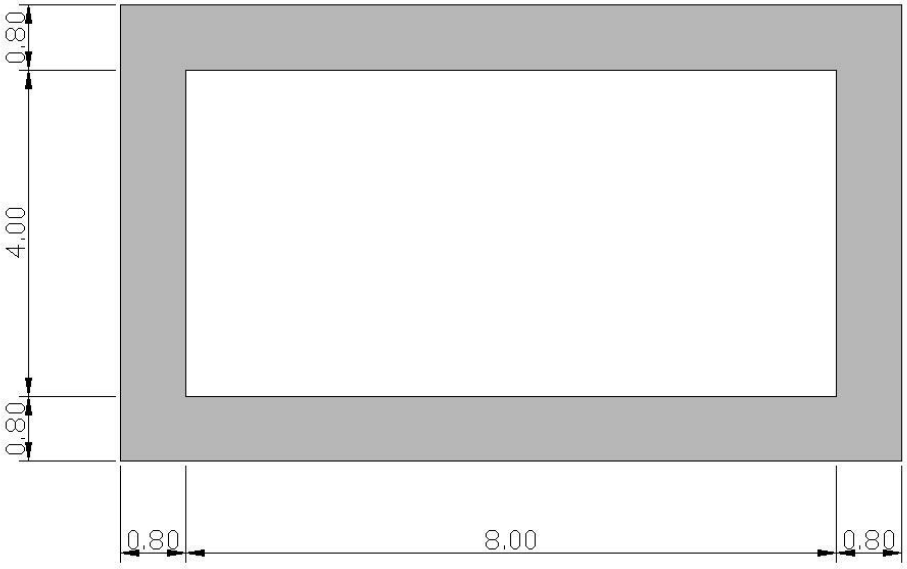

Figure B.2. Cross-sectional structure geometry and member dimensions of Structure 2

Cross-Sectional Properties of the Structural Members:

It can be observed from Figure B.1 and Figure B.2 that cross-sectional dimensions of the structural members are as defined below.

- For Structure 1 : 0.40 m x 1.00 m
- For Structure 2 : 0.80 m x 1.00 m

Cross-sectional properties of the sections are summarized in Table B.1.

Table B. 1. Cross-Sectional Properties

	Unit	0.40 m x 1.00 m	0.80 m x 1.00 m
Moment of Inertia, I	m^4	5.33 E-3	4.27 E-2
Area, A	m^2	4.00 E-1	8.00 E-1

Material Properties:

In accordance with current design of practice, concrete having grade of C30 have been used in the analyses. Although concrete has variety of properties, i.e. Modulus of Elasticity, Poisson Ratio, coefficient of thermal expansion, strength, etc., in this appendix only the modulus of the elasticity is going to be discussed.

As Ersoy and Özcebe (2001) indicated that since concrete is a highly nonlinear and inelastic material, it is very hard to determine a linear elastic parameter

such as Young's Modulus. Any factor, i.e. the rate and intensity of loading, creep, shrinkage, etc., affecting concrete strength and stress-strain relationship of concrete also affects the modulus of elasticity (Ersoy and Özcebe, 2001). Therefore, it is impossible to determine the modulus of elasticity precisely. Moreover, it is very unpractical to estimate a modulus of elasticity value by considering all possible factors simultaneously. So as to cope with this problem, several codes correlate modulus of elasticity with compressive strength for the sake of simplicity (Ersoy and Özcebe, 2001). Correlations of Turkish Reinforced Concrete Code (TS 500 – 2000) and Standard Specification for Highway Bridges, *American Association of State Highway and Transportation Officials* (AASHTO, 2002) are going to are going to be demonstrated.

- The formulation suggested in Turkish Reinforced Concrete Code (TS500-2000) is given in Equation B.1.

$$E_{c,28} = 3250 \times \sqrt{f_{c,28}} + 14000 \qquad \text{(B.1)}$$

If $f_{c,28}$ = 30 MPa is replaced;

$E_{c,28}$ = 3250 x $(30)^{1/2}$ + 14000 = 31800 MPa is obtained

- The formulation suggested by AASHTO 2002, Part 8.7.1 is given in Equation B.2.

$$E_c = 0.0428 \times w_c^{1.5} \times \sqrt{f_c'} \qquad \text{(B.2)}$$

If f'_c = 30 MPa and w_c = 25 kN/m^3 are replaced into Equation 2,

$$E_c = 0.0428 \times 25^{1.5} \times 30^{1/2} = 29303 \text{ MPa is obtained}$$

It is important to note that both Equation 1 and Equation 2 are derived for rapid loadings (Ersoy and Özcebe, 2001) which are, as expected, applicable for seismic excitations too.

The modulus of elasticity used in the analyses is 30000 MPa which is an acceptable estimate between the values estimated by TS 500-2000 and AASHTO, 2002.

APPENDIX C

EARTHQUAKE PROPERTIES

In Chapter 3, total of 14 earthquake records have been used. This appendix is devoted to the classification of earthquakes in the bases of PGA, PGV, and PGD as well as moment magnitude. Further, database codes of SGM records are also be given in the end of this appendix.

1. Classification According to Peak Ground Accelaration (PGA)

   The distribution of SGM records according to PGA bins is listed in Table C. 1 and illustrated in Figure C. 1.

Table C. 1. Classification of EQ Database according to PGA Bins

PGA Bin	PGA_{rep}	Number of EQ
0.01 g ≤ PGA < 0.15 g	0.075 g	4
0.15 g ≤ PGA < 0.30 g	0.225 g	4
0.30 g ≤ PGA < 0.45 g	0.375 g	4
0.45 g ≤ PGA < 0.60 g	0.525 g	2

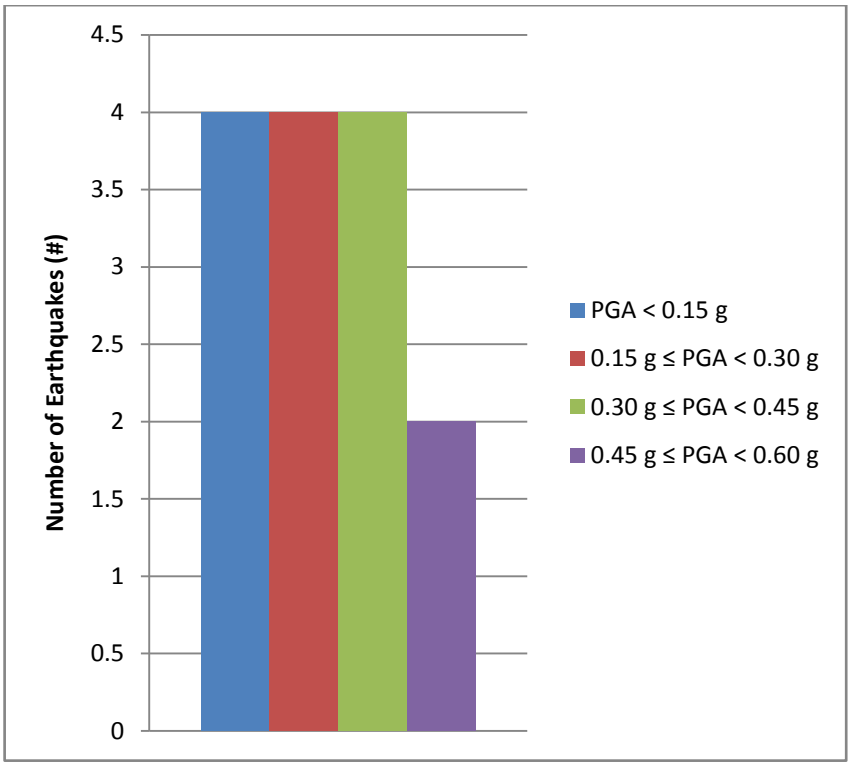

Figure C. 1. Number of Occurrences of EQ vs. PGA

2. Classification According to Peak Ground Velocity (PGV)

The distribution of SGM records according to PGV bins is listed in Table C. 2 and illustrated in Figure C. 2.

Table C. 2. Classification of EQ Database according to PGV Bins

PGV Bin	PGV_{rep}	Number of EQ
PGV < 15.00 cm/s	7.5	7
15.00 cm/s ≤ PGV < 30.00 cm/s	22.5	4
30.00 cm/s ≤ PGV < 45.00 cm/s	37.5	1
45.00 cm/s ≤ PGV < 60.00 cm/s	52.5	1
60.00 cm/s ≤ PGV < 75.00 cm/s	67.5	1

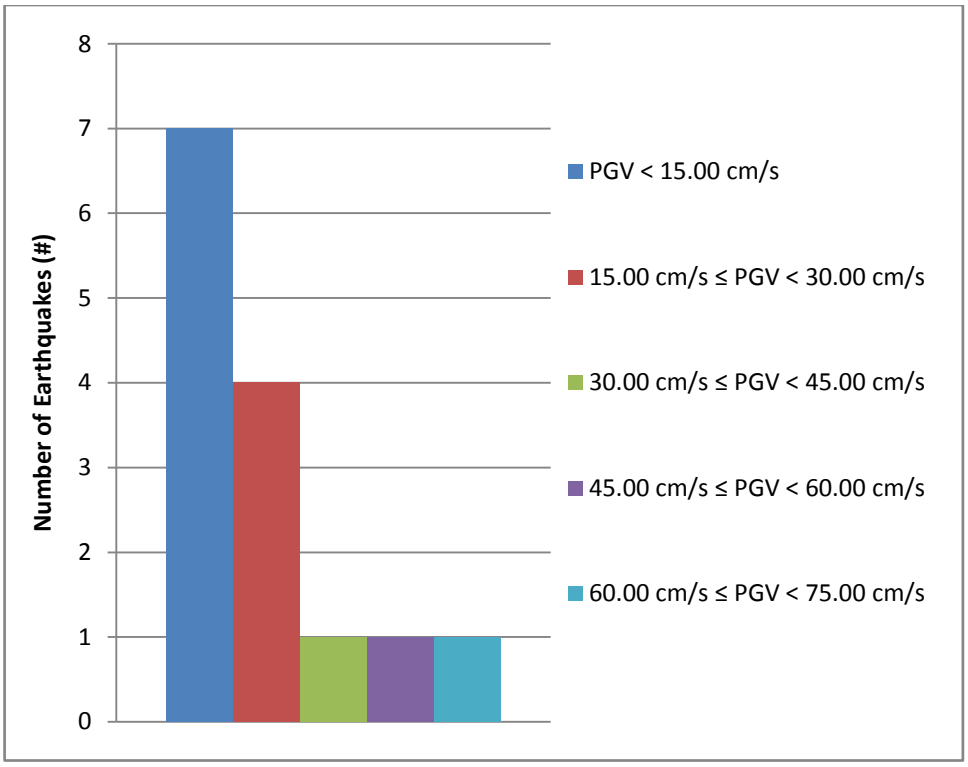

Figure C. 2. Number of Occurrences of EQ vs. PGV

3. Classification According to Peak Ground Displacement (PGD)

The distribution of SGM records according to PGD bins is listed in Table C. 3 and illustrated in Figure C. 3.

Table C. 3. Classification of EQ Database according to PGD Bins

PGV Bin	PGV_{rep}	Number of EQ
PGV < 15.00 cm/s	7.5	7
15.00 cm/s ≤ PGV < 30.00 cm/s	22.5	4
30.00 cm/s ≤ PGV < 45.00 cm/s	37.5	1
45.00 cm/s ≤ PGV < 60.00 cm/s	52.5	1
60.00 cm/s ≤ PGV < 75.00 cm/s	67.5	1

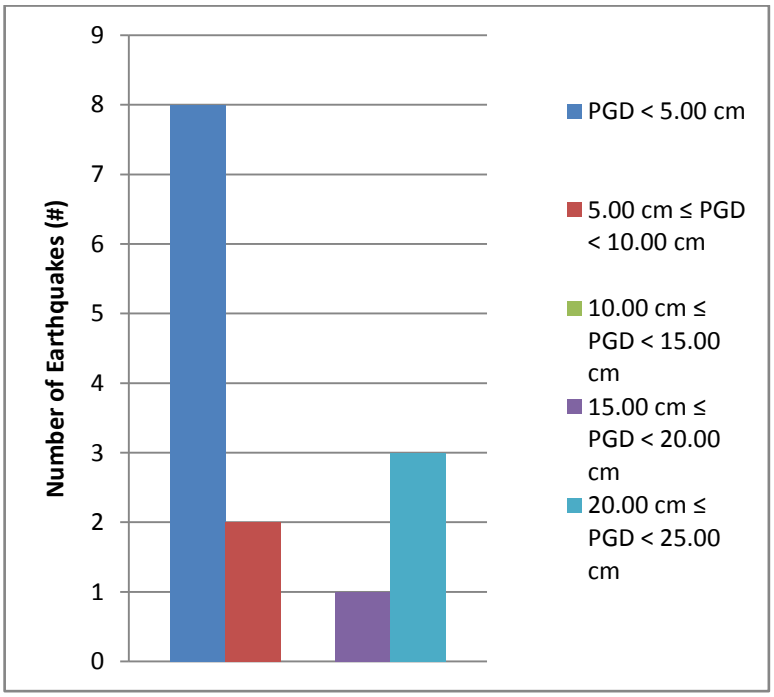

Figure C. 3. Number of Occurrences of EQ vs. PGD

4. Classification According to Moment Magnitude (Mw)

The distribution of SGM records according to Mw bins is listed in Table C. 4 and illustrated in Figure C. 4.

Table C.4. Classification of EQ Database according to PGD Bins

M_w Bin	$(M_w)_{rep}$	Number of EQ
$6.00 \leq M_w < 6.50$	6.25	2
$6.50 \leq M_w < 7.00$	6.75	8
$7.00 \leq M_w < 7.50$	7.25	4

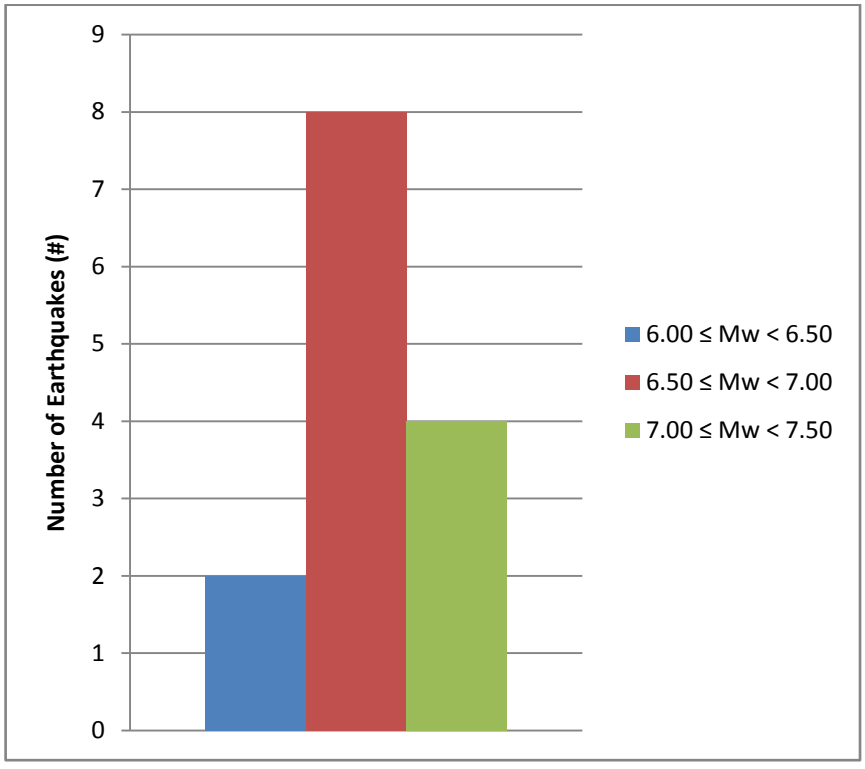

Figure C. 4. Number of Occurrences of EQ vs. Mw

5. Classification According to Both Moment Magnitude(Mw) and Peak Ground Accelaration (PGA):

Classification according to both M_w and PGA is presented in Figure C.5.

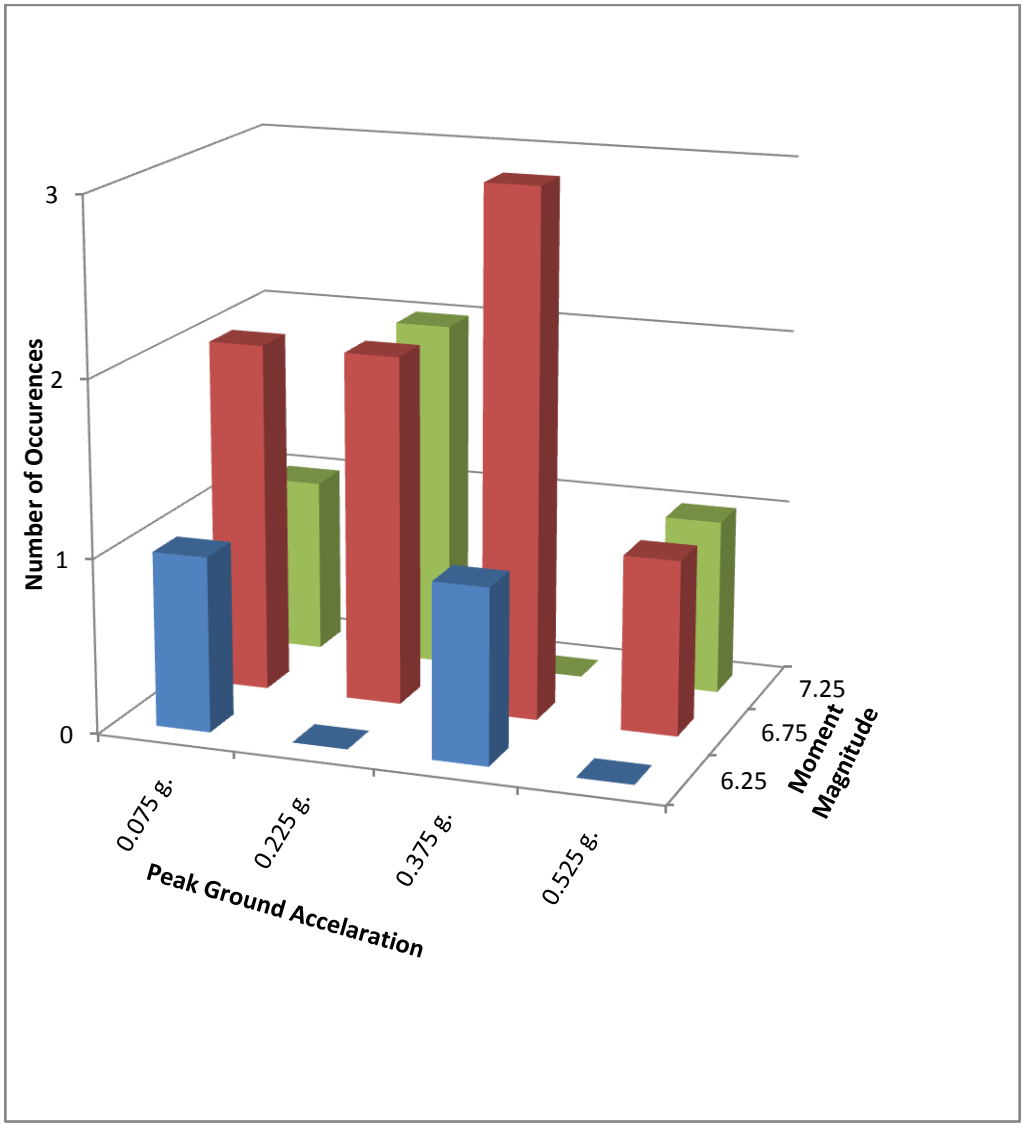

Figure C. 5. Number of Occurrences of EQ vs. Mw and PGA simultaneously

6. Classification According to Both Moment Magnitude(Mw) and Peak Ground Velocity (PGV) Simultaneously:

Classification according to both M_w and PGV is presented in Figure C. 6.

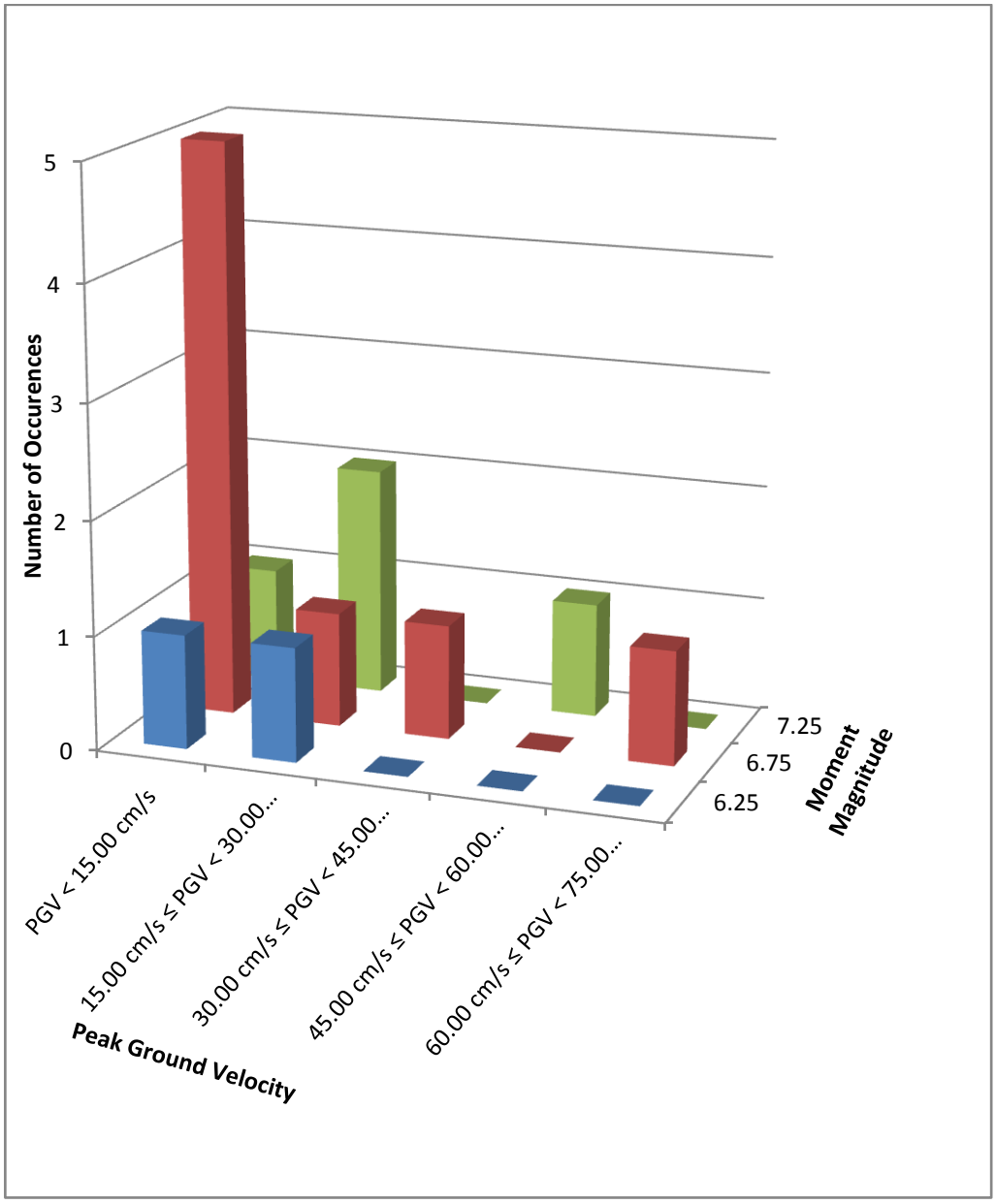

Figure C. 6. Number of Occurrences of EQ vs. Mw and PGV simultaneously

7. Classification According to Both Moment Magnitude(Mw) and Peak Ground Displacement (PGD) Simultaneously:

Classification according to both M_w and PGD is presented in Figure C. 7.

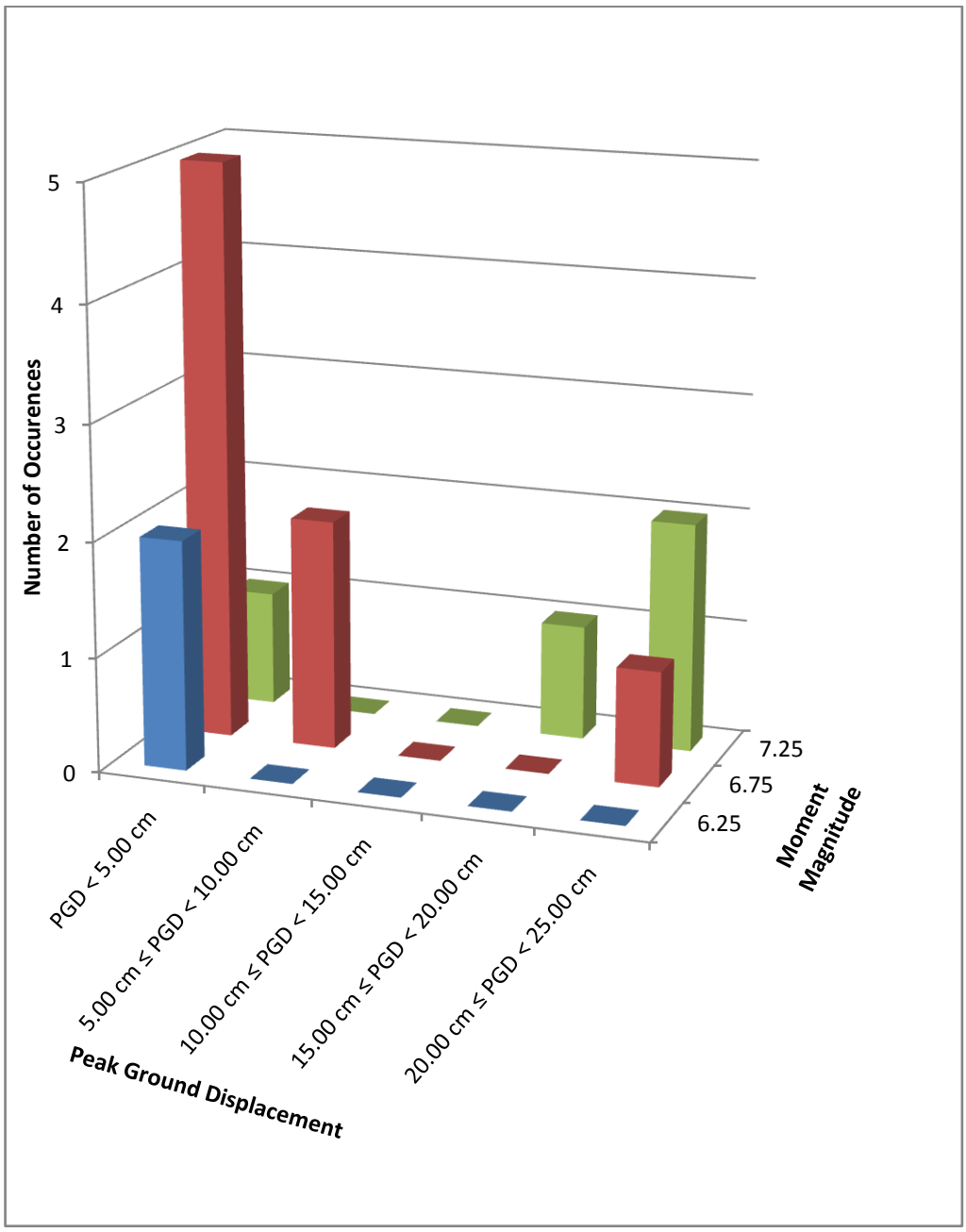

Figure C. 7. Number of Occurrences of EQ vs. Mw and PGD simultaneously

DATABASE CODES OF THE STRONG GROUND MOTION RECORDS

Database codes, present in the NISEE Online Database, of the SGM Records are listed in Table C. 5.

Table C. 5. Descriptive Properties of the SGM Records in NISEE Online Library

Name	Station	Component	Database Code
Loma Prieta	Piedmont Jr. High	045	PJH045.AT2
Landers	S. Valley Poppet	000	SIL000.AT2
Northridge	LA Wonderland	095	WON095.AT2
N. Palm Spr.	S. Valley Poppet	000	SIL000.AT2
Kocaeli	Izmit	090	IZT090.AT2
Northridge	L. Hughes #9	000	LO9090.AT2
Northridge	S. Gab.–E Grand Av.	270	GRN270.AT2
Loma Prieta	USCS	000	UC2000.AT2
W. Narrows	S. Gab. –E Grand Av.	180	A-GRN180.AT2
Hector Mine	Hec	000	HEC000.AT2
Loma Prieta	S. Cruz USCS Lick Obs.	000	LOB000.AT2
Loma Prieta	Gilroy Array #1	000	G01000.AT2
Loma Prieta	Los Gatos Lex. Dam	000	LEX000.AT2
Cape Mend.	Petrolia	000	PET000.AT2

APPENDIX D

SAMPLE ANALYSIS

This appendix is dedicated to one complete finite element analyses run performed by Plaxis 9. Step by step modeling procedure is detailly explained and illustrated in the following pages.

Before starting an illustrative run, site, earthquake, and structural information should be given.

Site Conditions : Soil profile of example NEHRP C1 is used. For further information, please see Appendix A and main text body of Chapter 3.

Earthquake Information : Loma Prieta earthquake record obtained from Los Gatos Dam is selected. Time and intensity domain parameters are defined in the main body of Chapter 3 and Appendix C.

Structural Information : Structure 1 is selected in the analysis. Further information can be reached from Chapter 3 and Appendix B.

Embedment Depth : Embedment depth equals to the height of the structure (i.e. z=H condition) is selected.

Methodology for the Finite Element Analysis:

1. Performing Site Response Analysis: Site response analysis is performed to obtain most critical free field deformation of the structure in time domain and degraded shear moduli of the layers. Figure D.1 shows the deformed shape in which the structure suffers the most critical free-field racking displacement.

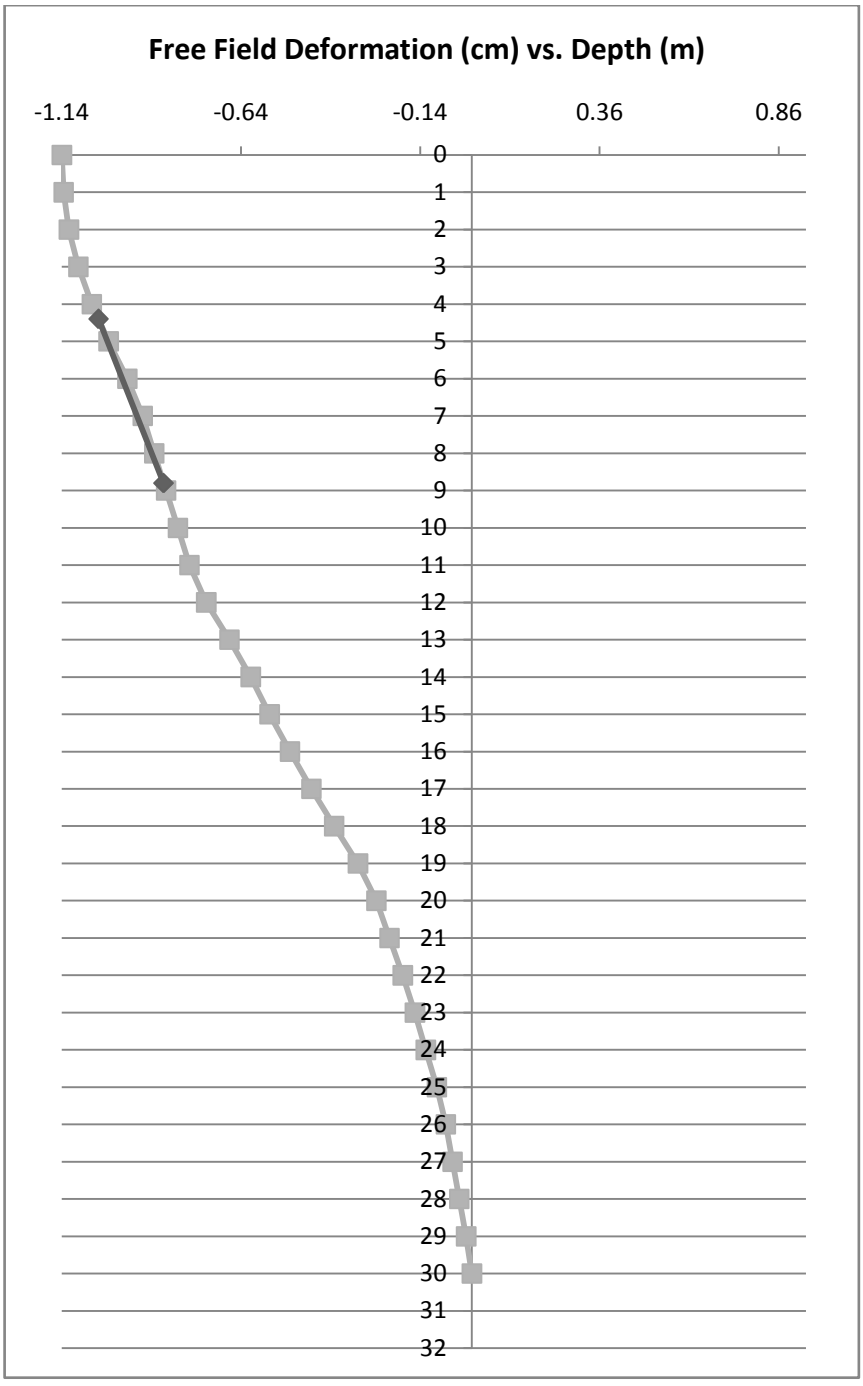

Figure D.1. Deformed shape of the soil profile in which the structure drawn with grey line suffers the most critical free field displacement in time domain

Table D.1 illustrates the degraded moduli of the soil profile.

Figure D.1. Degraded soil moduli

Layer	*z (m)*	*G (SI, kPa)*
1	0.5	255499
2	1.5	243897
3	2.5	239693
4	3.5	219114
5	4.5	220479
6	5.5	225095
7	6.5	254608
8	7.5	465856
9	8.5	519903
10	9.5	544547
11	10.5	604393
12	11.5	667446
13	12.5	385853
14	13.5	370866
15	14.5	514818
16	15.5	501436
17	16.5	489370
18	17.5	478515
19	18.5	468810
20	19.5	460172
21	20.5	854399
22	21.5	842568
23	22.5	831522
24	23.5	1058465
25	24.5	1047472
26	25.5	1037173
27	26.5	1732432
28	27.5	1729507
29	28.5	1726735
30	29.5	1724106
31	30.5	

2. Construction of Finite Element Model: Construction of model constitutes the following:

- *Definition of Geometry:* Geometries of 2D soil layer and cross-section of the structure are defined in this stage.

- *Assignment of Material Properties:* All soil layers, to be consistent with SHAKE 91 analysis, are defined as "Linear Elastic" materials. For all layers, degraded shear moduli obtained from SHAKE 91 analysis (Table D.1) and 0.49 have been defined as elasticity parameters, G and u, respectively. Structure is defined as "plate element" having a out of plane dimension of 1 m. The rest of cross-sectional properties are already defined in Appendix B and C.

- *Assignment of Restraints:* Horizontal restraints are assigned to side boundaries, and total fixities are assigned to bottom boundary. No boundary is assigned to the top boundary.

- *Assignment of Initial Boundary Displacements:* Prescribed displacements consistent with the deformed shape obtained from site response analysis are given from the right and left boundaries.

After completing first four steps Figure D.2 is obtained.

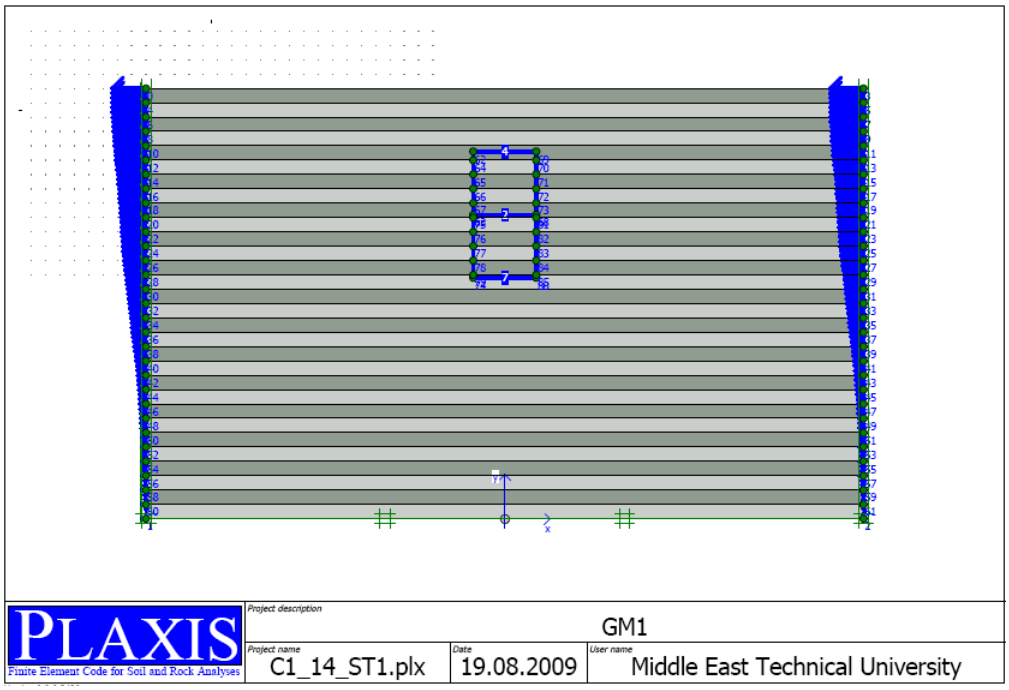

Figure D.2. After the definition of initial boundary displacements consistent with the deformed shape obtained from SHAKE 91

- *Meshing:* While meshing, triangular elements are chosen. Water table is not defined due to the fact that analysis performed in SHAKE 91 is in total stress space, i.e. not in effective stress space. After meshing Figure D.3 is obtained.

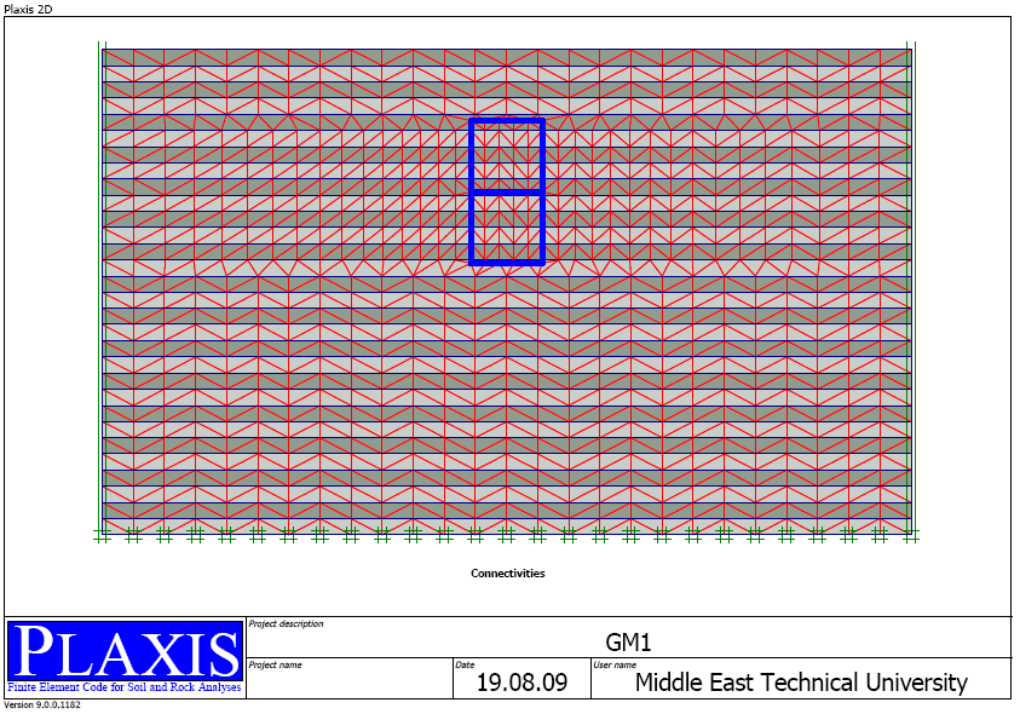

Figure D.3. Illustrative Meshing

- *Definition of Stages:* Stages are defined in the order of: initial condition, free-field deformation condition (structure is deactivated and no excavation is done), and soil-structure interaction deformation condition. Free-field deformation stage and soil-structure interaction stage are demonstrated in Figure D.4 and Figure D.5, respectively.

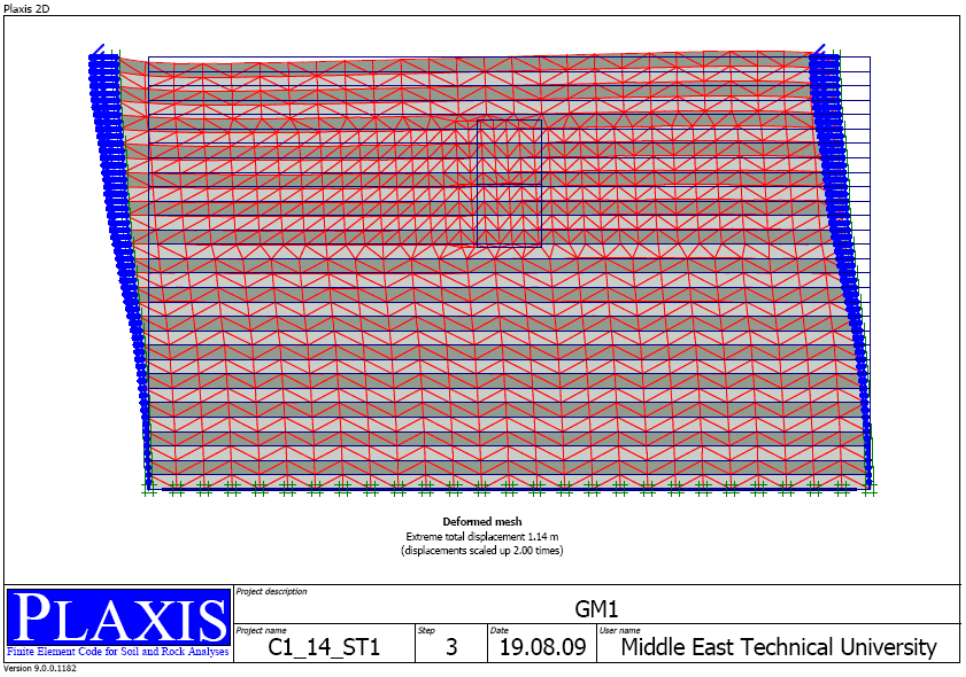

Figure D.4. Free-field deformation stage

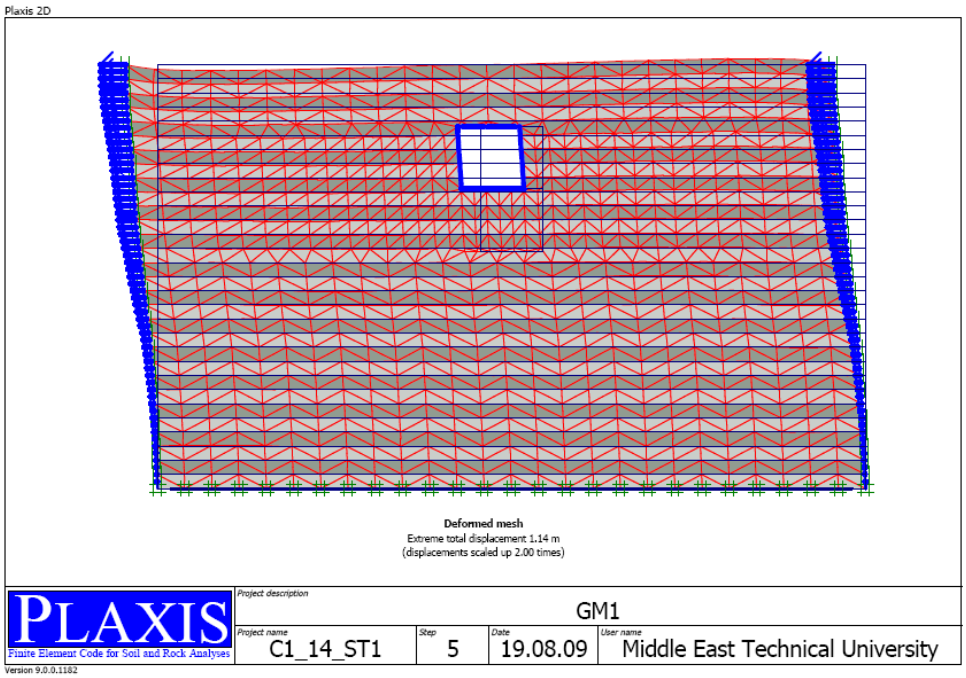

Figure D.5. Soil-structure interaction deformation stage

- *Performing an Iterative Procedure:* In this stage, by the help of total multipliers, extra effort is put on while scaling the deformation field defined at side boundaries until the relative displacement between the ceiling and the floor of the structure is equal to relative free-field deformation (Figure D.6).

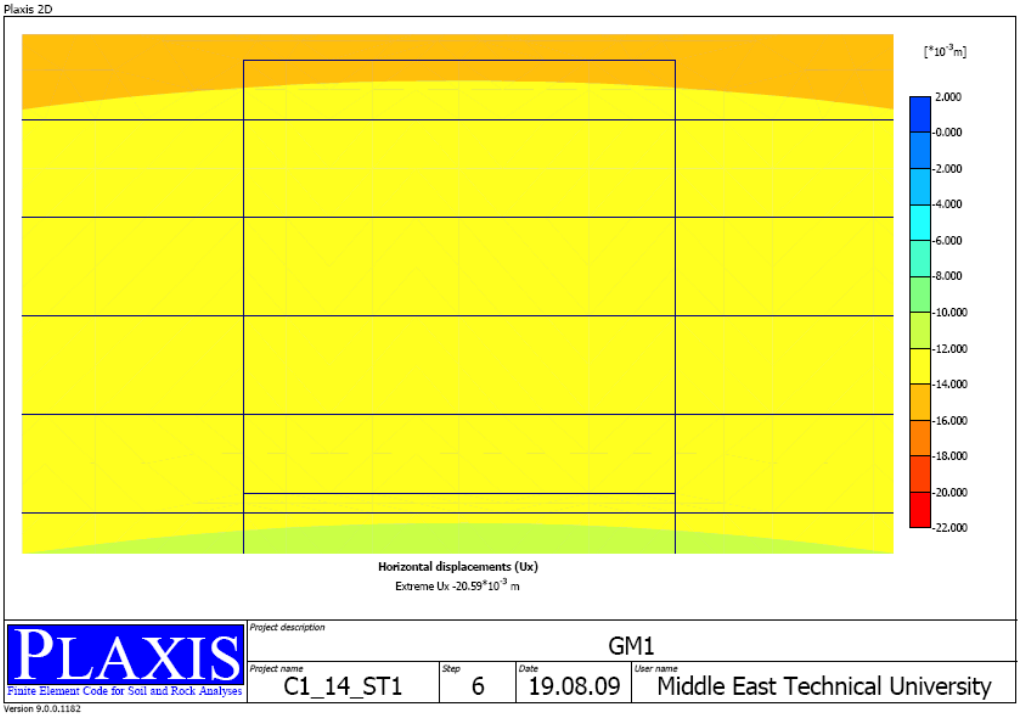

Figure D.6. Free-field displacements in shadings after necessary scaling

Table D.2 shows the free-field displacements of Figure D.6.

Table D.2. Free-field displacements and relative deformation between the top and the bottom

Location	Free-Field Displacement (cm)
Top	1.41
Bottom	1.21
Difference	**0.20**

- Determination of Racking Deformation: By means of total multipliers, same scaled deformation field is applied to soil-structure interaction (SSI) deformation stage in Figure D.5. Figure D.7 indicates the soil-structure interaction deformation in shadings type of notation.

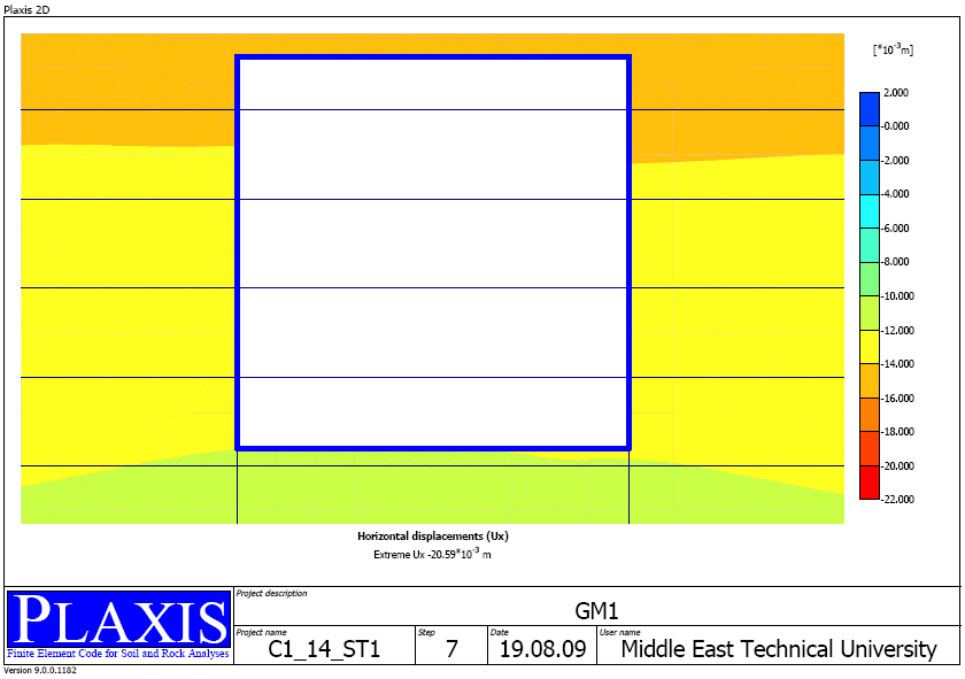

Figure D.6. SSI displacements in shadings after necessary scaling

Table D.3 shows the free-field displacements of Figure D.6.

Table D.3. Free-field displacements and relative deformation between the top and the bottom

Location	SSI Displacement (cm)
Top	1.46
Bottom	1.20
Difference	**0.26**

In this case,

Racking coefficient (R) = 0.26/0.20 = **1.3**

APPENDIX E

TABLE OF COMPARISON

Comparisons of closed form solutions under all combinations are given in Table E.1.

Table E.1. Comparison of Analytical SFA Methods

Class	Site	EQ	Str.	Depth	Racking Deformations (mm)			
					Δ_{FF}	Δ_{WANG}	$\Delta_{PENZIEN}$	Δ_{HUO}
B	1	1	1	H	0.23	0.38	0.44	0.63
B	1	1	1	2H	0.28	0.48	0.56	0.79
B	1	1	2	H	0.26	0.44	0.49	0.63
B	1	1	2	2H	0.32	0.53	0.60	0.78
B	1	2	1	H	0.16	0.27	0.31	0.44
B	1	2	1	2H	0.20	0.34	0.39	0.56
B	1	2	2	H	0.18	0.31	0.34	0.44
B	1	2	2	2H	0.22	0.38	0.43	0.56
B	1	3	1	H	0.43	0.73	0.84	1.19
B	1	3	1	2H	0.53	0.90	1.04	1.49
B	1	3	2	H	0.50	0.83	0.93	1.19
B	1	3	2	2H	0.59	1.00	1.13	1.46
B	1	4	1	H	0.43	0.73	0.85	1.20
B	1	4	1	2H	0.52	0.88	1.02	1.46
B	1	4	2	H	0.50	0.83	0.93	1.19
B	1	4	2	2H	0.58	0.98	1.11	1.44
B	1	5	1	H	0.31	0.51	0.60	0.84
B	1	5	1	2H	0.39	0.66	0.77	1.09
B	1	5	2	H	0.35	0.59	0.66	0.85
B	1	5	2	2H	0.44	0.74	0.84	1.09
B	1	6	1	H	0.59	0.99	1.15	1.62
B	1	6	1	2H	0.75	1.25	1.46	2.07

Table E.1 (cont'd). Comparison of Analytical SFA Methods

Class	Site	EQ	Str.	Depth	Racking Deformations (mm)			
					Δ_{FF}	Δ_{WANG}	$\Delta_{PENZIEN}$	Δ_{HUO}
B	1	6	2	H	0.68	1.14	1.27	1.63
B	1	6	2	2H	0.84	1.41	1.59	2.05
B	1	7	1	H	1.27	2.13	2.46	3.48
B	1	7	1	2H	1.55	2.61	3.03	4.30
B	1	7	2	H	1.45	2.44	2.71	3.46
B	1	7	2	2H	1.73	2.91	3.27	4.22
B	1	8	1	H	0.51	0.86	0.99	1.40
B	1	8	1	2H	0.64	1.07	1.24	1.77
B	1	8	2	H	0.58	0.98	1.10	1.40
B	1	8	2	2H	0.71	1.20	1.35	1.75
B	1	9	1	H	0.79	1.32	1.53	2.16
B	1	9	1	2H	0.99	1.67	1.93	2.75
B	1	9	2	H	0.90	1.52	1.69	2.16
B	1	9	2	2H	1.11	1.86	2.10	2.72
B	1	10	1	H	0.48	0.81	0.94	1.33
B	1	10	1	2H	0.60	1.01	1.17	1.67
B	1	10	2	H	0.55	0.93	1.04	1.33
B	1	10	2	2H	0.67	1.13	1.27	1.65
B	1	11	1	H	1.02	1.72	1.98	2.80
B	1	11	1	2H	1.27	2.13	2.48	3.52
B	1	11	2	H	1.17	1.97	2.19	2.80
B	1	11	2	2H	1.41	2.37	2.67	3.45
B	1	12	1	H	0.49	0.83	0.96	1.36
B	1	12	1	2H	0.64	1.07	1.25	1.77
B	1	12	2	H	0.57	0.96	1.07	1.37
B	1	12	2	2H	0.72	1.21	1.37	1.77
B	1	13	1	H	1.70	2.85	3.29	4.64
B	1	13	1	2H	2.09	3.52	4.08	5.79
B	1	13	2	H	1.94	3.27	3.63	4.61
B	1	13	2	2H	2.32	3.91	4.39	5.65
B	1	14	1	H	2.04	3.43	3.96	5.58
B	1	14	1	2H	2.55	4.29	4.98	7.06
B	1	14	2	H	2.34	3.94	4.37	5.55
B	1	14	2	2H	2.85	4.79	5.37	6.91
B	2	1	1	H	0.13	0.21	0.25	0.35
B	2	1	1	2H	0.19	0.31	0.37	0.52
B	2	1	2	H	0.15	0.25	0.28	0.37
B	2	1	2	2H	0.22	0.36	0.41	0.54
B	2	2	1	H	0.11	0.18	0.21	0.31

Table E.1 (cont'd). Comparison of Analytical SFA Methods

Class	Site	EQ	Str.	Depth	Racking Deformations (mm)			
					Δ_{FF}	Δ_{WANG}	$\Delta_{PENZIEN}$	Δ_{HUO}
B	2	2	1	2H	0.16	0.27	0.32	0.46
B	2	2	2	H	0.13	0.21	0.24	0.32
B	2	2	2	2H	0.19	0.32	0.36	0.48
B	2	3	1	H	0.27	0.46	0.54	0.77
B	2	3	1	2H	0.41	0.68	0.80	1.14
B	2	3	2	H	0.32	0.54	0.61	0.80
B	2	3	2	2H	0.47	0.79	0.90	1.18
B	2	4	1	H	0.29	0.49	0.57	0.81
B	2	4	1	2H	0.43	0.72	0.84	1.20
B	2	4	2	H	0.34	0.57	0.65	0.85
B	2	4	2	2H	0.49	0.83	0.95	1.24
B	2	5	1	H	0.21	0.35	0.41	0.58
B	2	5	1	2H	0.32	0.54	0.63	0.89
B	2	5	2	H	0.24	0.41	0.47	0.61
B	2	5	2	2H	0.37	0.62	0.71	0.93
B	2	6	1	H	0.64	1.08	1.25	1.79
B	2	6	1	2H	0.97	1.63	1.90	2.71
B	2	6	2	H	0.75	1.26	1.43	1.86
B	2	6	2	2H	1.12	1.88	2.15	2.81
B	2	7	1	H	0.66	1.11	1.30	1.85
B	2	7	1	2H	0.99	1.67	1.94	2.77
B	2	7	2	H	0.77	1.30	1.48	1.92
B	2	7	2	2H	1.14	1.93	2.19	2.87
B	2	8	1	H	0.27	0.45	0.52	0.75
B	2	8	1	2H	0.40	0.68	0.79	1.13
B	2	8	2	H	0.31	0.53	0.60	0.78
B	2	8	2	2H	0.47	0.79	0.90	1.18
B	2	9	1	H	0.61	1.02	1.19	1.69
B	2	9	1	2H	0.91	1.53	1.78	2.54
B	2	9	2	H	0.71	1.19	1.35	1.76
B	2	9	2	2H	1.05	1.76	2.01	2.63
B	2	10	1	H	0.28	0.47	0.55	0.78
B	2	10	1	2H	0.42	0.70	0.82	1.16
B	2	10	2	H	0.33	0.55	0.62	0.81
B	2	10	2	2H	0.48	0.81	0.93	1.21
B	2	11	1	H	0.71	1.20	1.39	1.99
B	2	11	1	2H	1.06	1.79	2.08	2.97
B	2	11	2	H	0.83	1.40	1.59	2.06
B	2	11	2	2H	1.22	2.05	2.34	3.06

Table E.1 (cont'd). Comparison of Analytical SFA Methods

Class	Site	EQ	Str.	Depth	Racking Deformations (mm)			
					Δ_{FF}	Δ_{WANG}	$\Delta_{PENZIEN}$	Δ_{HUO}
B	2	12	1	H	0.40	0.68	0.79	1.13
B	2	12	1	2H	0.62	1.04	1.21	1.72
B	2	12	2	H	0.47	0.79	0.90	1.17
B	2	12	2	2H	0.71	1.20	1.37	1.79
B	2	13	1	H	0.99	1.67	1.94	2.77
B	2	13	1	2H	1.50	2.52	2.94	4.18
B	2	13	2	H	1.16	1.95	2.22	2.88
B	2	13	2	2H	1.73	2.91	3.31	4.32
B	2	14	1	H	1.29	2.16	2.52	3.58
B	2	14	1	2H	1.97	3.31	3.85	5.49
B	2	14	2	H	1.51	2.53	2.87	3.73
B	2	14	2	2H	2.28	3.83	4.36	5.68
C	1	1	1	H	0.31	0.52	0.58	0.80
C	1	1	1	2H	0.30	0.51	0.59	0.82
C	1	1	2	H	0.33	0.53	0.59	0.71
C	1	1	2	2H	0.33	0.56	0.62	0.79
C	1	2	1	H	0.23	0.39	0.44	0.61
C	1	2	1	2H	0.24	0.40	0.46	0.64
C	1	2	2	H	0.25	0.40	0.45	0.55
C	1	2	2	2H	0.26	0.44	0.49	0.62
C	1	3	1	H	0.55	0.92	1.04	1.43
C	1	3	1	2H	0.56	0.94	1.08	1.51
C	1	3	2	H	0.59	0.94	1.05	1.26
C	1	3	2	2H	0.63	1.06	1.17	1.48
C	1	4	1	H	0.58	0.98	1.10	1.51
C	1	4	1	2H	0.60	1.01	1.16	1.63
C	1	4	2	H	0.63	0.99	1.11	1.34
C	1	4	2	2H	0.68	1.15	1.27	1.60
C	1	5	1	H	0.76	1.28	1.44	1.98
C	1	5	1	2H	0.80	1.34	1.53	2.14
C	1	5	2	H	0.82	1.29	1.44	1.72
C	1	5	2	2H	0.92	1.55	1.70	2.14
C	1	6	1	H	0.99	1.67	1.87	2.57
C	1	6	1	2H	1.05	1.77	2.02	2.82
C	1	6	2	H	1.06	1.67	1.86	2.22
C	1	6	2	2H	1.22	2.06	2.26	2.83
C	1	7	1	H	1.63	2.75	3.06	4.18
C	1	7	1	2H	1.57	2.65	3.01	4.18
C	1	7	2	H	1.70	2.65	2.95	3.49

Table E.1 (cont'd). Comparison of Analytical SFA Methods

Class	Site	EQ	Str.	Depth	Racking Deformations (mm)			
					Δ_{FF}	Δ_{WANG}	$\Delta_{PENZIEN}$	Δ_{HUO}
C	1	7	2	2H	1.84	3.10	3.38	4.21
C	1	8	1	H	1.47	2.48	2.77	3.79
C	1	8	1	2H	1.58	2.66	3.02	4.20
C	1	8	2	H	1.56	2.44	2.72	3.22
C	1	8	2	2H	1.88	3.17	3.45	4.30
C	1	9	1	H	0.97	1.64	1.84	2.52
C	1	9	1	2H	1.00	1.69	1.93	2.70
C	1	9	2	H	1.04	1.64	1.84	2.20
C	1	9	2	2H	1.15	1.94	2.13	2.68
C	1	10	1	H	1.04	1.76	1.97	2.69
C	1	10	1	2H	1.13	1.90	2.16	3.01
C	1	10	2	H	1.11	1.75	1.95	2.33
C	1	10	2	2H	1.33	2.24	2.45	3.06
C	1	11	1	H	1.83	3.08	3.43	4.67
C	1	11	1	2H	1.98	3.34	3.77	5.22
C	1	11	2	H	1.92	2.98	3.32	3.91
C	1	11	2	2H	2.39	4.03	4.37	5.41
C	1	12	1	H	0.96	1.61	1.81	2.48
C	1	12	1	2H	1.07	1.79	2.04	2.85
C	1	12	2	H	1.03	1.62	1.81	2.16
C	1	12	2	2H	1.26	2.11	2.31	2.90
C	1	13	1	H	1.82	3.06	3.40	4.64
C	1	13	1	2H	1.95	3.29	3.72	5.15
C	1	13	2	H	1.89	2.94	3.28	3.86
C	1	13	2	2H	2.37	4.00	4.33	5.36
C	1	14	1	H	2.19	3.68	4.09	5.56
C	1	14	1	2H	2.50	4.20	4.74	6.53
C	1	14	2	H	2.29	3.55	3.94	4.62
C	1	14	2	2H	3.08	5.03	5.58	6.87
C	2	1	1	H	0.32	0.55	0.60	0.82
C	2	1	1	2H	0.32	0.54	0.61	0.84
C	2	1	2	H	0.36	0.55	0.61	0.71
C	2	1	2	2H	0.34	0.55	0.62	0.75
C	2	2	1	H	0.39	0.66	0.73	0.99
C	2	2	1	2H	0.37	0.62	0.70	0.97
C	2	2	2	H	0.43	0.67	0.74	0.86
C	2	2	2	2H	0.39	0.63	0.70	0.85
C	2	3	1	H	0.68	1.14	1.25	1.69
C	2	3	1	2H	0.63	1.06	1.20	1.65

Table E.1 (cont'd). Comparison of Analytical SFA Methods

Class	Site	EQ	Str.	Depth	Racking Deformations (mm)			
					Δ_{FF}	Δ_{WANG}	$\Delta_{PENZIEN}$	Δ_{HUO}
C	2	3	2	H	0.74	1.13	1.25	1.44
C	2	3	2	2H	0.69	1.09	1.22	1.47
C	2	4	1	H	0.92	1.55	1.70	2.29
C	2	4	1	2H	0.84	1.41	1.59	2.19
C	2	4	2	H	1.00	1.53	1.69	1.94
C	2	4	2	2H	0.90	1.43	1.60	1.92
C	2	5	1	H	1.46	2.46	2.69	3.59
C	2	5	1	2H	1.69	2.84	3.15	4.29
C	2	5	2	H	1.61	2.42	2.66	3.01
C	2	5	2	2H	2.00	3.10	3.44	4.03
C	2	6	1	H	1.74	2.93	3.19	4.26
C	2	6	1	2H	1.88	3.17	3.53	4.80
C	2	6	2	H	1.90	2.85	3.13	3.53
C	2	6	2	2H	2.20	3.40	3.78	4.43
C	2	7	1	H	2.30	3.88	4.19	5.57
C	2	7	1	2H	2.29	3.85	4.27	5.79
C	2	7	2	H	2.46	3.62	4.00	4.46
C	2	7	2	2H	2.64	4.06	4.50	5.24
C	2	8	1	H	1.98	3.34	3.62	4.83
C	2	8	1	2H	2.20	3.70	4.10	5.57
C	2	8	2	H	2.15	3.21	3.53	3.97
C	2	8	2	2H	2.61	4.01	4.45	5.18
C	2	9	1	H	1.73	2.91	3.18	4.26
C	2	9	1	2H	1.69	2.85	3.19	4.36
C	2	9	2	H	1.88	2.84	3.12	3.53
C	2	9	2	2H	1.90	2.97	3.31	3.91
C	2	10	1	H	1.42	2.38	2.60	3.48
C	2	10	1	2H	1.56	2.63	2.93	4.00
C	2	10	2	H	1.55	2.34	2.57	2.92
C	2	10	2	2H	1.84	2.85	3.17	3.73
C	2	11	1	H	3.22	5.24	5.81	7.66
C	2	11	1	2H	3.34	5.62	6.16	8.27
C	2	11	2	H	3.39	4.90	5.42	5.96
C	2	11	2	2H	4.11	6.24	6.84	7.79
C	2	12	1	H	1.57	2.65	2.89	3.86
C	2	12	1	2H	1.79	3.01	3.35	4.56
C	2	12	2	H	1.72	2.59	2.85	3.22
C	2	12	2	2H	2.12	3.29	3.65	4.28
C	2	13	1	H	2.57	4.32	4.66	6.16

Table E.1 (cont'd). Comparison of Analytical SFA Methods

Class	Site	EQ	Str.	Depth	Racking Deformations (mm)			
					Δ_{FF}	Δ_{WANG}	$\Delta_{PENZIEN}$	Δ_{HUO}
C	2	13	1	2H	2.77	4.65	5.13	6.92
C	2	13	2	H	2.72	3.97	4.39	4.87
C	2	13	2	2H	3.35	5.12	5.64	6.49
C	2	14	1	H	2.83	4.63	5.13	6.78
C	2	14	1	2H	3.22	5.42	5.95	8.01
C	2	14	2	H	3.03	4.41	4.87	5.39
C	2	14	2	2H	3.94	5.99	6.58	7.52
D	1	1	1	H	1.15	0.86	0.93	0.83
D	1	1	1	2H	0.46	0.67	0.74	0.88
D	1	1	2	H	1.00	0.41	0.47	0.33
D	1	1	2	2H	0.45	0.56	0.62	0.61
D	1	2	1	H	2.87	1.53	1.72	1.44
D	1	2	1	2H	0.83	1.18	1.30	1.53
D	1	2	2	H	2.22	0.60	0.72	0.49
D	1	2	2	2H	0.84	1.03	1.12	1.09
D	1	3	1	H	3.98	1.88	2.15	1.76
D	1	3	1	2H	1.17	1.62	1.78	2.07
D	1	3	2	H	3.19	0.74	0.91	0.61
D	1	3	2	2H	1.14	1.35	1.48	1.42
D	1	4	1	H	1.64	1.19	1.30	1.15
D	1	4	1	2H	0.74	1.06	1.17	1.39
D	1	4	2	H	1.35	0.54	0.62	0.44
D	1	4	2	2H	0.75	0.93	1.01	1.00
D	1	5	1	H	12.86	3.07	3.73	2.84
D	1	5	1	2H	3.81	4.63	5.02	5.37
D	1	5	2	H	10.22	1.09	1.46	0.93
D	1	5	2	2H	3.68	3.69	3.98	3.50
D	1	6	1	H	7.92	2.39	2.79	2.16
D	1	6	1	2H	2.59	3.36	3.69	4.11
D	1	6	2	H	6.22	0.83	1.09	0.71
D	1	6	2	2H	2.52	2.71	2.98	2.72
D	1	7	1	H	5.06	1.95	2.25	1.79
D	1	7	1	2H	2.57	3.31	3.64	4.04
D	1	7	2	H	4.15	0.75	0.95	0.63
D	1	7	2	2H	2.47	2.64	2.89	2.63
D	1	8	1	H	4.31	1.62	1.86	1.47
D	1	8	1	2H	2.37	3.12	3.43	3.84
D	1	8	2	H	3.83	0.66	0.85	0.56
D	1	8	2	2H	2.49	2.73	3.01	2.78

Table E.1 (cont'd). Comparison of Analytical SFA Methods

Class	Site	EQ	Str.	Depth	Racking Deformations (mm)			
					Δ_{FF}	Δ_{WANG}	$\Delta_{PENZIEN}$	Δ_{HUO}
D	1	9	1	H	19.50	4.40	5.38	4.09
D	1	9	1	2H	3.15	3.98	4.37	4.81
D	1	9	2	H	14.65	1.48	1.98	1.27
D	1	9	2	2H	2.89	3.07	3.36	3.05
D	1	10	1	H	9.80	2.83	3.33	2.57
D	1	10	1	2H	3.35	4.16	4.55	4.94
D	1	10	2	H	7.87	1.02	1.34	0.86
D	1	10	2	2H	3.23	3.34	3.61	3.22
D	1	11	1	H	14.20	2.95	3.65	2.76
D	1	11	1	2H	7.01	7.62	8.37	8.52
D	1	11	2	H	12.63	1.17	1.58	1.00
D	1	11	2	2H	6.53	5.69	6.21	5.18
D	1	12	1	H	59.52	8.52	10.97	8.12
D	1	12	1	2H	6.19	6.50	7.05	7.04
D	1	12	2	H	45.81	3.02	4.13	2.61
D	1	12	2	2H	5.36	4.69	5.12	4.28
D	1	13	1	H	36.40	5.49	7.04	5.22
D	1	13	1	2H	7.87	8.09	8.68	8.55
D	1	13	2	H	26.50	1.82	2.49	1.57
D	1	13	2	2H	7.25	6.01	6.55	5.37
D	1	14	1	H	12.30	3.11	3.74	2.86
D	1	14	1	2H	7.33	7.77	8.46	8.49
D	1	14	2	H	12.27	1.41	1.87	1.20
D	1	14	2	2H	6.59	5.58	6.08	5.03
D	2	1	1	H	1.56	0.81	0.91	0.75
D	2	1	1	2H	0.70	0.84	0.92	0.97
D	2	1	2	H	1.34	0.37	0.44	0.30
D	2	1	2	2H	0.65	0.66	0.71	0.63
D	2	2	1	H	3.49	1.33	1.53	1.22
D	2	2	1	2H	1.03	1.17	1.30	1.36
D	2	2	2	H	3.01	0.56	0.71	0.47
D	2	2	2	2H	0.92	0.90	0.98	0.85
D	2	3	1	H	7.24	1.89	2.26	1.73
D	2	3	1	2H	2.24	2.34	2.53	2.52
D	2	3	2	H	6.01	0.74	0.98	0.63
D	2	3	2	2H	1.81	1.58	1.72	1.44
D	2	4	1	H	2.16	0.86	0.99	0.79
D	2	4	1	2H	1.68	1.85	2.04	2.10
D	2	4	2	H	1.83	0.37	0.46	0.30

Table E.1 (cont'd). Comparison of Analytical SFA Methods

Class	Site	EQ	Str.	Depth	Racking Deformations (mm)			
					Δ_{FF}	Δ_{WANG}	$\Delta_{PENZIEN}$	Δ_{HUO}
D	2	4	2	2H	1.42	1.32	1.44	1.23
D	2	5	1	H	42.10	3.97	5.27	3.84
D	2	5	1	2H	8.23	5.11	5.64	4.84
D	2	5	2	H	35.84	1.71	2.36	1.48
D	2	5	2	2H	5.83	3.21	3.61	2.69
D	2	6	1	H	11.04	2.00	2.52	1.89
D	2	6	1	2H	4.02	3.73	4.03	3.83
D	2	6	2	H	8.50	0.74	1.00	0.63
D	2	6	2	2H	3.25	2.54	2.75	2.21
D	2	7	1	H	8.68	1.84	2.27	1.71
D	2	7	1	2H	4.63	3.95	4.28	3.96
D	2	7	2	H	7.71	0.80	1.07	0.69
D	2	7	2	2H	3.68	2.64	2.90	2.28
D	2	8	1	H	5.09	1.12	1.37	1.04
D	2	8	1	2H	4.33	3.80	4.12	3.85
D	2	8	2	H	5.00	0.54	0.72	0.46
D	2	8	2	2H	3.39	2.51	2.74	2.17
D	2	9	1	H	27.77	3.48	4.53	3.34
D	2	9	1	2H	6.56	5.14	5.53	4.98
D	2	9	2	H	22.94	1.43	1.96	1.24
D	2	9	2	2H	4.80	3.25	3.60	2.79
D	2	10	1	H	36.93	3.72	4.92	3.59
D	2	10	1	2H	7.88	5.26	5.79	5.03
D	2	10	2	H	30.19	1.49	2.07	1.30
D	2	10	2	2H	5.81	3.31	3.70	2.77
D	2	11	1	H	20.94	2.60	3.39	2.50
D	2	11	1	2H	13.32	8.73	9.62	8.33
D	2	11	2	H	19.93	1.19	1.63	1.03
D	2	11	2	2H	9.69	4.87	5.56	4.07
D	2	12	1	H	117.42	7.91	10.70	7.73
D	2	12	1	2H	19.08	8.41	9.65	7.82
D	2	12	2	H	102.78	3.56	4.98	3.11
D	2	12	2	2H	12.90	5.14	5.96	4.21
D	2	13	1	H	53.32	4.11	5.52	4.00
D	2	13	1	2H	15.72	7.65	8.70	7.16
D	2	13	2	H	43.28	1.73	2.41	1.51
D	2	13	2	2H	12.02	5.61	6.46	4.67
D	2	14	1	H	24.19	2.56	3.37	2.47
D	2	14	1	2H	11.12	5.61	6.35	5.25

Table E.1 (cont'd). Comparison of Analytical SFA Methods

Class	Site	EQ	Str.	Depth	Racking Deformations (mm)			
					Δ_{FF}	Δ_{WANG}	$\Delta_{PENZIEN}$	Δ_{HUO}
D	2	14	2	H	23.71	1.40	1.92	1.21
D	2	14	2	2H	8.40	4.43	5.02	3.70

APPENDIX F

SAMPLE VBA CODE FOR SIMPLIFIED PROCEDURE

```
Dim gamma(999), GR(999), Err(999) As Double
Private Sub CommandButton1_Click()
    AccErr = 3#
    For i = 1 To 520
        gamma(i) = Worksheets("Girdi").Cells(4 + i, 40).Value
    Next i
    For m = 1 To 3
        d = 19 + (m - 1) * 6
        For a = 1 To 168
            minErr = 999
            optGR = 1
            dr = Cells(a + 4, 4).Value / 4.4
            Site = Cells(a + 4, 1).Value
            For b = 1 To 520
                Select Case Site
                    Case "BOLU"
                        f = 0
```

```
            Case "POLICE ST. "
                f = 2
            Case "SAND 1"
                f = 4
            Case "CLAY 1"
                f = 6
        End Select
        If (dr = 1) Then
            GR(b) = Worksheets("Girdi").Cells(4 + b, 41 + f).Value
        End If
If (dr = 2) Then
            GR(b) = Worksheets("Girdi").Cells(4 + b, 42 + f).Value
        End If
        If (dr = 3) Then
            GR(b) = Worksheets("Girdi").Cells(4 + b, 54 + f).Value
        End If
        Cells(a + 4, d).Value = gamma(b)
        Cells(a + 4, d + 1).Value = GR(b)
        Err(b) = Cells(4 + a, d + 5).Value
        If (Err(b) <= AccErr) Then
            optGR = GR(b)
            optgam = gamma(b)
```

```
            GoTo 300
        Else
            If (Err(b) < minErr) Then
                minErr = Err(b)
                optGR = GR(b)
                optgam = gamma(b)
                  End If
        End If
      Next b
300   Cells(a + 4, d).Value = optgam
      Cells(a + 4, d + 1).Value = optGR
    Next a
  Next m
End Sub
```

APPENDIX G

DESIGN FLOWCHART

Design flowchart for underground buried structure as defined in the next page (Figure G.1)

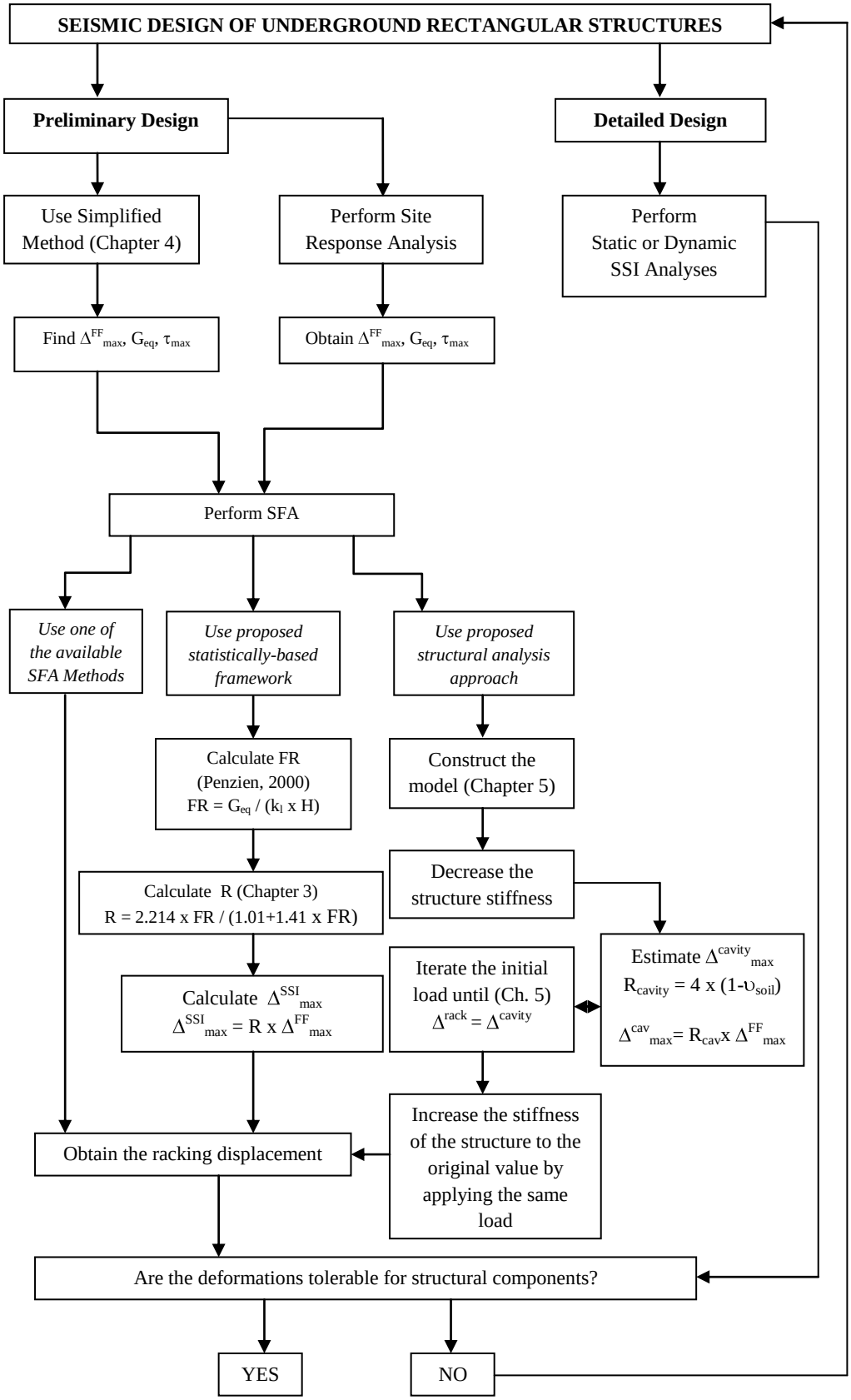

Figure G.1. Flowchart for seismic design of underground rectangular structures